UNIVERSITÀ
DI PAVIA

PhD IN BIOMEDICAL SCIENCES

DEPARTMENT OF MOLECULAR MEDICINE

UNIT OF BIOCHEMISTRY

INVESTIGATING THE PROTEASE/ANTIPROTEASE BALANCE IN BRONCHOALVEOLAR LAVAGE OF LUNG TRANSPLANT RECIPIENTS THROUGH A MULTIFACTORIAL APPROACH

PhD Tutor: Dott.ssa Simona Viglio

PhD dissertation of
Maddalena Cagnone

INDEX

INTRODUCTION

INTRODUCTION

1. Lung transplantation

By improving life quality of patients and increasing their survival rates, lung transplantation (LTx) is considered the best option in many end-stage lung diseases, such as emphysema, cystic fibrosis and pulmonary arterial hypertension [1]. The first lung transplantation was carried out in 1963 at the University Hospital of Mississippi on a patient affected by lung neoplasia. Despite the success of the surgical operation, unfortunately the patient died after 18 days for renal failure and infection [2].

With a 27% survival rate at 10 years, currently LTx has one of the poorest long-term outcomes compared to other solid organ transplantations, such as liver (70%), kidney (58%), heart (56%) or intestine (44%) [3]. Although double lung transplantation (DLTX) was demonstrated to be more effective than single transplantation (SLTX), it is more complicated being typically associated with increased perioperative complications and early mortality [4]. Thus, due to the lack of available organs, the SLTX option is usually preferred over the former [5,6]. Given the high probability of rejection that leads to either acute or chronic loss graft function [7], a major problem in solid organ transplantation is represented by acute allograft rejection (AR). This response is a well-known process in which the recipient organism does not recognize a new organ as self and, in the effort to destroy it, triggers immune response. Vertebrates have evolved sophisticated mechanisms that permit recognition of self from non-self-organs, enabling them to protect their integrity and respond to pathogens. This mechanism, called allo-recognition, is driven by T cells recognition from foreign major histocompatibility complexes (MHC I and II). The function of MHC molecules is to bind peptide fragments derived from pathogens and display them on the cell surface for recognition by the appropriate T cells. As a consequence, virus-infected cells are killed, macrophages are activated to wipe up bacteria living in their intracellular vesicles and B cells are activated to produce antibodies that neutralize extracellular pathogens.

These molecules are encoded by highly polymorphic genes located on the short harm of chromosome 6. In humans they are known as HLA (Human Leukocyte Antigen) and represent an important advantage against pathogens making individuals unique. The reverse of the medal is that this process creates problems after graft.

Both classes of MHC are involved in the direct and indirect pathways of recognition. MHC molecules of class I, expressed on the membrane of many cells, show exogenous and endogenous peptides to CD 8+ T cells. MHC molecules of class II are present on B lymphocytes and dendritic cells' surface and show exogenous peptides to CD 4+ T cells [8,9].

In the direct pathway, MHC molecules (both I and II classes) are exposed on the surface of antigen-presenting cells (APC) and are directly exposed to CD8+ and CD4+ T cells. In the indirect pathway, when APCs are destroyed, recipient dendritic cells expose antigens to CD4+ T cells [9,10].

Lung transplantation outcome is frequently unlucky also due to the constant exposure of lungs to environmental viruses, bacteria and fungi. The presence of pathogens [11] can cause infections which stimulate the immune response thus facilitating the onset of the acute rejection [12]. The most frequent type of acute rejection is mediated by T cells, in which CD4+ produces cytokines with the consequent activation of CD8+, neutrophils and alveolar macrophages. Moreover, interleukin 17 (IL-17) activates the neutrophilic migration triggering IL-8, a neutrophilic chemo-attractant cytokine [13,14].

The other type of rejection, also known as Chronic Lung Allograft Dysfunction (CLAD), is chronic and represents the most severe cause of long-term failure of lung transplantation. The term CLAD encompasses a myriad of clinical features (summarized in Table 1) that cause a lung allograft not to achieve or maintain normal function over time. [Update on Chronic Lung Allograft Dysfunction [15,16].

Table1. Clinical features of the two BOS phenotypes

	RAS	**BOS**
Onset	Late, but can occur at any time. It represents around 30% of CLAD cases	Late, 2-3 years post-transplant, but can also occur early. 70% prevalence at 10 years post-transplantation
Pathophysiology	Restrictive (for example FEV1 ≤ 80% and TLC ≤ 90% of the basal value)	Obstructive (FEV1 ≤ 80% of best-FEV1)
HRCT Imaging	Presence of parenchymal infiltrates and diffuse alveolar damage (DAD). ± Bronchiectasis, ± air entrapment	Air trapping often present. Absent or minimal infiltrates. ± Bronchiectasis.
Histopathology	Fibrosis, thickening of the septa and pleura. DAD often present. ± OB.	Bronchiolitis Obliterans (OB) difficult to diagnose by transbronchial biopsy
Clinical course	Generally progressive. Prognosis significantly worse than BOS	Generally progressive but can stabilize. A consistent chronic bacterial infectious state may be present

The holy grail of current CLAD research is the identification of novel molecular markers for the different subtypes of CLAD, not only to recognize patients who could potentially develop CLAD, but also to use as prognostic markers after CLAD onset [17].

At the beginning CLAD was used to describe obliterative bronchiolitis (OB) but, more recently, it was proved that it is the histological hallmark of a more heterogeneous condition [18,19]. This condition includes the following two distinct phenotypes:

• Bronchiolitis Obliterans Syndrome (BOS)

• Restrictive Allograft Syndrome (RAS)

It has been estimated that the probability to develop CLAD five years after LTx is about 50%. This valuation is given by the sum of the probability to contract BOS (35%) and that of developing RAS (15%). The survival rate, after 10 years, is of 16% for RAS and 31% for BOS [18,19]. From a clinical point-of-view, CLAD is defined as an irreversible decline in the forced expiratory volume in one second (FEV1) often due to acute rejection [20].

RAS, which is also called restrictive CLAD or rCLAD, is characterized by restrictive chronic decline of FEV1 of at least 20% and a decline in total lung capacity (TLC) of at least 10% compared to post-operative baseline TLC. It can occur at any time after transplantation. The average survival time after the onset is of about 541 days and this makes RAS one of the most significant causes of death after the development of CLAD. From the histological analysis of the lung this phenotype shows alveolar damage, an extensive fibrosis in the alveolar interstice, visceral pleura and interlobular septa.

2. Bronchiolitis Obliterans Syndrome

According to the last report of the International Society for Heart and Lung Transplantation (ISHLT) registry, median survival after lung transplantation is 6.5 years [1].

BOS, the most common phenotype of chronic rejection, is characterized by a persistent and irreversible obstructive pulmonary function defect. It is a heterogeneous condition in which 5 stages with an increasing rate of severity, have been evidenced. The classification of this disorder is shown in Table 2.

Table 2. Different stages of BOS

Stage	FEV1 levels
0	FEV1 > 90% of baseline & FEF25-75% > 75% of baseline
0-p	FEV1 81-90% of baseline &/or FEF25-75% ≤ 75% of baseline
I	FEV1 66-80% of baseline
II	FEV1 51-65% of baseline
III	FEV1 ≤ 50% of baseline

As shown in the Table above, the classification is mainly based on changes in FEV1 i.e. the maximum post-transplant FEV1 of 100% predicted value (the mean of the two best post-operative FEV1 values with at least 3 weeks interval between the measurements) and the reduction in the mean Forced Expiratory Flow during the middle half of the forced vital capacity (FEF 25-75%). These are the parameters used as an early marker for BOS or potential BOS. It was also estimated that the average survival rate is from 3 to 5 years and it has

been proved that patients with an early (< 2 years post-transplant) or a high degree of onset (FEV1 decline >35%) have less survival compared to patients with late and low -grade onset [21].

BOS is a chronic obstructive disease: it can arise during the first year after transplantation and the developmental rate increases in the following years (Fig.1). A high percent (30-50%) of patients develops BOS three years after transplantation and after ten years this percent raises to 90% [22]. The pathology is histologically characterized by diffused obliterative bronchiolitis (OB) lesions, with a high level of myo-fibroblasts, but a relatively intact peripheral lung tissue [19].

As mentioned above, the histological hallmark of BOS is OB, an inflammatory/fibrotic process affecting bronchioles. It is characterized by sub-epithelial fibrosis which can lead to partial or complete luminal occlusion [23, 24].

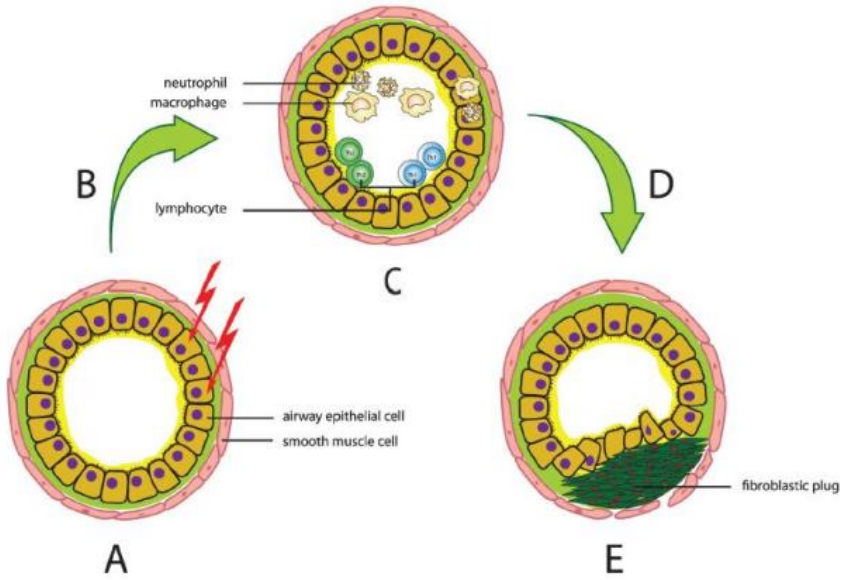

Figure 1. Schematic figure of chronic obstructive disease

2.1. Pathogenesis and risk factors

While being driven by alloimmune and non-alloimmune mechanisms, due to its complexity, the precise pathogenesis of BOS is still unclear [25, 27]. The current hypothesis predicts at first a lymphocytic infiltration in the sub-mucosa, followed by the epithelial damage which can cause a chronic inflammation that leads the epithelial to mesenchymal cell transition (EMT) mediated by fibroblasts [20]. This causes the formation of myo-fibroblasts and continues with the development of fibrosis and the complete obliteration of the airway lumen. The development of BOS can be summarized in the three steps (epithelial damage, cellular bronchiolitis, aberrant reparation) shown in the scheme of Figure 2 [18].

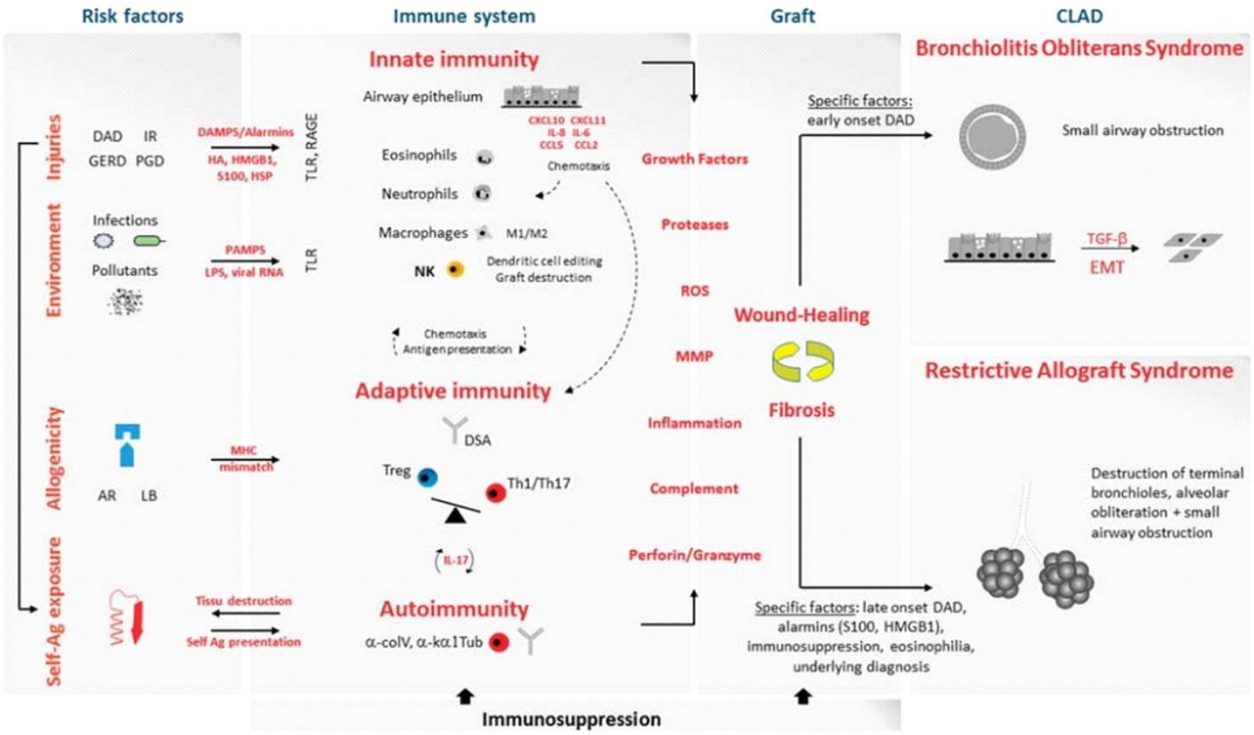

Figure 2. Biochemical steps which involve the development of BOS

Briefly, due to the constant exposition of lungs to external environment, pathogens and allergens, the *first step* that activates the innate immune response involves the Toll Like Receptors (TLR). TLR is a family of receptors (13 types) which are exposed by hematopoietic and parenchymal cells involved in pathogens recognition [24]. This leads to bronchiolar epithelial damage and consequent necrosis with mucosal ulceration. Pollution and genetic features of the donor and of the recipient can be the cause of several non-immunological risk factors such as viral infections, acute rejection or gastro-esophageal reflux. All these factors up-regulate dendritic cells in the epithelium mainly attracting lymphocytes followed by the epithelial damage with consequent stimulation of inflammation and ending with the production of chemo- and cytokines [17, 28].

In the *second step* of the mechanism, as a consequence of the epithelial damage worsening, dendritic cells can secrete cytokines which increase inflammation by activating other inflammatory cells such as lymphocytes, macrophages, neutrophils [18]. With the obliteration of the airway lumen the immune response becomes chronic. Among the produced cytokines, IL-17 and IL-8, involved in the activation of neutrophils (that is a characteristic of BOS), should be mentioned [13, 17]. IL-8 remains the most important factor involved in the neutrophil recruitment and activation after lung transplantation [29]. Neutrophils increase the epithelial damage through the production of mediators such as reactive oxygen species (ROS) and proteases such as elastase and metalloproteins [30]. Other cells involved in the pathology of BOS are: Th1, Th2, Th17 and Treg [31]. These cells work at the reparation of the epithelium for which a fragile balance

between effector type immune responses (type Th1, Th2, Th17) and regulatory type immune response (Treg) is required. The disruption of this balance may lead to fibro-obliteration of airways and consequent BOS.

Th17 mediates the production of cytokines IL-17 and IL-23 and is associated with autoimmunity; its job is to recruit neutrophils. The epithelial damage can also activate the auto immunity process with the production of antibodies which are formed after the exposure of antigens by damaged epithelium. These antibodies degrade lungs tissue through granzymes [18].

The *third step* is characterized by an aberrant reparation in which a fibro-proliferative phase occurs. This reaction is triggered by growth factors such as Platelet Derived Growth Factor (PDGF), Fibroblast Growth Factor (FGF), TGF beta and TNF alpha. All these factors increase the action of fibroblasts and myoblasts ending with fibrosis and collagen deposition which obliterates the lumen of small airway tissues [32].

The numerous factors which increase the probability to develop BOS are classified as alloimmune acute (acute rejection and HLA mismatch) and non-alloimmune factors (infections, gastroesophageal reflux and genetic features). Acute rejection represents the most common cause in BOS development. Although it can present with recurrent, severe or late episodes, all of them contribute to the injury. The severity of acute rejection is indicated as “A” and “B” grades. The grade “A” indicates the infiltration of perivascular inflammatory cells into the interstice and alveolar space. “B” grade, also known as lymphocytic bronchiolitis (LB), is characterized by peri-airway lymphocyte infiltration [33].

~~In humans, MHC molecules, also known as~~ Human leukocytes antigens (HLA), mediate the T cell response and have an important role in the defense against pathogens. While being well-known that allograft reject is caused by the cytotoxic effect of CD4+ and CD8+ T cells, it has also been proved to be associated with an increasing number of HLA mismatches between donor and recipient. Also, the production of HLA antibodies is involved in chronic rejection [7, 33].

The other group is composed by non-alloimmune dependent risk factors, such as chronic low-degree infections which can amplify inflammatory responses and increase the risk of BOS. Infection by cytomegalovirus (CMV) results in increased epithelial cell HLA I and II expression causing an up-regulation of pro-inflammatory cytokines and allergenic response. In addition to Epstein-Barr virus that can increase the risk of BOS onset [7, 23, 34], other examples are bacterial infections with *Chlamydia pneumoniae* and *Aspergillus* [31, 35]. It can be speculated that inflammation caused by all these infections induce a condition of chronic inflammation that leads to BOS.

A very common consequence of lung transplantation is Gastroesophageal (GE) reflux which may play a role in BOS pathogenesis as suggested by the presence of bile acids and pepsin in samples of bronchoalveolar lavage fluid (BALf) [36].

Despite the rapid advances in lung transplant surgery, the unknown pathogenesis of BOS and the inefficacy of treatment remain the Achilles’ Heel for long-term survival [37].

3. Role of proteases and protease inhibitors in lung homeostasis

Proteases are a group of enzymes able to hydrolyze peptide bonds. This feature makes their role essential in the control of multiple biological processes in all living organisms [38]. Indeed, proteases regulate the fate, localization, and activity of many proteins, modulate protein-protein interactions, create new bioactive molecules, contribute to cellular information, influence proliferation and differentiation, tissue morphogenesis, homeostasis, inflammation, immunity, cell death and can have pro- and anti-fibrotic activities.

Based on their specificity, they can be divided into the following four classes:

- serine proteases
- cysteine proteases
- aspartic acid proteases
- metallo proteases

In normal physiological conditions, proteases and their inhibitors (anti-proteases) are in tight balance, any alteration in proteolytic systems leading to different pathological conditions such as cancer, neurodegenerative disorders and inflammatory and cardiovascular diseases (Fig. 3) [39].

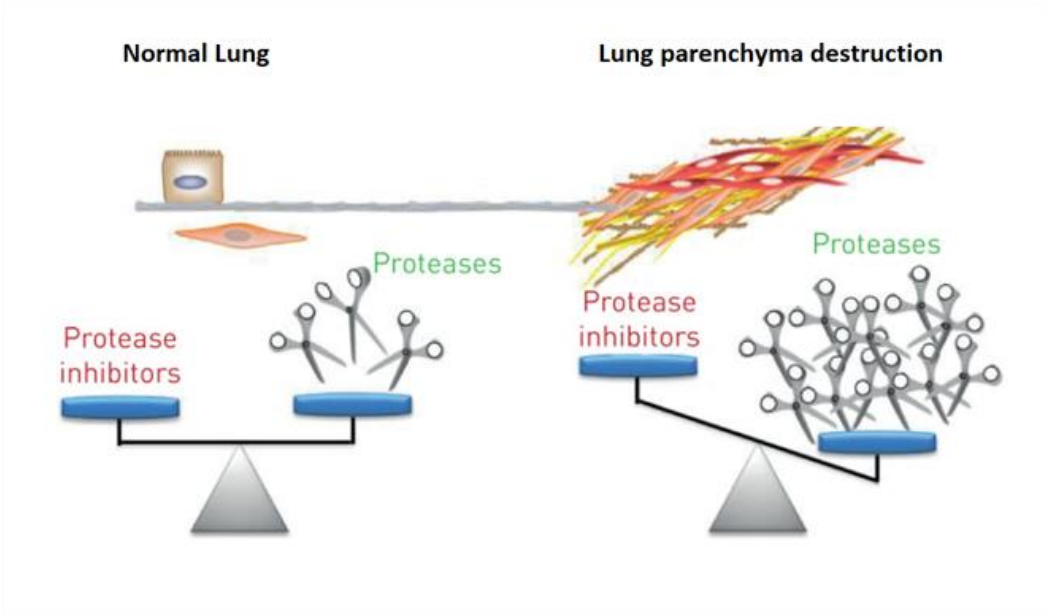

Figure 3. Lung protease and antiproteases balance

For example, the deficiency of anti-proteases and their decreased activity in chronic obstructive pulmonary diseases (COPD) contributes to the development of emphysema and mucus hypersecretion. This protease/anti-protease imbalance has been suggested to result from neutrophil infiltration in lung [40].

Mainly for this reason, the majority of research into the role of neutrophil serine proteases in the lung has been so far focused on human neutrophil elastase (HNE).

3.1. Serine-Proteases

Neutrophil elastase, proteinase 3 (PR3), and cathepsin G (Cat G) are the most important serine-proteases associated with lung damage [41]. They are coded by ELANE, PRTN3, CTSG genes respectively. All three are members of the chymotrypsin family and are expressed by neutrophils. [42]

As mentioned above, neutrophils play an important role during disease pathogenesis. They are able to carry out phagocytosis, release lytic enzymes and produce reactive oxygen intermediate (ROI) which have antimicrobial function [43-45]. Furthermore, a high number of these cells was evidenced by the analysis of BAL fluid samples from patients affected by CLAD [40]. Neutrophils secrete proteolytic enzymes which can, under appropriate conditions, cause tissue damage. This is the rationale for considering neutrophils an important marker of CLAD.

Serine proteases belong to the largest endo-proteases family and are characterized by the presence of a nucleophilic serine residue in the active site [46]. The serine target is the carboxyl moiety of the peptide with which it forms an acyl-enzyme intermediate [47]. The nucleophilic feature is given by the presence of a group of three amino acids (Asp-His-Ser) which, while being far in the primary structure, are close to each other in the tertiary one [48].

The secondary structure of proteases is usually characterized by the presence of two β-barrel domains, each of them composed of six antiparallel β-sheet connected through a linker segment and a C-terminal α helix [48-50]. Three catalytic residues are located at the junction of the two β-barrels and the active cleft is perpendicular to the junction [42] allowing Serine 195 to carry out the catalytic reaction. The structural conformation is shown in Figure 4.

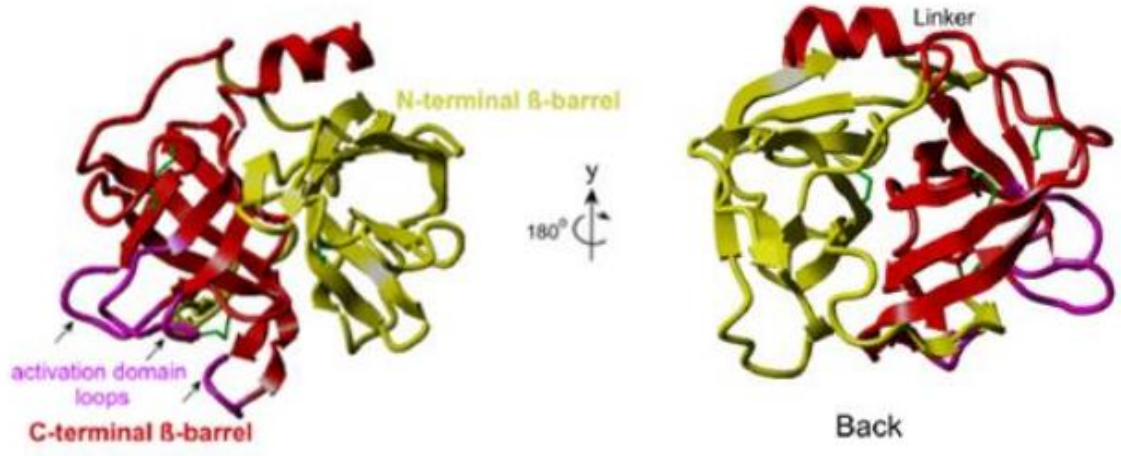

Figure 4. Protease's structure.

Proteases are present in all kingdoms and in viral genome too, although with different distribution.

Serine proteases may be classified in four types, two of which PA (chymotrypsin-like) and SB (subtilisin-like) are well-represented by chymotrypsin and subtilisin, respectively, while the other two SC (α/β-hydrolase fold) and SF (Signal peptidase I) contain several less specific peptidases. PA clan (about 75% of human serine proteases) is divided into three subfamilies based on their substrate specificity: trypsin-like proteases that usually cleave proteins after a positively charged residue (such as lysine and arginine); chymotrypsin-like that process their substrate after large hydro-phobic residues (leucine and alanine) and elastase-like serine proteases that group neutrophil elastase and proteinase 3. They usually cleave substrate after a valine residue [51].

While being involved in many fundamental processes such as digestion, coagulation and immune response [52] these enzymes can be a threat for the cells (Fig. 5). For this reason, many strategies have been developed during the evolution to control their activity.

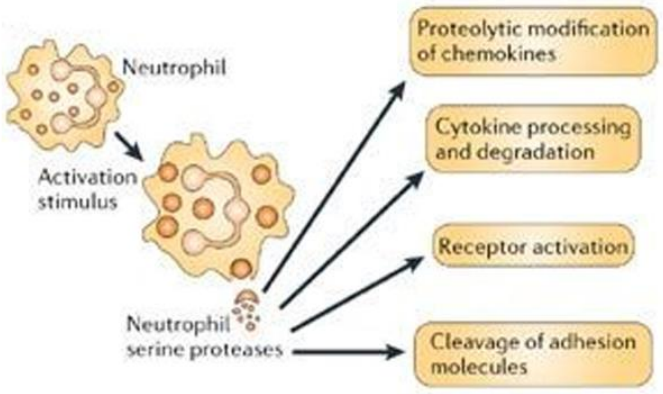

Figure 5. Neutrophil degranulation's

The first is the production of all proteases as inactive zymogens that are subsequently activated upon cleavage by other proteases. Often the localization of enzymes modulates their activity or they can be stored in granules bound to proteoglycans, avoiding the contact with their cytoplasmic targets. Furthermore, the low pH value inside granules maintains proteases less active. Another factor is the presence of serine proteases inhibitors, called serpins whose action is based on a suicide mechanism which traps proteases in an irreversible stable complex (Fig. 6A and Fig. 6B).

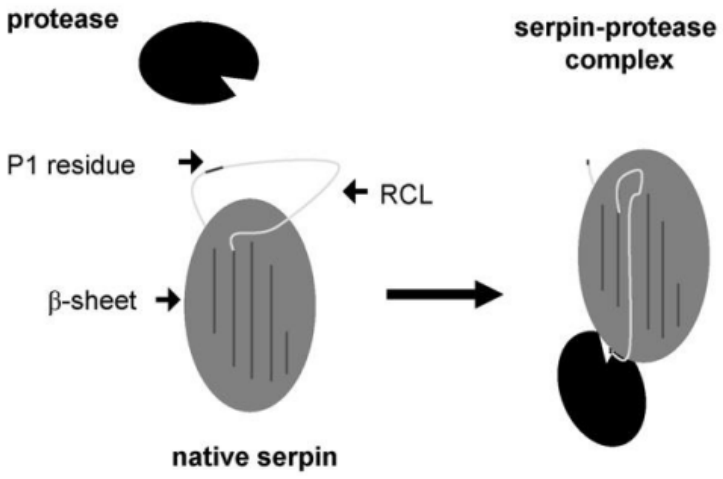

Figure 6B. Trapping mechanism

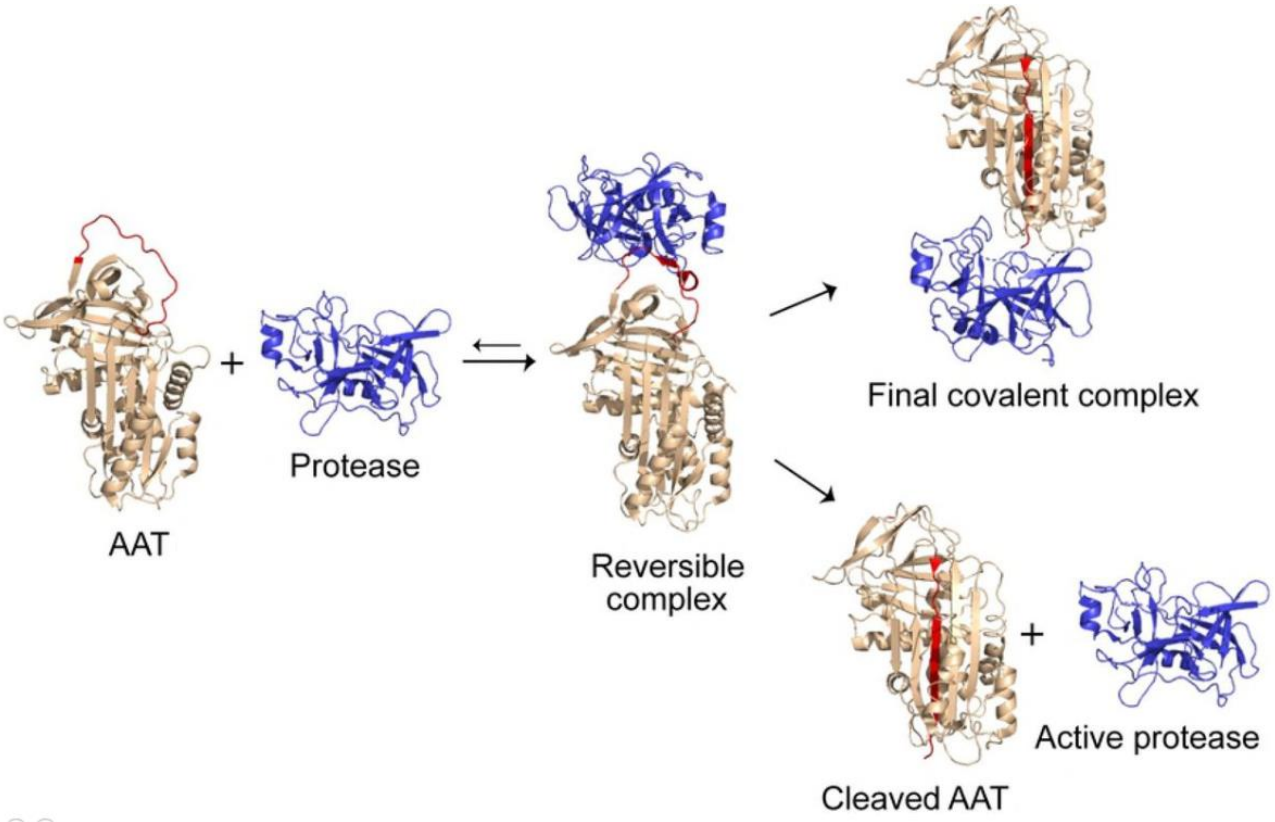

Figure 6B. Trapping mechanism of serine by serine protease inhibitor

The protease binds and cleaves the reactive center loop (RCL) of serpins, a homogeneous family of glycoproteins found especially in eukaryotes, but also in bacteria, archea and viruses. This bond causes a conformational change known as stressed-to-relaxed transition that closely links RLC into the serpin body [53-55].

Neutrophil elastase

Neutrophils are produced in the bone marrow from pluripotent stem cells and then released in the bloodstream where, in healthy people, they reach a concentration of 1.5 to 5 x 10^9 cells/liter.

Although in blood of healthy individuals neutrophils survive about eight hours, upon inflammation their longevity increases up to five days [56]. When inflammation bursts in peripheral tissues, they are soon recruited in that site. Neutrophils are composed by granules and, upon infection, they migrate through the blood stream and, rolling along the endothelium, they activate and move themselves in the interstice. In the activated state, intracellular granules fuse with cell membrane and, through degranulation, they release a variety of proteases.

Their targets are small hydrophobic residues such as Ala, Val, Ser or Cys and they are considered highly cationic proteases because of their important content of positively charged residues located in the activation domain loop [42]. One of the most important lytic enzymes studied in current research on proteases is neutrophil elastase [57]. Its release is triggered by inflammatory stimuli such as TNFα, G-CSF and C5a, being strongly increased by contact with ECM or cellular surfaces [44].

HNE is a 218 amino acids glycoprotein encoded by the ELANE (and PRTN3) gene located in the terminal region of short arm of chromosome 19. The coding genes have five exons and four introns [58, 59]. The protease binding site defines the substrate specificity of protease. For example, the pocket of HNE S1 is characterized by hemispheric and hydrophobic moieties, formed by the presence of Val190, Phe192 Ala213, Val216, Phe228, and of the disulfide bridge Cys191–Cys220 [60]. HNE acts intracellularly with antimicrobial peptides and the membrane-associated NADPH oxidase system which produces reactive oxygen metabolites to kill pathogens inside the phagolysosome [62].

The active enzymes are released in the extracellular space where they may meet inhibitors protease proteins which usually are in plasma and bind them, maintaining a balance between protease and its inhibitor.

The elastase level in the protease liberation site of healthy people overcomes that of antiproteases, but, farther away, this level decreases and elastase can be neutralized (Fig. 7) [62-64].

When elastase concentration is not correctly balanced by that of its inhibitor (Alpha 1 antitrypsin, AAT), many inflammatory diseases that compromise tissue integrity may develop. This is exactly what has been observed in a group of patients affected by COPD in which the excess of proteases results in a lung tissue damage [65].

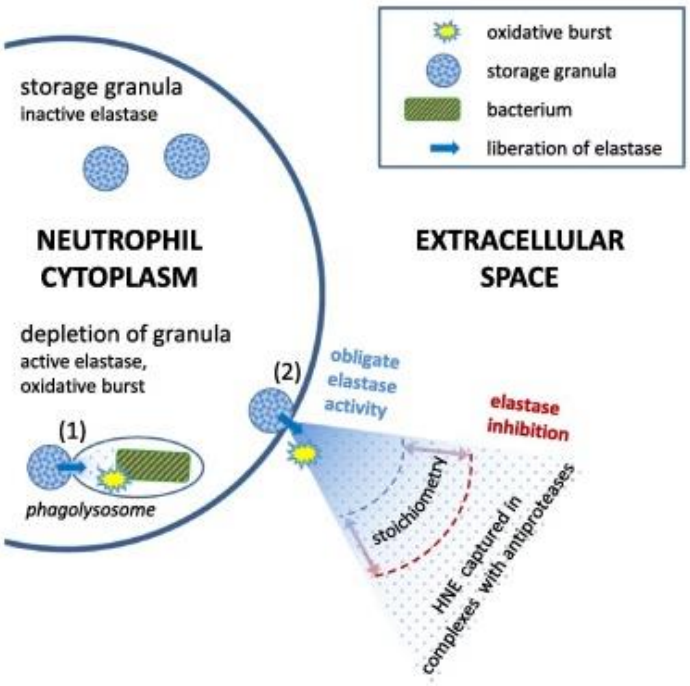

Figure 7. Schematic representation of the human neutrophil elastase (HNE) life cycle

3.2. Serine protease inhibitors (Serpins)

Cells have developed many strategies to neutralize protease's activity, a typical example being the production of inhibitors. The largest family of protease inhibitors is represented by Serpins (Serine Protease Inhibitor). More than 1000 types, classified by a distinctive three-dimensional (3D) structure, have been identified in the different kingdoms [66, 67]. They are divided in 16 groups, nine of which are characteristic of humans [54]. Serpin family is composed by homologous glycoproteins the first of which was described by Hunt in 1980 [68]. To allow proteolysis to occur only when it is necessary, their production in an organism is regulated. They are involved in many intracellular and extracellular processes, such as coagulation, apoptosis and cell migration [69-71].

Serpins are characterized by the presence of a homogeneous core domain composed of 350-500 amino acids although the total length can vary based on the glycosylation level and on N- and C-terminal extension [72]. In native conformation amino acids fold in an N-terminal helical domain and a β-barrel domain at the C-terminal (Fig. 8).

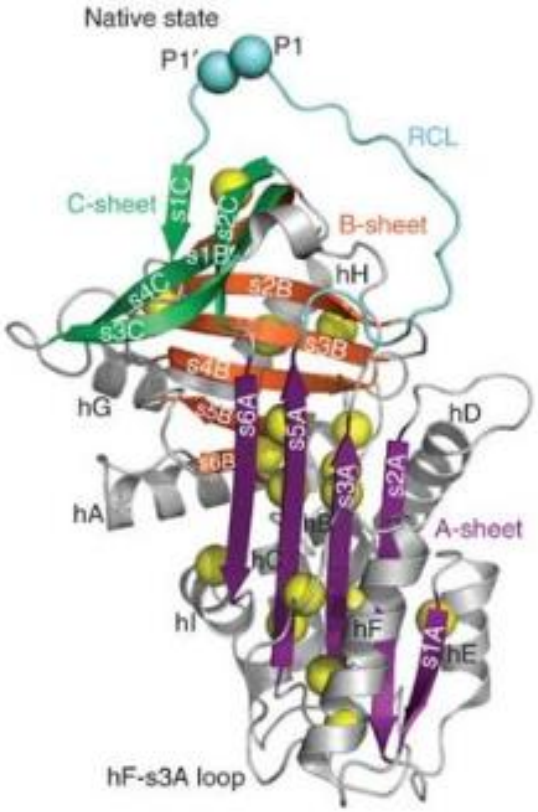

Figure 8. Serpin's structure

The conserved region is characterized by nine α helices (hA-hI), three β sheets (A, B, C) and a reactive center loop (RCL) which is fundamental to interact with the target active site cleft of protease. The RCL is flexible and composed by 20-24 residues with a sequence which is similar to that of the natural protease's target.
The most important residue in RCL defines the inhibitory specificity of the serpin and is indicated as P1. The surrounding residues (P4-P4') play an important role in protease's recognition by increasing the affinity of the interaction [53, 73, 74]. To increase their stability, serpins must incorporate RCL into the β sheet A, forming a metastable state where RCL acts as a bait for target proteases, followed by serpin cleavage between P1 and P1' residues [53, 72, 73]. Although the protease-anti protease linkage is not a key-and-lock mechanism, it allows to regulate serpins activity by modulating the RCL accessibility. This binding between protease and its inhibitor, also known as stressed-to-relaxed transition, increases serpin stability.
The protease binds its inhibitor through an ester bond formed between the catalytic Ser 195 of protease and the carbonyl group of P1 residue, forming the acyl enzyme intermediate. The protease catalytic loop results relaxed by the RCL which pulls serpin against its target and, thanks to this clash, the oxyanion hole is broken (Fig.9). The loss of protease affinity for Ca^{2+} suggests a disorder in the binding site [75]. In this conformation, protease is stably bound with its inhibitor although the complex can be broken by low density lipoprotein receptor related proteins. As shown by fluorescence studies [76] this determines a distortion in the final structure and a high level of disorder (compared to native conformation) that prevents the acyl intermediate hydrolysis [53, 72, 77].

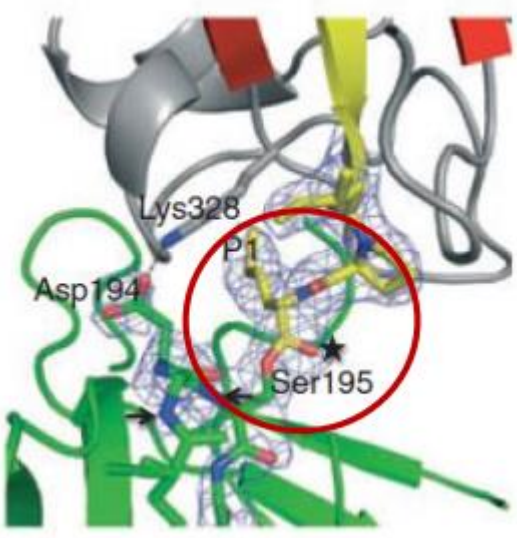

Figure 9. Covalent bond between protease's Ser195 and P1 Met. The narrows show that in normal condition there is the formation of an oxyanion hole and a salt bridge between Asp 194 of protease and Lys 328 of serpin

Alpha 1 antitrypsin (AAT)

As cited above, one of the major proteinase inhibitors is AAT, an acute phase protein that, while being mainly produced by hepatocytes, is also synthesized by monocytes, macrophages, lungs cells and some cancer cells. It circulates in blood stream with a molecular weight of 52 kDa and a half-life of 4-5 days [78]. Human body produces ~34 mg/kg/day of AAT and the plasma concentration of this protein is 1-2 g/L. Circulating levels can increase upon infection and inflammation [79].

Its natural substrate is the serine protease HNE, which binds to Met358-Ser359, and the interaction between these proteins is considered one of the strongest linkages known in biology, the association constant being 6.5×10^{7} M^{-1} s^{-1}.

Nevertheless, it is also able to neutralize cathepsin G, proteinase 3, myeloperoxidase and α-defensin produced by neutrophils, chymase and tryptase from mast cells, trypsin from pancreas, granzyme B from T-lymphocytes and the serine proteases of coagulation cascade. With more than 90% of activity, this makes AAT the most important anti-protease in human organisms.

Increasing evidence demonstrates that AAT, besides its well-known anti-protease properties, reduces production of pro-inflammatory cytokines, induces anti-inflammatory cytokines, and interferes with maturation of dendritic cells. As shown by the increased pulmonary levels of AAT upon lung infection, its action in lungs is fundamental because not only it modulates inflammation, but also protects tissues from pathogens [80, 81]. During acute response phase, the enzyme moves from plasma to interstitial tissues and it can reach biological fluids, such as alveolar fluid, saliva, tears, milk, bile, semen, urine and cerebrospinal fluid [82, 83]

Molecular structure

AAT is characterized by a conserved structure that contains three β sheets (A, B and C), nine α helices and the exposed active loop (Fig. 10). It is composed by 394 amino acids and 3 glycosylated side chains which are linked to 3 asparagine residues (Asn46, Asn83, Asn247). This post-transcriptional modification occurs in the endoplasmic reticulum (ER) and represents a sort of quality-control mechanism because only proteins which are correctly folded can leave the ER [84].

It was evidenced by crystallographic analysis that the enzyme has a globular structure, the active site being located on a surface protrusion which contains the reactive amino acid i.e. a Met in position 358. The conversion of this Met in Met sulfoxide (i.e. by oxidants from cigarette smoke) makes the protein less potent in its function [85].

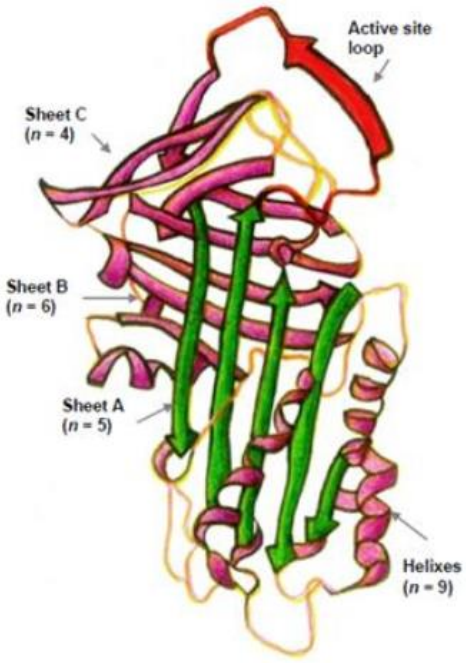

Figure 9. Alpha-1-antitrypsin structure.

Genetics information

SERPINA1, the alpha 1 antitrypsin coding gene, is located on the long arm of chromosome 14 (14q32.1). The gene is composed by four coding, three untranslated exons and six introns (Fig. 11). This gene has different starting sites and alternative splicing sites which may potentially produce various transcripts. For example, while the promoter in hepatocytes is located on exon C1, in monocytes it is located upstream exon 1B [84, 86, 87].

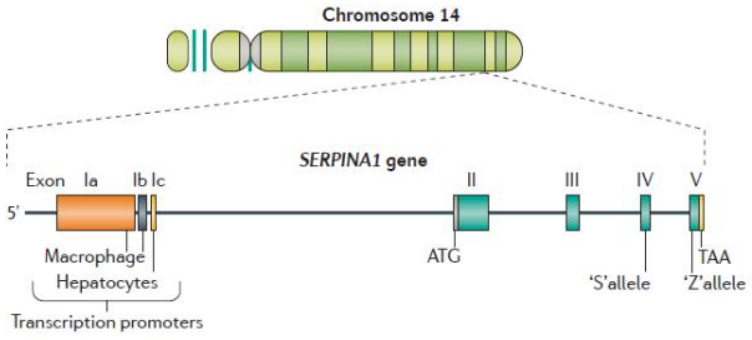

Figure 11. SERPINA 1 gene's structure

Basal expression in steady state is regulated by promoters, while other elements on DNA, known as enhancers, modulate the expression during inflammation. Upstream hepatocytes' starting site many regions

able to modulate basal expression, such as nuclear factor-1α (HNF-1α) binding site are evidenced. Humoral regulation is modulated by interleukins (IL-1, IL-6), β-interferon and oncostatin-M which work through a 3' enhancer located downstream promoter [84, 88]. In monocytes and other cell types, SERPINA1 gene is regulated by a different group of transcription factors, known as Sp1 family [89]. SERPINA1 is a highly polymorphic gene characterized by more than 150 mutations. Different alleles formed are involved in severe pathological conditions.

Each variant is classified based on its electrophoretic migration speed in a pH gradient, the two most common mutated alleles being S (slow) and Z (very slow) compared to the normal variant M.

Based on their effect, variants are divided in four classes: normal, functional, deficient and null which reflect a mutated level of the protein in the blood stream.

The extraordinary impact of serpins on multiple molecular regulatory pathways is evident in genetic abnormalities wherein regulation of normal functions by serpins is lost. In the genetic serpinopathies, genetic mutations can cause either loss of function or pathologic aggregates leading to loss of local function.

The most frequent and severe is the Z variant which is caused by a mutation on exon 5 leading to a substitution of glutamic acid at position 342 for a lysine. Other point mutations (i.e. Glu264Val) have been described in the literature [90].

The null variants, also known as Q0, cause the detection of very low levels of AAT in the blood due to the presence of a truncated protein. The most important variant, characterized by a severe deletion involving an important portion of the gene, is called *Q0 Isola di Procida*. Another important variant is *Q0 granite falls* which presents a frame shift mutation that causes abnormalities in mRNA splicing. The protein is totally absent in serum of patients characterized by this genotype who, usually, develop emphysema [91]. The absence of protein can be explained by two mechanisms, i.e. its intracellular degradation, like in M *heerlevariant*, or intracellular accumulation as in the case of *M malton* variant [92].

Although protein has a low affinity in binding its target, functional variants present a normal protein concentration in the blood stream. An example is the *Pittsburg variant* which binds thrombin instead of proteases [82]. This condition can lead to the protein misfolding and polymerization with a consequent accumulation in the endoplasmic reticulum of hepatocytes. This process increases the probability that these people develop a chronic liver disease.

Alpha 1 antitrypsin deficiency (AATD)

Alpha 1 antitrypsin deficiency was first reported in 1963 by Laurell and Eriksson who noted a link between low serum level of this protein and symptoms of pulmonary emphysema [93]. It is a pathological condition, inherited in an autosomal codominant manner, characterized by low circulating levels of this protein. Its clinical features are pulmonary emphysema, liver cirrhosis and, less frequently, skin disease panniculitis.

As mentioned before, the most severe among the high number of pathologic mutations of this protein, is the Z variant. Patients with this variant accumulate AAT in endoplasmic reticulum of hepatocytes increasing cells stress level, mitochondrial dysfunction and autophagy that lead to chronic liver disease. ER stress is caused by an accumulation in this organelle of unfolded proteins where they are eliminated by two possible mechanisms: autophagy or ER-associated protein degradation machinery (ERAD).

As demonstrated by Stockley and colleagues [94], alpha 1 antitrypsin level correlates with lung pathology, the lack of this antiprotease activity being associated with premature development of pulmonary emphysema. The lung damage is probably associated to cigarette smoke that, as mentioned before, is able to oxidize the active methionine reducing the functioning protein's level. This increases the number of neutrophils and consequently of serine proteases in the airway epithelium (Fig.12).

These data lead to the conclusion that the balance between protease and inhibitors is crucial for a correct homeostasis [93].

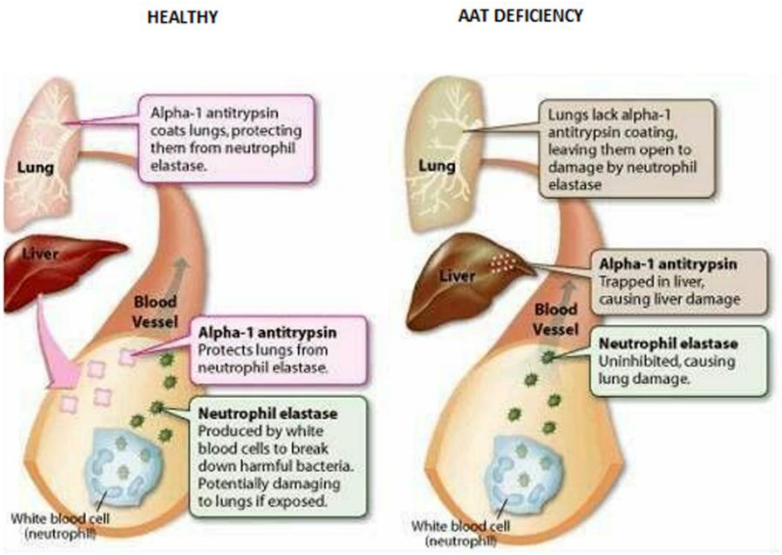

Figure 12. SERPINA 1 gene's structure

AIM

AIM

Early and long-term graft and patient survival after lung transplantation continue to be challenged by primary graft dysfunction and by chronic allograft dysfunction or bronchiolitis obliterans syndrome (BOS). While the neutrophilic component is known to play an important role in the pathogenesis and maintenance of this condition, the exact pathogenesis of BOS is still unknown. It has been speculated that it may result from the combination of several triggers which, by causing innate/adaptive immune reactions, lead to immune activation responsible for the induction of the neutrophilic inflammation. This inflammatory phase is ultimately followed by a fibro-proliferative phase of fibrocytes/fibroblasts originating from mesenchymal stromal cells.

The current research aimed at the identification of potential biomarkers of BOS that could be useful not only for a better diagnosis of the disease but also for the development of novel drugs that can improve the quality of life of patients. The identification of markers that could predict the development and progression of BOS is crucial for preventing the irreversible phase of the disorder with the final goal of improving the survival of lung transplant recipients.

My presentation has been divided into four chapters as follows:

Chapter 1: Proteomics

The application of the MudPIT technology and of bioinformatics tools described, allowed me to identify a number of proteins differentially expressed in ~~a~~ pool of Stable (n= 10), BOS0p (n= 10), BOSI (n= 10) and BOSII/III (n= 6) individuals.

A few, from among these proteins, evidence that oxidative stress and inflammation play an important role in the progression of the disorder.

Chapter 2: Metabolomics

This approach was applied “in parallel” with the proteomic analysis to the same samples described in previous chapter. Aim of this investigation was to characterize the level of metabolites in BALf from stable and BOS patients (BOS0p and BOSI; BOSII/III have not been considered). The results of this approach confirmed that the release of ROS species by neutrophils and macrophages during inflammatory states could play a role in lung injury with the consequent increase of mucus secretion and development of BOS.

Chapter 3: Proteases and Anti-Proteases study

Given the importance of neutrophilic components in BOS pathogenesis, this pilot work aimed to obtain a global picture of the protease/antiprotease balance in the BALf of 7 stable and 6 BOSII/III lung transplant

recipients. Proteases are secreted by neutrophils whose recruitment may enhance their concentration thus causing an unbalance in the equilibrium between proteases (HNE) and protease inhibitors (AAT). To understand whether AAT and other anti-proteases still maintain their full capacity to inhibit elastase, electrophoretic and western blotting profiles of samples from these individuals have been analyzed and compared.

Chapter 4: Current Studies

Current researches should focus on the development of a specific and sensitive assay to detect a HNE-specific fibrinogen degradation product (Aα-Val360) and on AAT augmentation therapy.

DEMOGRAPHIC AND CLINICAL FEATURES OF PATIENTS

● **Patients analyzed**

In this work a group of 36 patients from Pneumology ward of Fondazione IRCCS Policlinico San Matteo, Pavia, Italy, was analysed. Based on their clinical features they were classified as stable (S, n=10), potential BOS (BOS 0p, n=10), BOS I (BOS I, n=10), BOS II and BOS III (BOS II + III, n=6). From a clinical point-of-view, stable were individuals that, at >2 years post-transplant, came up with still stable lung function, in the total absence of acute rejection or infection. BOS diagnosis and severity grades have been assessed according to published guidelines [95, 96]. The current classification of BOS severity is based on FEV1changes ~~in~~ and is indicated as BOS 0p if FEV1 is 81−90% of the best FEV1 value obtained after transplantation; BOS I when FEV1 is 66−80% of the best value; BOS II when FEV1 is 51−65% of the best and BOS III if FEV1 is ≤50%.

All patients were Caucasian nonsmokers, the female/male ratio was 4:1 and their median age was 51 years (range 45-73 years). BALf samples were collected between 2014 and 2015.

All subjects underwent clinical analysis to exclude a possible genetic alpha 1 antitrypsin deficit and none of them resulted positive for this condition before transplantation. Furthermore, patients which showed any kind of infection were excluded from this project.

All of them signed an informed consent to undergo bronchoscopy.

The experimental procedures to which these patients have been submitted are summarized in Table 3.

Table 3: Number of patients investigated and experimental procedures applied.

Experimental Approaches	**Stable (n=10)**	**BOS 0p (n=10)**	**BOS** I **(n=10)**	**BOS** II **+BOS** III **(n=6)**
Gel-based techniques (Cap.1)	4	3	-	6
Gel-free techniques (Cap.1)	10	10	10	6
NMR Analysis (Cap.2)	10	10	10	-
1-DE Analysis (Cap.3)	4	3	-	6

● **Clinical treatment of patients**

After transplantation, an immunosuppression protocol (IS) must necessarily be applied. However, over the years, some changes have occurred to front pathologies correlated with a long-term therapy. In fact, while until 2007 the administered drugs were Ciclosporin A, Azathioprine and Prednisone, currently drugs designed are Tacrolimus, Mycophelonate and Prednisone. This therapy was often modulated during the years because of many side effects, such as kidney failure [95].

Selected subjects underwent a program of surveillance and on-need bronchoscopy at 1; 3; 6; 12; 24 months and upon clinical needs, such as a decline in lung function and at diagnosis of chronic lung rejection. Biopsy-proven episodes of acute rejection (AR) were treated with steroid boluses and, in case of AR recurrence or persistence, with a standard anti-thymoglobulin course and a modulation of the IS regimen.

BOS diagnosis and severity were based on recent guidelines [97, 98] and BOS 0p patients were treated for 3 months with a low dose of azithromycin, a treatment that was demonstrated to decrease airway neutrophils and IL-8 and increase FEV_1 in BOS-affected people [98].

All patients underwent analysis to exclude gastroesophageal reflux. In affected subjects, a massive anti-reflux therapy was carried out.

Since 2003, when lungs failure associated with CLAD diagnosis occurred, patients were referred to the Apheresis Unit for compassionate ECP treatment [99]. Also the cytomegalovirus surveillance protocol was detailed elsewhere [100].

All patients gave their informed consent to BAL collection.

BAL FLUID COLLECTION AND PROCESSING

Bronchoalveolar lavage (BAL) is a procedure in which a bronchoscope is passed through the mouth or nose into the lungs and fluid is flushed into a small part of the lung and then recollected for examination. BAL is the most common manner to sample the components of the epithelial lining fluid and to determine the protein composition of the pulmonary airways.

BAL lavage fluid samples were obtained from patients during fiberoptic bronchoscopy performed for routine to monitor organ rejection. Briefly, the distal tip of the bronchoscope was wedged into the middle lobe or lingular bronchus; a total of 150 ml of warm sterile saline solution was instilled in five subsequent 30 ml aliquots which were sequentially retrieved by gentle aspiration. The first aliquot collected (20 ml) was used for a series of analysis including microscopic and cultural examination of common bacteria and fungi and direct/cultural investigations for respiratory viruses. The returned fluid from the second to the fifth aliquots was pooled and further processed as the BALf. Cells were recovered by centrifugation at 1,500 rpm for 10 min and supernatant divided in aliquots (30 ml each) which were stored immediately after processing at -80°C until use.

CHAPTER 1

Proteomics

MATERIAL AND METHODS

● **Two-dimensional electrophoresis (2-DE)**

Two-dimensional electrophoresis separates proteins based on their isoelectric point (first dimension) and molecular weight (second dimension).

After precipitation with TCA, BALf proteins (200 μg) were dissolved in 125 μl of rehydration buffer and loaded on a non- linear immobilized pH gradient (pH 3-10, 7 cm IPG) strips. The 2-DE protocol is described in Table 4.

Table 4: 2-DE protocol.

Time	Voltage Applied	Temperature
1h	0 V (rehydration)	20 °C
8h	30 V	16 °C
1h	120 V	16 °C
30 min	300 V	16 °C
3h	From 330 V to 3500 V (linear ramping)	16 °C
10 min	500 V	16 °C
Overnight (>7h)	Constant 7950 V (to reach a total of 62 KV/h)	16 °C

Six hours after the start, Isoelectrofocusing (IEF) run was stopped, pieces of paper were positioned between IGP strip and the electrodes and IEF restarted [101].

Reduction/alkylation steps were applied between the first and the second dimension. The focused IPG strips were incubated for 15 min at room temperature in 6 M urea, 2% w/v dithiothreitol (DTE) and for 15 min in an equilibration buffer containing 2,5% w/v iodoacetamide (IAA).

The second dimension was carried out on 12% SDS-polyacrylamide gels at a constant current of 10 mA per strip.

At the end of the electrophoretic run, gels were left in a fixative solution, containing methanol (40%) and acetic acid (7%), for 1 h and then were stained with ‘‘Blue silver’’ (colloidal Coomassie G-250 staining), according to Candiano et al [102].

● **In-situ digestion**

Briefly, the selected electrophoretic spots were carefully excised from the gel, placed into Eppendorf tubes, broken into small pieces and washed in 100 mM ammonium bicarbonate buffer pH 7.8 and 50% acetonitrile (ACN) until complete destaining. The gels were then dehydrated by addition of 200 µl ACN until the pieces became opaque-white color. ACN was finally removed, gel pieces were dried under vacuum for 10 min and then rehydrated by addition of 75 µL of 100 mM ammonium bicarbonate buffer pH 7.8, containing 20 ng/µl sequencing grade trypsin (Promega, Madison,WI, USA). The digestion was performed by incubating the mixture overnight at 37°C and the resultant peptides were extracted from gel matrix by a three-step treatment with 50 µl of 50% ACN, 5% trifluoroacetic acid (TFA) in water and finally with 100% ACN [103]. Each extraction involved 10 min of stirring followed by centrifugation and removal of the supernatant. The first supernatant and those obtained from extraction were pooled, dried and stored at -80°C until mass spectrometric analysis. At the moment of use, the peptide mixture was solubilized in 0,1% formic acid (FA).

● **LC-MS/MS**

The analyses were performed on a liquid chromatography-mass spectrometry (LC-MS, Thermo Finnigan, San Jose, CA, USA) system consisting in a thermostated column, a Surveyor auto sampler controlled at 25°C, a quaternary gradient Surveyor MS pump equipped with a diode array (DA) detector, and a Linear Trap Quadrupole (LTQ) mass spectrometer with electrospray ionization (EI) ion source controlled by Xalibur software 1.4. Analytes were separated by reverse-phase high performance liquid chromatography (RP-HPLC) on a Jupiter (Phenomenex, Torrance, CA, USA) C_{18} column (150 x 2 mm, 4 µm, 90 Å particle size) using a linear gradient (2-60% solvent B in 60 min) in which solvent A consisted of 0,1% aqueous FA and solvent B of ACN containing 0,1% FA. Flow rate was 0.2 ml/min. Mass spectra were generated in positive ion mode under constant instrumental conditions: source voltage 5.0 kV, capillary voltage 46 v, sheath gas flow 40 (arbitrary units), auxiliary gas flow 10 (arbitrary units), sweep gas flow 1 (arbitrary units), capillary temperature 200°C, tube lens voltage -105 V. MS/MS spectra, obtained by CID studies in the linear ion trap, were performed with an isolation width of 3 Th *m/z*, the activation amplitude was 35% of ejection RF amplitude that corresponds to 1.58 V. Data processing was performed using Peaks studio 4.5 software.

● **Protein detection**

The 2-DE gels were stained with “Blue silver” (colloidal Coomassie G-250 staining) [102]. This staining method has a sensitivity of 5-10 ng per spot and is compatible with mass spectrometry detection.

In the first step, proteins were fixed in the gel by treatment with 40% methanol and 7% acetic acid for 1 h. Then, gels were incubated overnight in the staining solution (10% ortophosphoric acid, 10% ammonium sulfate, 20% methanol and 0,12% Coomassie Brilliant Blue G-250). Gels were initially bleached with 5% acetic acid and then with water until a transparent background was obtained.

● **Reproducibility of the study**

To verify the reproducibility of the study, 2-DE maps were obtained in triplicate for each of the analyzed pool (see Table 3). Those presented in this report are the best representative gels among all generated that showed spots consistently present. Experimental steps concerning sample preparation, electrophoretic run and gel staining were performed "in parallel" on both pools.

● **PD- quest analysis**

Digital image of stained gels was acquired using the VersaDoc Imaging Model 3000 (Bio Rad) equipment and then subjected to qualitative and quantitative analysis using the PD-Quest version 8.0.1 software (Bio Rad). Thanks to the advanced algorithm of the software, the scanned images were filtered and smoothed to remove background noise, vertical or horizontal streaking and gel artefacts. They were also normalized to eliminate the variability of each sample. The software then determined the number of spots present and calculated their intensity by applying the following algorithm: peak value (ODs/image units) *σx*σy (standard deviations in x and y). The following step was the creation of a "Match Set" necessary to compare all the gels of a single group and to match the spots present. A synthetic image (called Master Gel) containing the information about all the spots of Match Set was created. The Master Gels of every group were finally compared each other through a Higher Master Set to create a Higher Master Gel (HGM) that contained all information about the whole analysis.

● **2DC-MS/MS ANALYSIS**

Two-dimensional chromatography coupled to tandem mass spectrometry (2DC-MS/MS) was applied for the analysis of the whole BALf proteome. In Multidimensional Protein Identification Technology (MudPIT), BALf peptide mixture (5 µg from each pool) was loaded onto a strong cation exchange column (PolyLC-SCX column 0.3 i.d. x 100 mm, 5µm, 300 Å, PolyLC), eluted stepwise with salt solutions of increasing molarity (10, 20, 40, 80, 120, 200, 400, 600, 700 mM) and captured onto peptide traps for concentration and desalting prior to final separation by reverse phase C_{18} column (Biobasic-C_{18}, 0.18 i.d. x 100 mm, 5µm, 300 Å, Thermo Fischer). The peptides, gradually eluting from the C_{18} column (3 min of column conditioning followed by a 65 min gradient of 5-95% CH_3CN/0.1% HCOOH, flow rate of 130 µL/min), were analyzed by a mass spectrometer equipped with a NSI-ESI ion source and LTQ-Orbitrap XL mass analyzer (Thermo Fisher Scientific). The spray capillary voltage was set at 2.4 kV and the ion transfer capillary temperature was held at 220°C. For each step of peptides eluted from the C_{18} column, full MS spectra were recorded over a 400–1600 *m/z* range in positive ion mode, followed by five MS/MS events sequentially generated in a data-dependent manner on the Top 5 ions selected from the full MS spectrum (at 35% collision energy), using dynamic exclusion of 0.5 min for

MS/MS analysis. System MudPIT management was performed by Xcalibur data system v.1.4 (Thermo Fisher Scientific, San Josè, CA, USA).

● **Data Analysis**

All data generated by MudPit were searched using the 3.3.1 Bioworks version, based on SEQUEST algorithm (Thermo Fisher Scientific, San Jose, CA, USA). The experimental MS/MS spectra were correlated to tryptic peptide sequences by comparison with the theoretical mass spectra obtained by *in silico* digestion of the human protein database (about 228763 entries), downloaded in January 2013 from the National Centre for Biotechnology Information (NCBI) website. To allow identification of peptide sequences and related proteins the following criteria were applied: trypsin as enzyme; three missed cleavages *per* peptide were allowed; mass tolerances of 50 ppm for precursor ions (threshold) and 0.8 Da for fragment ions were used. Validation based on separate target and decoy searches and subsequent calculation of classical score-based false discovery rates (FDR) were used for assessing the statistical significance of the identifications (FDR ≤ 1%). Finally, to assign a final score to proteins, the SEQUEST output data were filtered as follows: 1,5; 2.0; 2.25 and 2.5 were chosen as minimum values of correlation score (Xcorr) for single-; double-; triple- and quadruple -charged ions, respectively. A total of 7 protein lists for each sample was obtained by averaging of the technical replicates.

To improve the identification of differentially expressed proteins, two different approaches have been used: Linear Discriminant Analysis (LDA) and DAve and DCI indices inserted in MAProMa software [104].

● **Linear Discriminant Analysis (LDA)**

Protein lists obtained by MudPIT replicate analyses have been aligned by Multidimensional Algorithm Protein Map (MAProMa), normalized through the Total Signal normalization methods [105] and processed by Linear Discriminant Analysis [106], to perform a reduction of data dimensions. LDA has been applied using a common covariance matrix and the protein selection was performed considering F ratio≥ 4 and p-value ≤ 0.05.

● **DAve - DCI INDICES**

Protein lists obtained by MudPIT replicate analyses were aligned and, for each protein, the average spectral count (aSpC) corresponding to each analyzed condition (Stable and BOS) was calculated. Based on a direct correlation between the SpC (or SEQUEST-based score) and the relative abundance of the identified proteins [107], the four subgroups were pairwise compared by Differential Average (Dave) and Differential Confidence Index (DCI) indexes of the homemade MAProMa software [107].

In particular, DAve, which evaluates changes in protein expression, is defined as (X-Y)/(X+Y)/0.5, while DCI, that evaluates the absolute of differential expression, is defined as (X+Y)*(X-Y)/2, where the X and Y terms

represent the SpC of a given protein in two compared samples. To select differentially expressed proteins, a threshold of 0.4 and 50 was applied to DAve and DCI, respectively.

RESULTS

The goals of the present study were the following:

- obtaining the proteomic profile of BALf from BOS patients
- identifying the proteins differentially expressed between cohorts

As shown in the scheme of Figure 12, a typical protocol for proteome analysis usually follows these essential steps: sample preparation, cleavage of proteins, separation of peptides followed by mass spectrometry analysis and database searching.

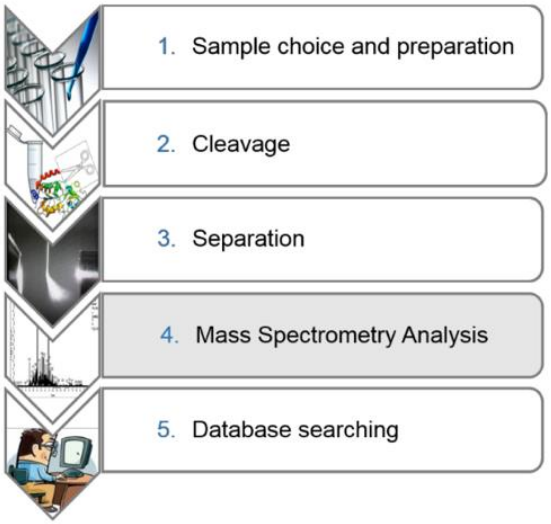

Figure 12. Proteomics Workflow. The scheme shows the typical protocol for proteome analysis.
Both in-gel and gel-free techniques have been applied to perform the proteomic studies described in this work.

● **GEL BASED TECHNIQUE**: **Two-dimensional electrophoresis with nonlinear pH 3-10 gradient range**

To identify proteins differentially expressed in BALf of stable and BOS subjects, 2-DE analyses were performed "in parallel" on pooled (four Stable + three BOS0p patients and six BOSII+III patients) samples. Gels were scanned and spots were detected using the spot detection wizard tool, after defining and saving a set of detection parameters. The original gel scans were filtered and smoothed to clarify spots, remove vertical and horizontal streaks, and remove speckles. Three dimensional Gaussian spots were then created from filtered images. Three images were created from the process: the original raw 2-D scan, the filtered image and the Gaussian image. A match set for each pool was then created for comparison after the gel image had been aligned and automatically overlaid. If a spot was saturated, irregularly shaped, or otherwise of poor quality, then the Gaussian model was unable to accurately determine the quantity. In these cases, the spot was defined in the filtered image using the spot boundary tools. Thus, for each pool, a master gel was produced which included protein spots only if present at least in two out of the three gels. The master gel from pools showed similar patterns of proteins such that they could be matched each other. This facilitated the correlation of the gels and the creation of a virtual image, indicated as high master gel (HMG), comprehensive of all matched spots derived from master gels. The HMG produced by PD-Quest analysis confirmed the presence of differentially expressed proteins in BALf of these individuals. Spots indicated in red in Figure 13 were unique to stable individuals; spots in blue were unique for BOS patients and spots in green were common to both cohorts. The differences evidenced in the proteomic profiles of these individuals support the view that the lung status is different between the cohorts. A few differential spots were excised, destained, digested with trypsin, and peptides were submitted to LC-MS/MS. The MS fragmentation data were searched against the SwissProt studio 4.5 software. Unfortunately, the poor quality of MS spectra (most likely due to the small amount of the material) did not allow to identify/characterize the proteins that could discriminate the two cohorts investigated.

.

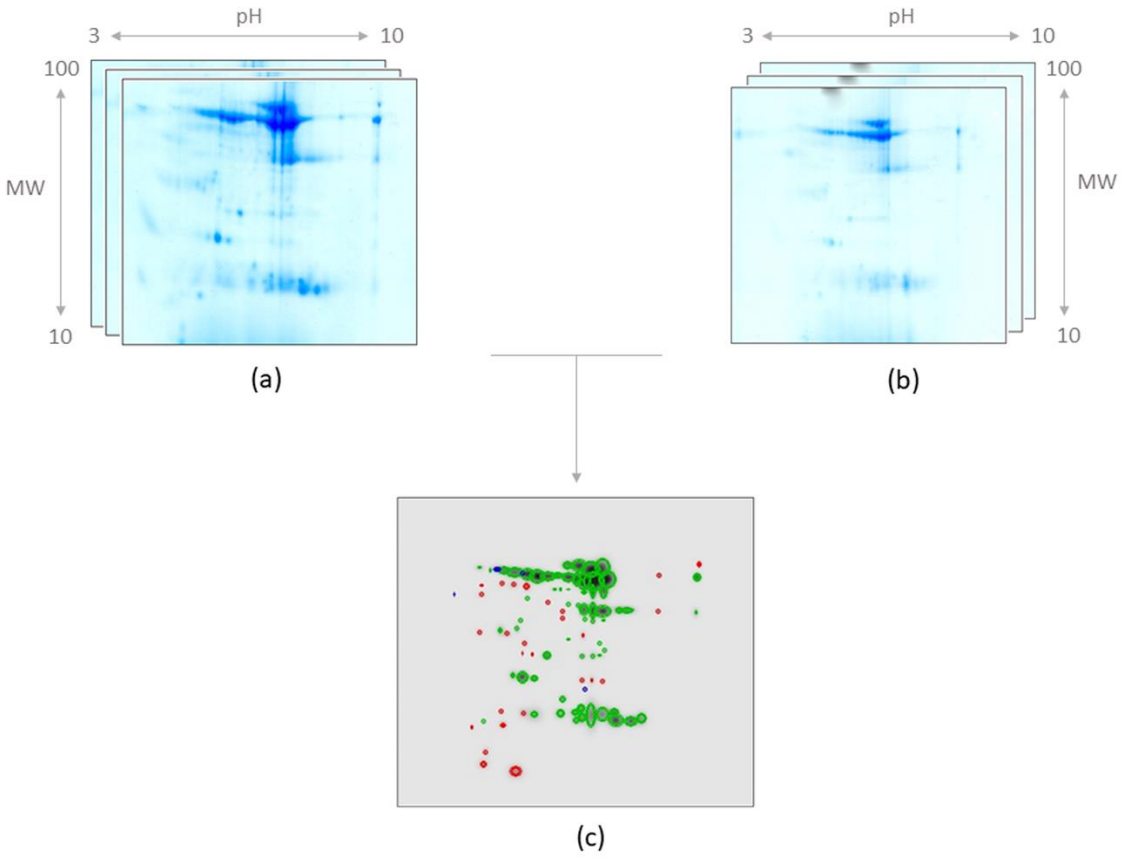

Figure 13. Two-dimensional gel Electrophoresis of pool from BALf samples. 2DE maps obtained by performing IEF on 7 cm IPG strips with 3-10 NL pH range and SDS-PAGE in the second dimension on 12.5% T gels (a) 2DE of pool from stable patients; (b) 2DE of pool from BOS patients; (c) High Master Gel of BALf samples: Labelled in green: common spots between the two groups; Labelled in red/blue: unique spots of stable (red) and BOS (blue)

Thus, to collect information on these proteins, a gel-free approach referred to as Multidimensional Protein Identification Technology (MudPIT), characterized by resolution and sensitivity higher than 2-DE, was explored.

The MudPIT experiments have been carried out in the laboratories of the National Council Research (CNR) of Milan, where this sophisticated two-dimensional liquid-chromatographic system is available.

● **GEL-FREE TECHNIQUE: Multidimensional Protein Identification Technology (MudPIT).**

Multidimensional Protein Identification Technology (MudPIT) is based on the use of two-dimensional chromatography coupled to tandem mass spectrometry (2DLC-MS/MS) (Fig.14). Briefly, following enzymatic digestion of a protein mixture, peptides are separated by a liquid chromatographic system consisting of a strong cation exchange (SCX) process as the first dimension followed by a reverse-phase (RP) process as the second. Peptides are then automatically delivered to a tandem mass spectrometer and MS/MS spectra are acquired and used to query protein sequence databases. MudPIT represents a technology that simultaneously allows separation of peptides, their sequencing and the identification of the corresponding proteins. By this way, mixtures of proteins within a wide isoelectric point (pI) and molecular weight (MW) range can be quantitatively characterized.

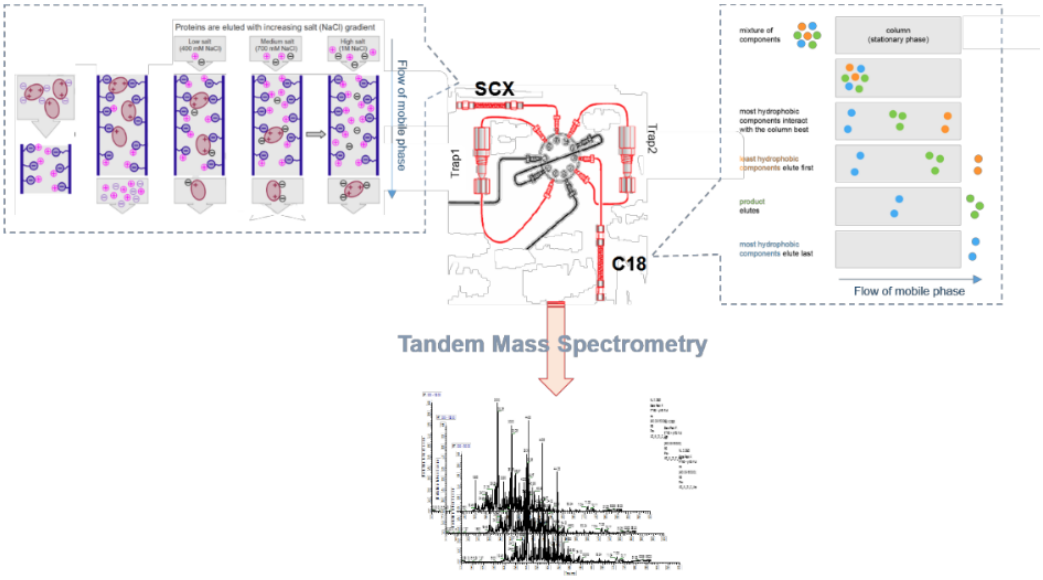

Figure 14. Multi-dimensional protein identification technology (MudPIT). MudPIT combines ion-exchange with reversed-phase chromatography of peptide mixtures obtained from direct digestion of a protein extracts. Peptides are first loaded onto a strong cation exchange (SCX) column and then separated using different steps of increasing salt concentration. After this, the peptides are captured onto C_{18}-traps (Trap1 and Trap2) and subsequently loaded into reverse phase C_{18} column. The peptides are eluted from hydrophobic column by means of acetonitrile gradient and the eluate is analyzed by high-resolution mass spectrometer (2DC-MS/MS).

The above-mentioned approach applied to the BALf samples (ten Stable, ten BOS0p, ten BOS1 and six BOSII+III patients) allowed to identify 10253 unique peptides and 3519 distinct proteins. All identified proteins were plotted according to their theoretical molecular weight (MW) and isoelectric point (pI). As

shown in the dendrogram (Fig. 15), a rapid visualization of the proteins that change upon comparison of two or more conditions, are evident in terms of color changes.

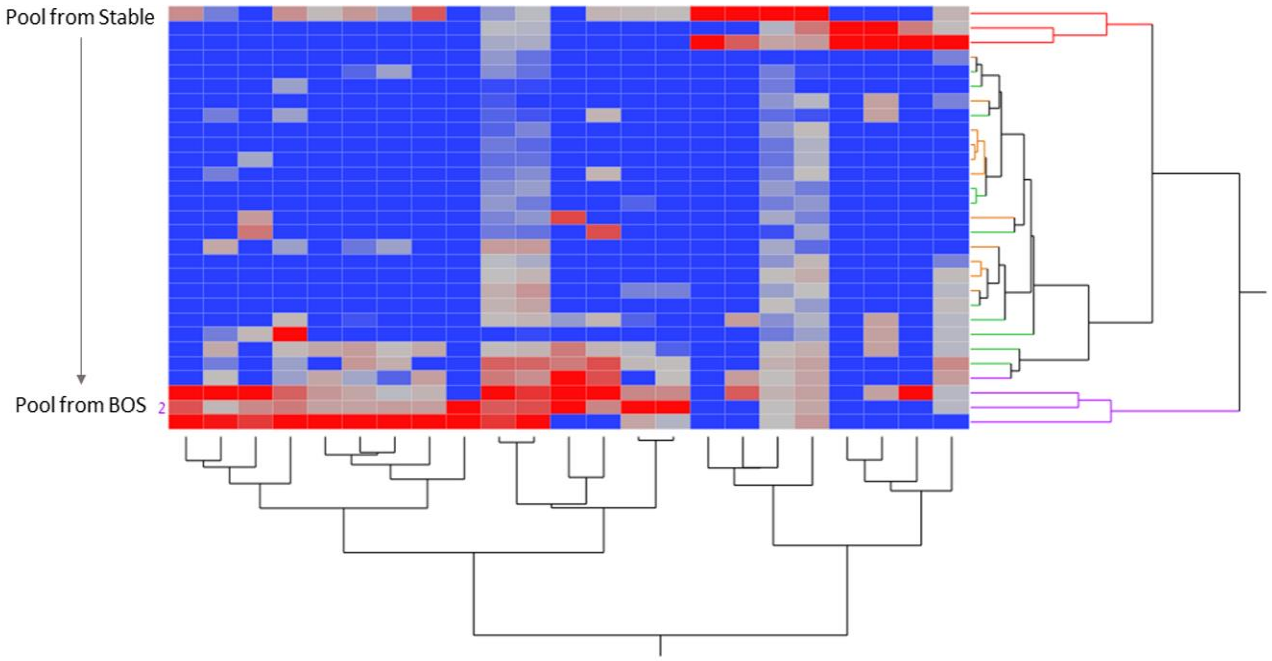

Figure 15. Hierarchical Clustering. Heatmap and dendrogram of protein lists from BALf pools of stable, BOS0p, BOSI, BOSII+BOSIII and their technical replicates. Clustering was performed by computing the average spectral count (aSpC) value of proteins selected by Linear Discriminant Analysis (LDA). The blue and red colors indicate the different level of expression (under-expressed or over-expressed respectively).

Applying the Linear Discriminant Analysis (LDA) with $p<0.01$, about 300 LDA Significant Proteins (LDA-SP), including 147 differentially expressed proteins (DEP), were extracted as discriminants. Using DAve and DCI algorithms, MAProMa generates a figure (Figure S2) showing these 147 DEPs: 35 were the distinct proteins that resulted differentially expressed between stable and BOS 0p subjects (figure S1, panel a); 54 between stable and BOS1 (figure S1, panel b); 58 between stable and BOS II + BOS III (figure S1, panel c). The complete list of differential proteins for each comparison is reported in Supplementary Material (Tables S1, S2 and S3). Moreover, from a comparison among the three categories (Stable *vs* BOS0p; Stable *vs* BOS I; Stable *vs BOS* II + III), interesting processes in which proteins with different level of expression were involved came to light**.** The function of proteins identified was rather heterogeneous. According to the literature, a significant proportion of these proteins was associated with general metabolism; others were related to immunological response and inflammation, tissue repair and proliferation, antioxidative processes, cytoskeleton.

In particular, as far as the inflammatory processes are concerned, 25 DEP proteins were identified that confirmed the importance of neutrophilic components and oxidative stress in the onset of bronchiolitis [108-113].

These proteins are listed in Table 5.

Table 5. Inflammatory DEPs identified in BOS specimens analyzed by MudPIT.

Reference	Accession	pI	MW	Stable	BOS0p	BOS1	BOS2+3
				Score			
Matrix metalloproteinase-9 OS=Homo sapiens OX=9606 GN=MMP9 PE=1 SV=3	P14780	6,06	78400	1,00	0,00	0,00	4,75
Zinc finger protein 655 OS=Homo sapiens OX=9606 GN=ZNF655 PE=1 SV=3	Q8N720	7,14	57400	0,67	0,00	0,00	0,00
Ubiquitin carboxyl-terminal hydrolase MINDY-2 OS=Homo sapiens OX=9606 GN=MINDY2 PE=1 SV=2	Q8NBR6	4,51	67100	0,67	0,00	0,00	0,00
Immunoglobulin heavy constant alpha 2 (Fragment) OS=Homo sapiens OX=9606 GN=IGHA2 PE=1 SV=1	P01877	6,1	36500	11,00	9,73	10,64	35,75
Myeloperoxidase OS=Homo sapiens OX=9606 GN=MPO PE=1 SV=1	P05164	8,97	83800	1,33	0,00	0,73	14,75
Immunoglobulin kappa constant OS=Homo sapiens OX=9606 GN=IGKC PE=1 SV=2	P01834	6,52	11800	72,67	36,18	31,55	53,00
Immunoglobulin heavy constant alpha 1 (Fragment) OS=Homo sapiens OX=9606 GN=IGHA1 PE=1 SV=1	P01876	5,64	42800	17,00	14,64	15,09	42,50
Lactotransferrin OS=Homo sapiens OX=9606 GN=LTF PE=1 SV=6	P02788	8,12	78100	0,33	0,64	0,82	13,00
Mucin-5B OS=Homo sapiens OX=9606 GN=MUC5B PE=1 SV=3	Q9HC84	6,64	596000	2,67	0,18	1,27	26,25
Keratin, type II cytoskeletal 4 OS=Homo sapiens OX=9606 GN=KRT4 PE=1 SV=4	P19013	6,61	57300	0,00	0,45	0,73	6,25
Immunoglobulin kappa variable 3D-11 OS=Homo sapiens OX=9606 GN=IGKV3D-11 PE=3 SV=6	A0A0A0MRZ8	5,29	12600	1,67	0,00	0,09	0,75
Cathepsin G OS=Homo sapiens OX=9606 GN=CTSG PE=1 SV=2	P08311	11,19	28800	3,67	0,00	0,36	7,25
Annexin A3 OS=Homo sapiens OX=9606 GN=ANXA3 PE=1 SV=3	P12429	5,92	36400	0,00	0,64	1,00	6,75
Immunoglobulin lambda variable 3-21 OS=Homo sapiens OX=9606 GN=IGLV3-21 PE=1 SV=2	P80748	5,29	12400	2,00	0,09	0,36	0,25
S phase cyclin A-associated protein in the endoplasmic reticulum OS=Homo sapiens OX=9606 GN=SCAPER PE=1 SV=2	Q9BY12	7,44	158200	0,00	0,00	0,00	1,00
Immunoglobulin heavy constant gamma 1 (Fragment) OS=Homo sapiens OX=9606 GN=IGHG1 PE=1 SV=1	P01857	6,96	43900	139,67	26,55	30,09	53,75
Mucin-5AC OS=Homo sapiens OX=9606 GN=MUC5AC PE=1 SV=4	P98088	7,02	585200	2,33	0,18	0,73	28,75

Neutrophil gelatinase-associated lipocalin OS=Homo sapiens OX=9606 GN=LCN2 PE=1 SV=1	P80188	8,5	22800	1,33	0,09	1,45	5,25
Protein S100-A9 OS=Homo sapiens OX=9606 GN=S100A9 PE=1 SV=1	P06702	6,13	13200	10,00	0,27	5,55	34,75
Patched domain-containing protein 3 OS=Homo sapiens OX=9606 GN=PTCHD3 PE=1 SV=3	Q3KNS1	6,24	86800	1,00	0,00	0,00	0,50
Immunoglobulin heavy variable 6-1 OS=Homo sapiens OX=9606 GN=IGHV6-1 PE=3 SV=1	A0A0B4J1U7	9,2	13500	0,33	0,09	0,82	2,25
Immunoglobulin heavy constant mu (Fragment) OS=Homo sapiens OX=9606 GN=IGHM PE=1 SV=1	A0A1B0GUU9	6,15	51900	9,00	0,73	1,64	2,75
Protein S100-A8 OS=Homo sapiens OX=9606 GN=S100A8 PE=1 SV=1	P05109	7,03	10800	1,00	0,27	2,09	23,75
Alpha-1-antitrypsin OS=Homo sapiens OX=9606 GN=SERPINA1 PE=1 SV=1	P01009	5.37	46736	37,33	70,09	66,00	15,50
Neutrophil elastase OS=Homo sapiens OX=9606 GN=ELANE PE=1 SV=1	P08246	9.35	28500	0.33	0	0,09	1,26

A few words about the most representative proteins.

Lactotransferrin (Lf) is a component of mucosal fluid and consists in a "chemical barrier" against external aggressions before adaptive immune response starts. In this respect, it is noteworthy that Lf concentrations are locally elevated in inflammatory disorders [114-117].

Cathepsin G (CatG) is a serine protease with trypsin- and chymotrypsin-like specificity. It is released by neutrophils in response to pro-inflammatory mediators leading to a progressive degradation of elastin, a hallmark in several lung diseases with fibrotic features [118, 119].

Annexin A3 (Anxa3) plays a role in the regulation of cellular growth and in signal transduction pathways. The changes in expression levels or localization of annexin may contribute to the pathological consequences and sequelae of human diseases. In particular, Anxa3 up-regulation was found to facilitate the metastases of lung adenocarcinoma [120].

Matrix metalloproteinase-9 may play an essential role in local proteolysis of the extracellular matrix and in leukocyte migration. It is an enzyme secreted by several cell types, including neutrophils and airway epithelial cells, as well as macrophages, which can be involved in COPD pathogenesis. MMP-9 provides the physiological remodeling of lung tissue but, when misregulated, may be associated with the development of lung diseases and their severity [121, 122].

Airway mucin concentrations may serve as a hallmark of the failed mucus transport and intrapulmonary mucus accumulation that are central to the pathogenesis of chronic bronchitis [123].

Finally, the extracellular functions of Protein S100-A8 involve pro-inflammatory, antimicrobial, oxidant-scavenging and apoptosis-inducing activities. Its pro-inflammatory activity includes recruitment of leukocytes, promotion of cytokine and chemokine production, and regulation of leukocyte adhesion and migration.

It has already been proved that the levels of S100-A9 in inflammatory BAL were increased compared to those of BAL from healthy subjects [124].

The level of these proteins in the different cohorts is shown in Fig. 16.

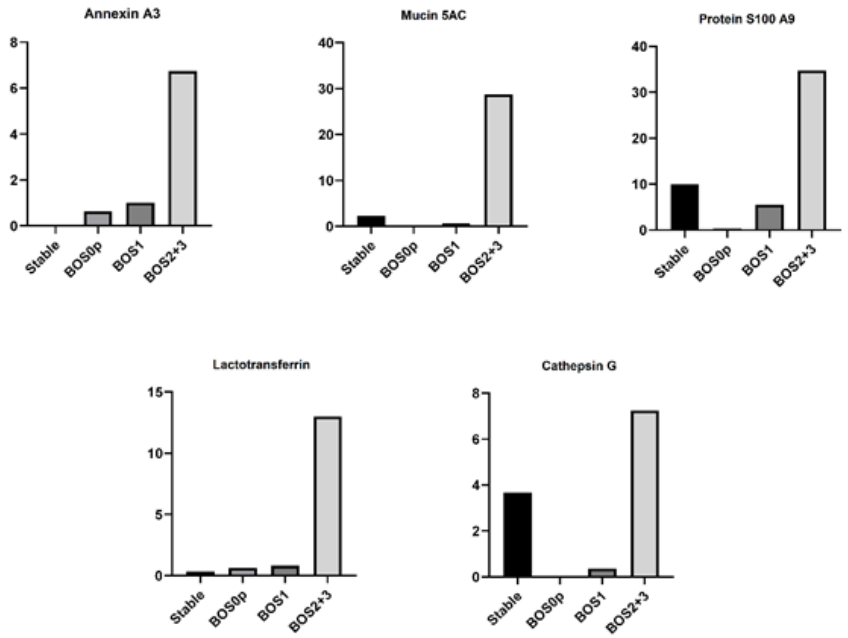

Figure 16. Levels of the most representative proteins identified by LC-MS/MS.

BOS is histologically characterized by early bronchiolar wall infiltration by lymphocytes, followed by a fibrotic process leading to small airway obliteration due to tissue remodeling and extracellular matrix (ECM) deposition. While it has been hypothesized that repeated epithelial injuries resulting from both alloimmune and non-alloimmune mechanisms contribute to the fibrotic process and airway obstruction [108], the cellular processes involved in BOS remain unclear.

The action of neutrophilic proteases strongly supports the progression and speeds up this process promoting a quick remodeling of the ECM that stimulates fibrogenesis. The focal point concerning the hypothesis of COPD pathogenesis is the protease-antiprotease imbalance as reported in the Introduction [125].

A classic example of this phenomenon is represented by the deficiency of *AAT* which is commonly known as a major genetic factor in emphysema development [126].

AAT play a pivotal role against the destructing action made by these enzymes; thus, it appears clear that the balance between proteases and antiproteases is an efficient endogenous control mechanism essential for the effective resolution of inflammatory lung diseases. That AAT plays a pivotal role in the inhibition of proteases was demonstrated by observing the weak control of the neutrophilic proteases activity in the lower airways of AAT deficient patients with inflammatory episodes [127].

The role of pulmonary AAT in the development of major complications in lung transplant recipients is still unclear. Further investigations are needed to obtain a clinical rationale for the AAT treatment in long-term post-transplant complications. With the aim of extending the survival of lung transplant recipients, we hope that our work will contribute to understand as quickly as possible when the irreversible phase of BOS begins. As stated above, the immune-modulator and anti-inflammatory AAT effect in this setting of patients has been previously suggested and investigated.

The preliminary data provided by the MudPIT analysis indicate that the amount of HNE in BOS II/III patients is higher than in stable. As expected, the content of AAT in the same patients is lower than in stable (Fig. 17). The fact that AAT content in BOS0p/BOS I is higher than in BOS II/III subjects seems to confirm the capacity of the formers to counteract the inflammation.

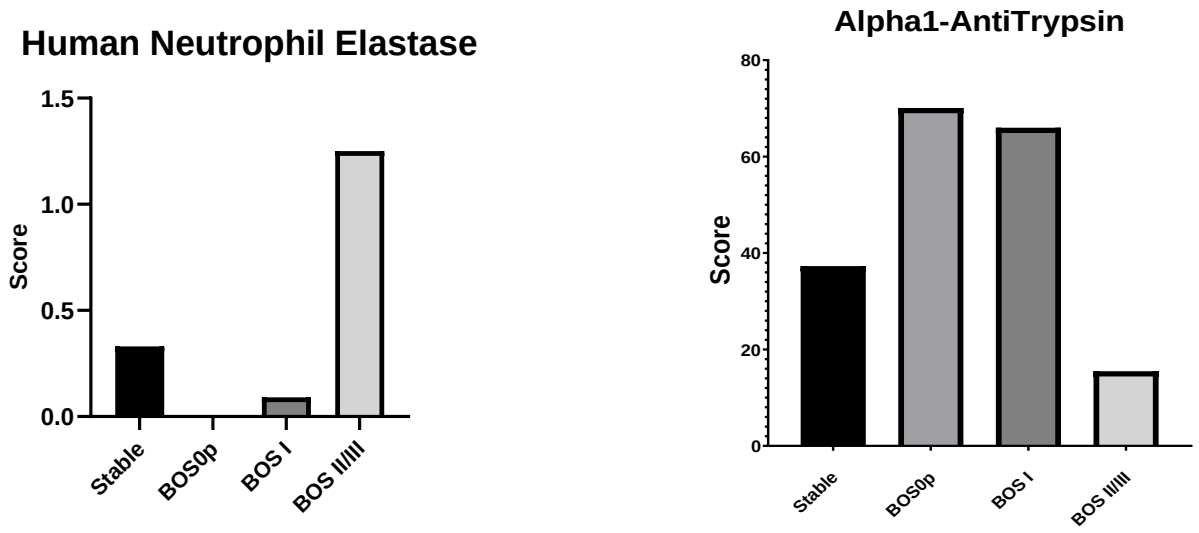

Figure 17. HNE and AAT levels among the categories

CHAPTER 2

Metabolomics

MATERIALS AND METHODS

● **Nuclear Magnetic Resonance (NMR) Analysis**

To evaluate different experimental conditions, BALf samples were submitted or not to a lyophilization step prior to their analysis. Freeze-dried samples were reconstituted in 10 mM deuterated phosphate buffer, pH 7.4, either at the same concentration of the original sample or at higher concentration (1.75x, 3.5x, 5x or 10x). Non-lyophilized ones were analyzed simply after adding 10% D2O to sample solution. 4,4-dimethyl-4-silapentane-1-sulfonic acid (DSS, final concentration 0.1 mM) was added to all samples as internal reference of both concentration and chemical shift. The pH of each sample was verified with a Microelectrode (Mettler-Toledo) for 5 mm NMR tubes and adjusted to pH 7.4 with small amounts of NaOD or DCl. All pH values were corrected for the isotope effect. The acquisition temperature was 298 K. All spectra were acquired on a Bruker AVANCE III 600 MHz NMR spectrometer equipped with a QCI (^{1}H, ^{13}C, ^{15}N/^{31}P and ^{2}H lock) cryogenic probe. 1D ^{1}H-NMR spectra were recorded with water suppression (cpmgpr1d or noesygppr1d pulse sequences in Bruker library) and 1024 scans, spectral width of 20 ppm, relaxation delay of 5 s. They were processed with a broadening of 0.3 Hz and automatically phased and baseline corrected. Chemical shifts values were internally calibrated to the DSS peak at 0.0 ppm.

Metabolite identification and assignment were performed with the support of 2D NMR experiments, the Human Metabolome Database, the Biological Magnetic Resonance Data Bank, In particular, ^{1}H,^{1}H-TOCSY (TOtal Correlation SpectroscopY) spectra (dipsi2esgpphpp pulse sequence in Bruker library) were acquired with 120 scans and 512 increments, a mixing time of 80 ms and the relaxation delay was 2 s. ^{1}H,^{13}C-HSQC (Heteronuclear Single Quantum Coherence) spectra (hsqcetgppr pulse sequence in Bruker library) were acquired with 180 scans and 256 increments, a relaxation delay of 2.5 s.

NMR spectra processing and peak peaking were performed by Mnova software package of Mestrelab (MestReNova v 9.0, 2013 Mestrelab Research S.L.). Before starting with the analysis of all samples, the reproducibility of runs was checked by assessing within-day and between-day repeatability, according to the protocol previously described and validated.

● **Statistical analysis**

Data were subjected to multivariate analyses in both unsupervised (through principal component analysis, PCA) and supervised mode (by orthogonal partial least squares discriminant analysis, OPLS-DA). Leave-one-out-cross validation (LOOCV) has been applied to validate the model. OPLSDA models have been validated in order to understand whether the separation was statistically significant or due to random noise. This hypothesis was tested using the permutation tests in each permutation, as implemented in Metaboanalyst: an OPLSDA model was built between the data (X) and the permuted class labels (Y) using the optimal number

of components determined by previous cross validation calculations and based on the original class assignment. The pathway analysis was performed through the respective module present in MetaboAnalyst.

RESULTS

NMR spectroscopy is a robust and nondestructive metabolic method for probing the dynamics of metabolites in biological samples without the need for elaborate sample preparation [128, 129].

This approach was applied to the same samples described in previous chapter. Aim of this investigation was to characterize the level of metabolites in BALf from stable and BOS patients in hope to identify potential diagnostic biomarkers which might aid in the diagnosis and/or treatment of lung diseases. NMR experiments have been carried out in the laboratories of the Department of Biotechnology and Biosciences, University of Milano-Bicocca, Milano, where this sophisticated system is available. A scheme of the procedure is shown in Figure 18.

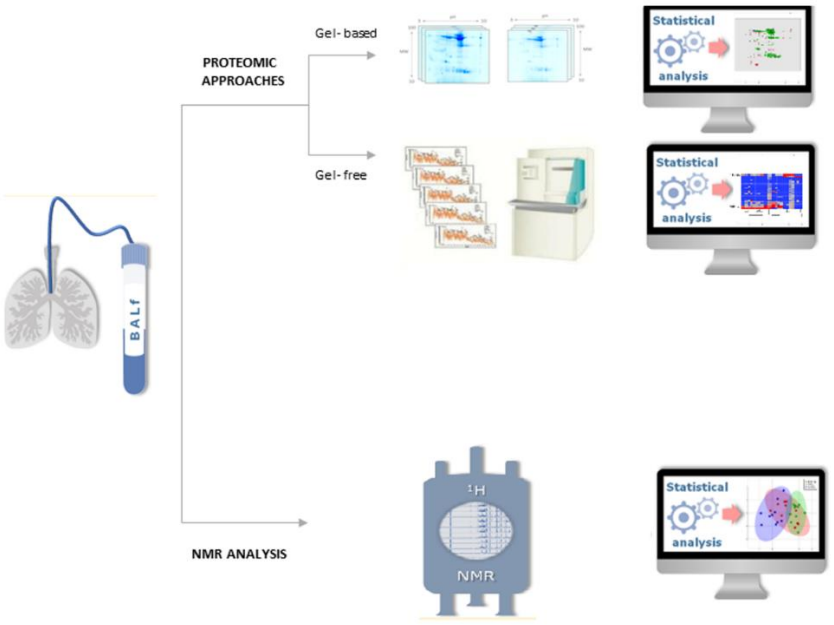

Figure 18. Scheme of experiments performed in chapter one and two

Exploiting the NMR spectra, 38 polar metabolites, including amino acids, Krebs cycle intermediates, mono- and disaccharides, nucleotides, and phospholipid precursors, were identified in BALf samples. A typical profile, representative of all other obtained in this work, is shown in Figure 19.

A careful observation of these profiles also shows the constant presence of two signals of high intensity (at 2.19 and 7.25 ppm), unambiguously identified as lidocaine. Given that topical lidocaine is usually administered through the flexible bronchoscope to reduce excessive coughing and patient discomfort during BAL collection, this finding was not that surprising.

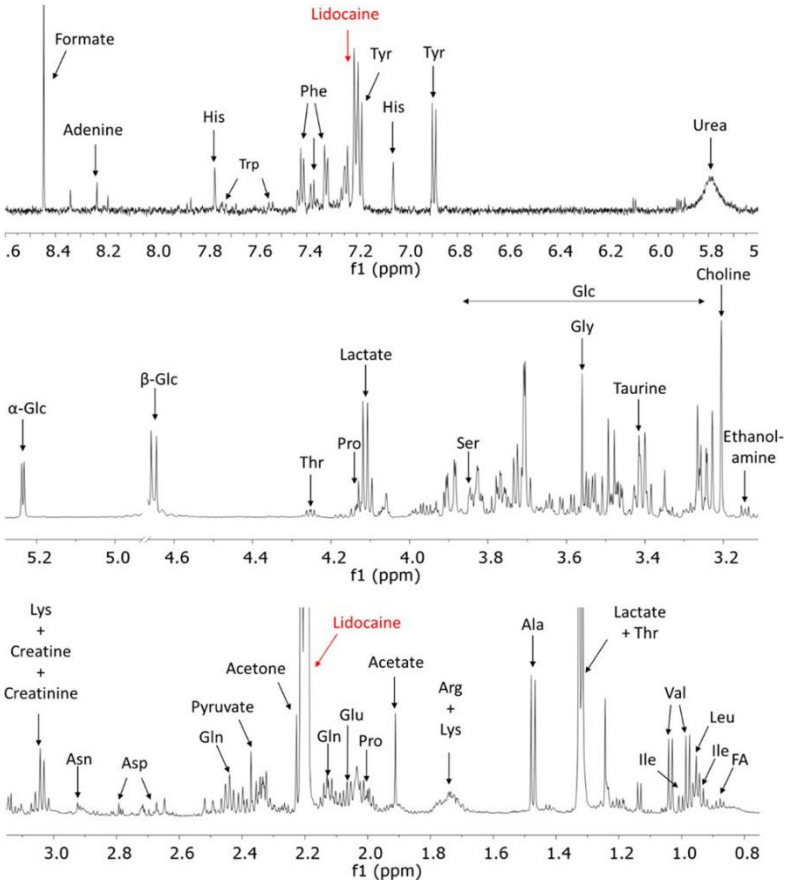

Figure 19. Expansion of different regions of the 1 H NMR spectrum of a BALf sample (representative of all others) with the assignment of the most abundant metabolites. His, histidine; Trp, tryptophane; Phe, phenylalanine; Tyr, tyrosine; Glc, glucose; Thr, threonine; Pro, proline; Ser, serine; Gly, glycine; Lys, lysine; Asn, asparagine; Asp, aspartate; Gln, glutamine; Glu, glutamate; Arg, arginine; Ala, alanine; Val, valine; Ile, isoleucine; Leu, leucine; FA, fatty acids.

The absolute concentrations (μM) of the metabolites that are mainly responsible for the discrimination among the three classes (S, BOS 0p, and BOS I), represented as mean values ± SEM for each group, is shown in Table 6.

Table 6. Absolute concentrations (μM) of the metabolites that are mainly responsible for the three classes (S, BOS 0p, and BOS I) discrimination, represented as mean values ± SEM for each group

	Stable		**BOS0p**		**BOS I**	
	Mean	SEM	Mean	SEM	Mean	SEM
Acetate	0.583	0.204	1.176	0.326	0.928	0.228
Acetone	0.207	0.073	0.337	0.120	0.790	0.376
Alanine	0.353	0.130	0.591	0.181	1.173	0.381
Creatine	0.116	0.043	0.408	0.148	0.392	0.070
Ethanolamine	0.250	0.122	0.873	0.225	1.265	0.323
Formate	0.250	0.068	0.873	0.170	1.265	0.150
Glucose	0.250	0.568	0.873	2.135	1.265	1.826
Glutamate	2.099	0.698	5.180	1.787	8.857	2.563
Glycerol	2.004	0.710	5.167	1.227	6.738	1.083
Isoleucine	0.439	0.249	0.194	0.088	0.444	0.113
Lactate	1.652	0.536	4.351	0.800	7.387	1.697
Leucine	0.907	0.380	0.644	0.215	1.834	0.512
Taurine	1.273	0.458	5.640	1.424	6.619	1.083
Threonine	1.637	0.590	2.524	0.804	3.510	0.796
Valine	0.475	0.246	0.323	0.097	0.436	0.101

The observation that the levels of these metabolites were different in the three cohorts prompted further investigations aimed at evaluating the usability of the same analyses on samples from transplanted subjects without BOS (stable, S, n = 10) or with BOS at different levels of severity (BOS 0p, n = 10; BOS I, n = 10), in an effort to detect signatures that could be correlated with proteomic results. BALf samples from BOS II and BOS III patients were not included in this part of the work due the intrinsic difficulty to obtain specimens from individuals severely affected that made the number of patients belonging to these categories very poor.

When the experimental data sets were submitted to PCA analysis, the score plot obtained, while being able to discriminate totally Stable from BOS I subjects, showed a partial overlapping of BOS 0p to both S and BOS I samples (Fig. 20). These data were not surprising since BOS stage 0p (BOS 0p) is a clinical parameter detected on pulmonary function tests (PFTs) after lung transplantation to identify patients at risk to develop BOS.

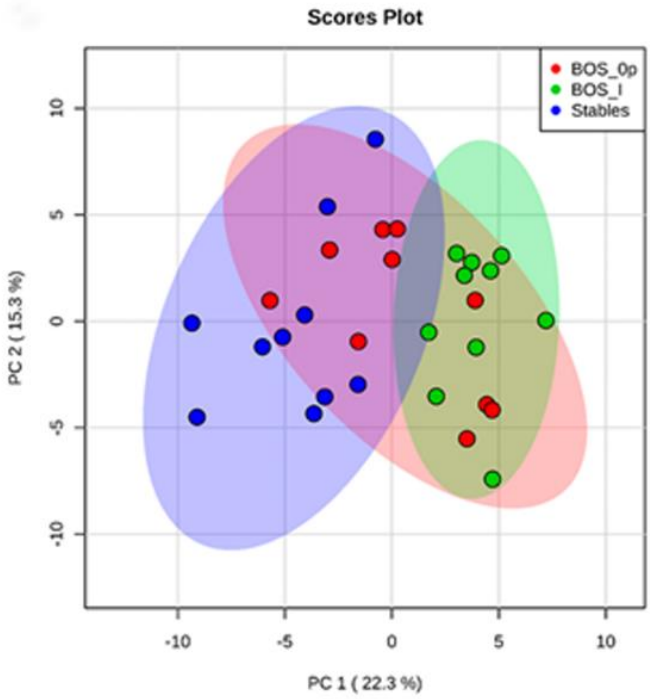

Figure 20. PCA score plots between S, BOS 0p and BOS 1 samples (Reprinted from Ciaramelli et al [130])

The loading plots from PCA allowed identification of the peaks responsible for S, BOS 0p, and BOS I separation and assignment of them to the corresponding metabolites (see Table 6). The concentrations of the most relevant metabolites for class discrimination were calculated integrating the corresponding signal(s). Interestingly, it can be observed that, while these metabolites are present in the NMR spectra of all groups, their different concentration allows to discriminate among groups.

The MetaboAnalyst 3.0 platform, applied to list of metabolites identified using “human” as the specific model organism, allowed generation of a pathway analysis aimed at defining the relationships among them (Fig. 21). This plot revealed that, among the pathways observed in this study, a critical role is played by the pyruvate and the taurine/hypotaurine pathways.

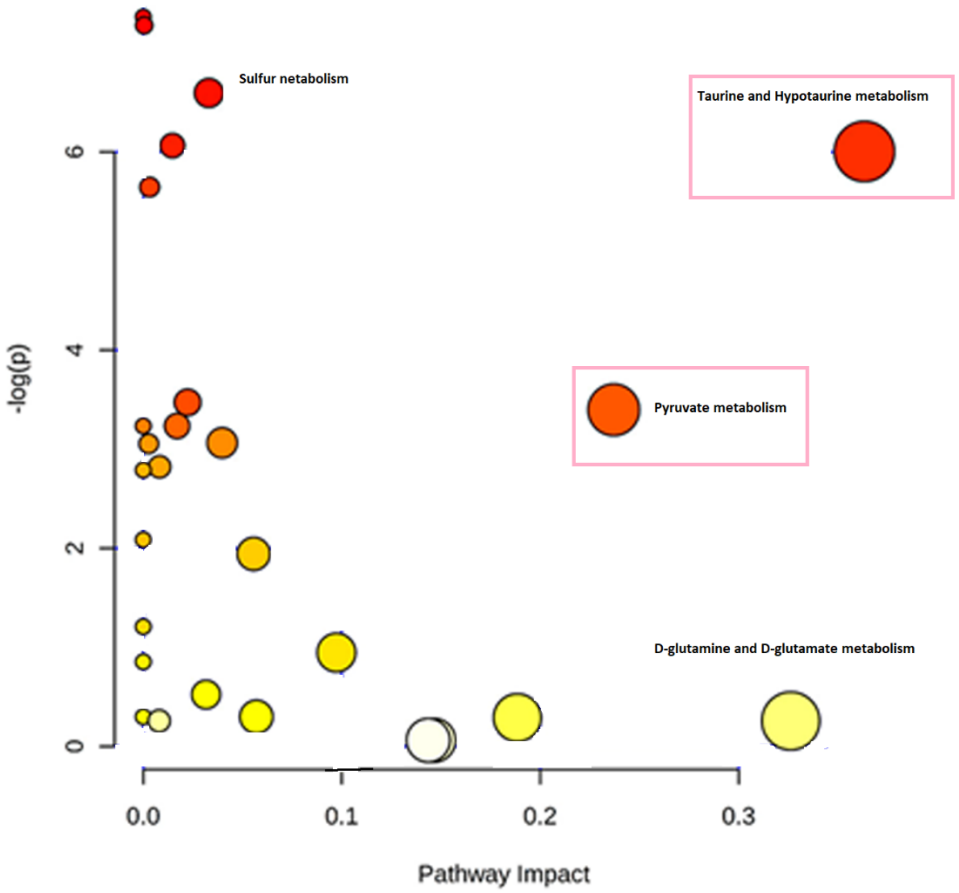

Figure 21. Summary of pathway analysis

The detection of a few metabolites which may be related to the former pathway was not a matter of surprise. For example, lactate was previously shown to be present in airway secretions [131] and, based on experimental evidence, an increase in lactate production was found to be triggered by lung inflammation [132]. This allowed us to speculate that the increased lactate levels in BOS patients at different stages of severity could be consistent with an increased inflammatory state. The finding that the levels of a good number of branched chain amino acids (valine, leucine, isoleucine) was increasing with the severity of the disease somehow supported this hypothesis. In fact, that the amount of these amino acids secreted in BALf is correlated with different inflammatory states, such as sepsis, was previously demonstrated [133].

Taurine is also acknowledged for having a role in the regulation of cell volume, as a membrane stabilizing agent, and for its antioxidative, anti-inflammatory, and antiapoptotic effects [134-136]. Furthermore, the activity of the taurine transporter (Tau-T) is strongly down-regulated by acidification, osmotic cell swelling, and exposure to reactive oxygen species (ROS).

In summary, based on proteomic and metabolomic approaches, the release of ROS species by neutrophils and macrophages during inflammatory states, together with the production of eicosanoids by leukocytes,

could play a role in lung injury with the consequent increase of mucus secretion and development of BOS. Given the clinical features of BOS 0p and BOS I patients, the fact that these cohorts can be separated much less efficiently than stable subjects may be considered a confirmation of data reliability. The possibility to include in the study also BOS II and BOS III patients would be the essential step to definitively confirm this speculation and to allow identifying which, among the metabolites detected, may be the best biomarker(s) of this disease.

Part of this work was published on the Journal of proteome research [130].

CHAPTER 3

Proteases and Anti-Proteases

MATERIALS AND METHODS

● **Reagents**

The Bicinchoninic Acid (BCA) Protein Assay kit was obtained from Thermo Scientific (Rockford, USA). Antibodies for detection of α1-AT and anti-mouse secondary antibodies were obtained from Abcam (Cambridge, UK). Antibody against Neutrophil Elastase was from Thermo Scientific (Rockford, USA). The standard p-nitroaniline (p-NA) and the peptide substrates MeOSuc-Ala-Ala-Pro-Val-NA and Suc-Ala-Ala-Pro-Phe-NA used for the determination of human neutrophil elastase and cathepsin G activities were obtained from Bachem (Bachem GmbH, Germany). Unless otherwise stated, all other reagents were purchased from Sigma-Aldrich (St. Louis, MO) and were of analytical grade. Double-distilled water used for the preparation of all buffers and solutions was prepared with a Millipore (Bedford, MA, USA) Milli-Q purification system.

● **AAT measurement**

AAT was measured in BAL by a rate immune nephelometric method (Immage 800 Immunochemistry System, Beckman-Coulter, USA).

● **BCA Protein Assay**

To obtain the exact protein concentration of each sample, the Bicinchoninic Acid (BCA) assay was applied [101]. Bovine serum albumin (BSA), in the range of concentration between 5 and 25 µg/ml, was the standard protein used to produce calibration curves.

● **Monodimensional electrophoresis (1-DE)**

An aliquot of each sample (50 µl containing 20 µg of proteins) was submitted to protein precipitation with trichloroacetic acid (TCA) according to the procedure of Yvon *et al* [137]. The pellets obtained after centrifugation were reconstituted in 10 µl of 50 mM Tris–HCl pH 8.3 containing 5% 2-mercaptoethanol, 2% sodium dodecylsulphate (SDS), 0.1% bromophenol blue (BPB) and 10% glycerol. Samples were incubated at 90 °C for 10 min and then loaded on gel slabs.

Electrophoresis was performed according to Laemmli [138] in 5% stacking gel and 12% running gel by applying a voltage of 150 V for 1 h.

Gels were stained with ‘‘Blue silver’’ (colloidal Coomassie G-250 staining), according to Candiano *et al* [102].

● **Western Blotting**

Western blot (WB) analyses were performed starting from 10 µg of proteins submitted to precipitation with trichloroacetic acid (TCA, 1,22 M), separated by SDS-PAGE and transferred onto a Millipore polyvinyldivinyl

fluoride (PVDF) membrane (Billerica, MA, USA) by using a Trans Blot turbo system (BioRad). After 1h incubation in 5% milk (10 ml) diluted in PBS and three additional washes with PBST (10 ml), the membrane was incubated overnight with AAT antibody (ab9400, Abcam) at a 1:2500 dilution in 1% milk. After washing the membrane three times with PBST (10 ml), incubation with the secondary antibody Rabbit Anti-Mouse IgG H&L (HRP) (ab6728, Abcam) was carried out for 1 h at room temperature at a 1:2000 dilution in 1% milk in PBST. The membrane was finally washed three times with PBS and incubated in ECL Westar ηC Ultra (Cyanagen, Bologna, Italy) solution according to the provided protocol. Immunoblots were acquired with the ImageQuant LAS 4000 analyzer (GE Healthcare). The same procedure was applied for the identification of free and complexed HNE by using the anti HNE antibody (PA5-29659, Thermo).

● **In-Situ Digestion**

Enzymatic digestion of proteins was performed as previously described [103]. Briefly, the selected bands were carefully excised from the gel, placed into eppendorf tubes, broken into small pieces and washed with 100 mM ammonium bicarbonate (AmBic) buffer pH 7.8 containing 50% ACN until complete destaining was achieved. The gel pieces were then dehydrated by adding 200 µL of ACN until they became opaque-white color. ACN was finally removed, gel pieces were dried under vacuum for 10 min and then rehydrated by adding 75 µL of 100 mM AmBic buffer pH 7.8 containing 20 ng/µL sequencing grade trypsin (Promega, Madison, WI, USA). The digestion was performed overnight upon incubation of the mixture at 37 ◦C and the resultant peptides were extracted from gel matrix by a three-step sequential treatment with 50 µL of 50% ACN, 5% TFA in water and finally with 100% ACN. Each extraction involved 10 min of stirring followed by centrifugation and removal of the supernatant. All supernatants were pooled, dried and stored at -80 °C until mass spectrometric analysis. At the moment of use, the peptide mixture was solubilized in 0.1% FA.

● **Liquid Chromatography Tandem Mass Spectrometry (LC–MS/MS)**

Analyses were performed on a liquid chromatography-mass spectrometry system (Thermo Finnigan, San Jose, CA, USA) consisting of a thermostated column, a surveyor auto sampler controlled at 25 ◦C, a quaternary gradient surveyor MS pump equipped with a diode array (DA) detector, and a linear trap quadrupole (LTQ) mass spectrometer with electrospray ionization (ESI) ion (Phenomenex, Torrance, CA, USA) C_{18} column (150 × 2 mm, 4 µM, 90 Å particle size) using a linear gradient (2–60% solvent B in 60 min). Solvent A consisted of 0,1% aqueous FA and solvent B of ACN containing 0.1% FA. Flow rate was 0.2 mL/min. Mass spectra were generated in positive ion mode under constant instrumental conditions: source voltage 5.0 kV, capillary voltage 46 v, sheath gas flow 40 (arbitrary units), auxiliary gas flow 10 (arbitrary units), sweep gas flow 1 (arbitrary units), capillary temperature 200 ◦C, tube lens voltage -105 V. MS/MS spectra, obtained by collision-

induced dissociation (CID) studies in the linear ion trap, were performed with an isolation width of 3 Th m/z, the activation amplitude was 35% of ejection RF amplitude that corresponds to 1.58 V. Data processing was performed using Peaks studio 4.5 software.

● **Enzymatic assays**

The following simple colorimetric assay was utilized for the determination of HNE and Cat G activities: 400 µl of each sample were lyophilized, the pellet resuspended in 400 µl of incubation buffer (50 mM Tris HCl pH 7,8 containing 500 mM NaCl) and the reaction started by adding 5 µl of the appropriate substrate (MeOSuc-Ala-Ala-Pro-Val-NA for HNE and Suc-Ala-Ala-Pro-Phe-NA for CatG; final concentrations 2 mM and 20 mM respectively). The mixture was incubated at 37 °C for 10 min and the reaction was stopped by addition of 40 µl of 0.27 M TCA. The content of nitroaniline (NA) released by peptide hydrolysis was determined by measuring the absorbance at 410 nm. One unit of enzyme activity was defined as the amount of enzyme required for the release of 1 µmol/min of NA.

PREMISE

In accordance with what was discussed in the previous chapter, AAT/HNE balance plays an important role in homeostasis of the lung. It has been speculated that BOS results from several noxious triggers which cause innate/adaptive immune reactions, leading to immune activation (mainly T helper 17, Th-17) responsible for inducing the neutrophilic inflammation characteristic of the disorder. Given the tissue-protective and anti-inflammatory properties of AAT, the interest in its influence in early and long-term complications post lung transplant has increased in recent years, also in light of the poor knowledge of complications which involve a high neutrophil recruitment, e.g., ischemia reperfusion injury and BOS [139-145].

In a healthy lung, antiproteases maintain a homeostatic balance with proteases, preventing damage that results from the excess of proteases activity [140, 141]. In many lung diseases, the inability of these anti-proteases to regulate their specific proteases might contribute in part to the disease. Inherited α1-antitrypsin deficiency (AATD) is a clear example that the balance between proteases and antiproteases is one of the most important aspects of lung homeostasis.

To get insights into this mechanism of control in BOS, possible proteomic variations in BALf from 13 lung transplanted patients classified as stable and BOS based on their clinical features (see paragraph *Demographic and clinical features of patients*) have been previously investigated.

Data from electrophoretic and western blotting analyses were compared with those acquired from LC–MS. The neutrophil count, together with the determination of HNE and of Cat G activities provided information on the functionality of AAT, its balance with HNE, and its correlation to the degree and type of inflammation of the deep graft.

RESULTS

The workflow of the experimental procedure is schematized in Figure 22.

.

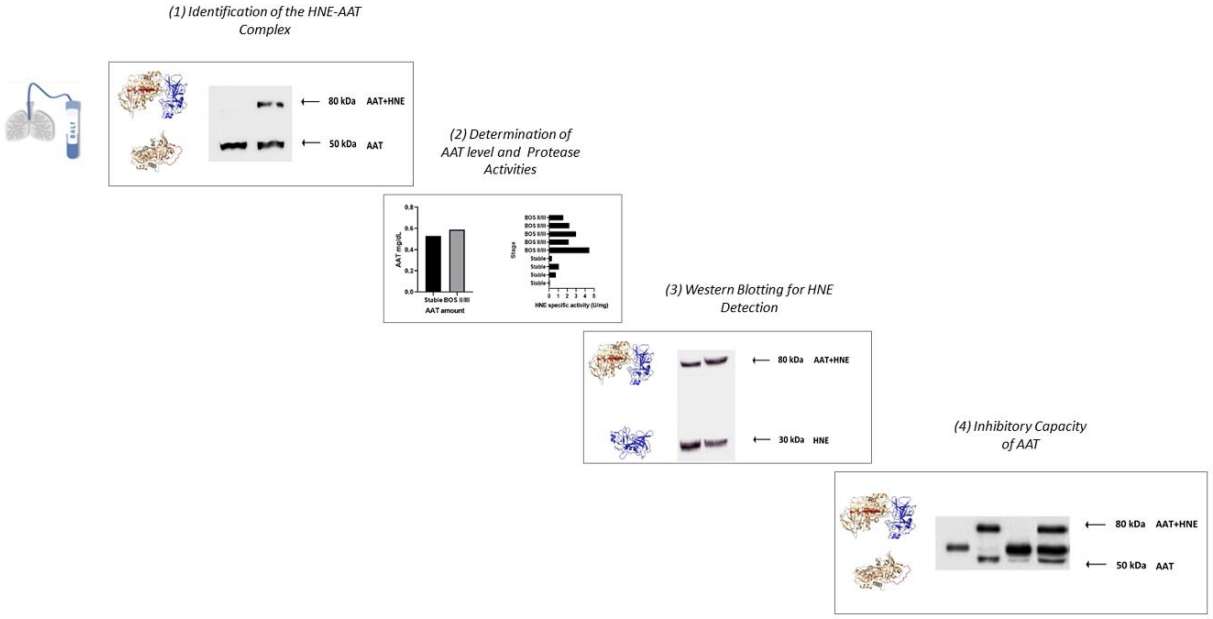

Figure 22. Workflow of the experimental procedure.

1) Identification of the HNE-AAT Complex

The results of the electrophoretic runs performed on BALf of all subjects investigated are shown in Figure 23. Lanes 1 to 7 refer to the subjects belonging to Group 1 (Stable and BOS 0p) and 8 to 13 to those in Group 2 (BOSII and BOSIII). It can be observed that two bands, at approximately 80 and 55 kDa, exceed in abundance over others.

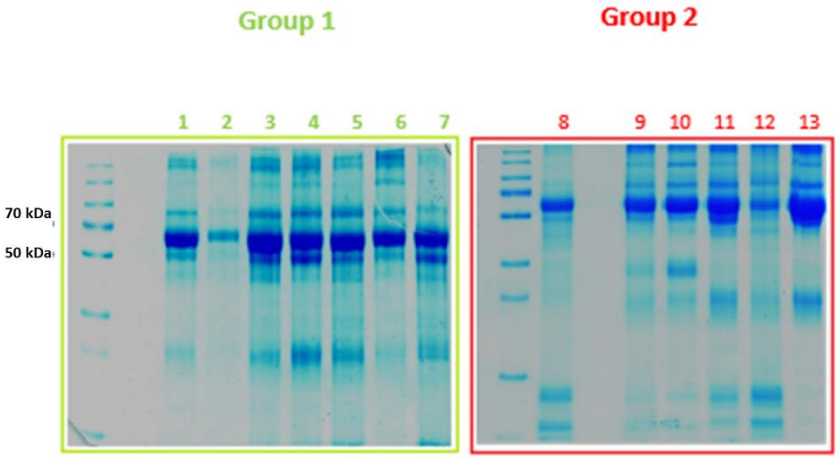

Figure 23. 12.5% SDS-PAGE showing the protein profile of all the bronchoalveolar lavage fluid (BALf) samples considered. Group 1: lanes 1–7, Group 2: lanes 8–13

Information on these two bands was obtained by blotting the gels on a PVDF membrane that was later incubated with an anti-AAT antibody. The results are shown in Figure 24.

Figure 24. Western blotting with anti-AAT antibody of the same samples as in Fig 23. Group 1: lanes 1–7, Group 2: lanes 8–13

Based on the presence/absence of the immune-reactive band at 80 kDa, individuals belonging to Group 1 could be divided in two sub-classes: subjects who did not exhibit this band (lanes 1 to 3) and those who showed it (lanes 4 to 7). Conversely, the image of the PVDF membrane obtained from patients belonging to Group 2 (lanes 8 to 13), mirrored that of the starting gel. In fact, the 80 kDa band was evident, although at different intensity, in all profiles, regardless of whether the BALf belonged to BOS II or BOS III patients. Based on the well-known molecular mass of AAT (Mr 52,0 kDa), the band at approximately 55 kDa was attributed to this protein. Likewise, on the basis of the sum of the theoretical molecular weights of AAT and HNE, the band at 80 kDa was tentatively attributed to the complex between these two proteins. While experimental

evidence was still lacking, the reactivity of the material under this band against the anti-AAT antibody was circumstantial evidence that it contained AAT.

The presence of a band at approximately 80 kDa in SDS-PAGE had been previously observed only *in vitro* by other authors who speculated that it could correspond to the HNE-AAT complex [146, 147]. To definitively prove the existence of this inhibitory complex in BALf samples that showed this band, it was carefully excised, the protein extracted and submitted to the procedure detailed in the experimental section. Peptides generated from tryptic digestion were separated by LC–MS/MS and fragmentation data searched against the Swiss-Prot database [148, 149]. Data relative to the proteins present under the 80 kDa band (shown in Fig.25) allowed us to unambiguously identify both HNE and AAT [150]. The same procedure was applied to the band at approximately 55 kDa to confirm that it contained AAT. The data of Table 2 show that this band contained AAT contaminated by proteins with similar molecular weight which co-migrated with the former due to the resolution limits of 1D electrophoresis. Additional information concerning the primary sequence of all peptides identified for each protein analyzed is included in Table S4 of Supplementary material.

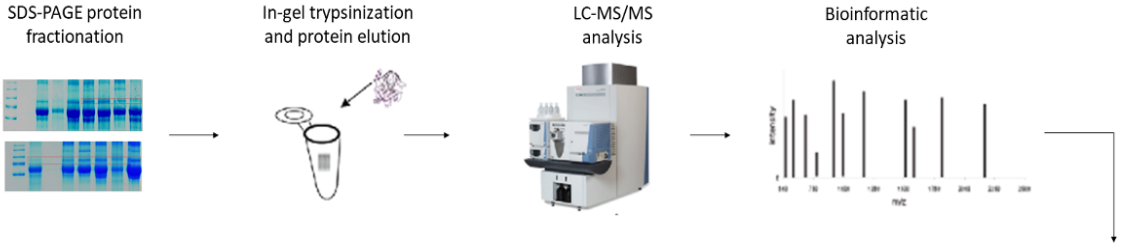

Molecular Weight	Accession	Mass (kDa)	Score (%)	Coverage (%)	Description
80kDa	sp|P01009|A1AT_HUMAN	46,737	67	9.33%	α1-antitrypsin OS = *Homo sapiens* GN = SERPINA1 PE = 1 SV = 3
	sp|P08246|ELNE_HUMAN	28,518	62	3.37%	Neutrophil elastase OS = *Homo sapiens* GN = ELANE PE = 1 SV = 1
55kDa	sp|P02768|ALBU_HUMAN	69,367	98	11.82%	Serum albumin OS = *Homo sapiens* GN = ALB PE = 1 SV = 2
	sp|P01009|A1AT_HUMAN	46,737	85	6.70%	α1-antitrypsin OS = *Homo sapiens* GN = SERPINA1 PE = 1 SV = 3
	sp|P01859|IGHG2_HUMAN	35,901	60	4.29%	Ig γ-2 chain C region OS = *Homo sapiens* GN = IGHG2 PE = 1 SV = 2

Figure 25. Extraction procedure and identification of proteins under bands at 50 and 80 kDa by liquid chromatography–mass spectrometry (LC–MS/MS).

Based on these data, the lack of the HNE-AAT complex in some subjects seems to be correlated with the low level of pulmonary inflammation. As shown below, this hypothesis is supported by the count of neutrophils and the determination of HNE/AAT activities in these subjects.

2) Determination of AAT level and Protease Activities

To answer the question of whether HNE had fully complexed AAT or was still partially present in BALf as a free, active enzyme, its activity was determined in all samples. The results summarized in Table 7 pointed out that significant levels of HNE activity were detectable only in BALf samples presenting the 80 kDa band

(Fig. 24). Conversely, the amount of AAT did not differ significantly among the samples with and without complex (Fig. 26).

Table 7. Biochemical features of all samples analyzed.

Sample #	Clinical Classification of the Disorder	AAT Assay (mg/dL)	Neutrophil Count	Elastase Specific Activity (mU/mg)	Cathepsin G Specific Activity (mU/mg)	Presence of the 80 kDa Complex
1	Stable	0.57*	1	n.d. **	n.d. **	NO
2	Stable	1.00	1	0,08	n.d.	NO
3	Stable	0.32	1	n.d.	n.d.	NO
4	Stable	0.79	34	0,725	n.d.	YES
5	Stable	0.37	30	1,06	0.14	YES
6	Stable	0.40	1	n.d.	n.d.	YES
7	BOS 0p	0.26	28	0,29	n.d.	YES
8	BOS II	2.50	94	4,44	0.57	YES
9	BOS II	0.56	56	2,16	0.254	YES
10	BOS II	0.12	40	2,98	n.d.	YES
11	BOS II	0.12	5	2,23	n.d.	YES
12	BOS III	0.13	10	n.d.	n.d.	YES
13	BOSIII	0.13	15	1,56	n.d.	YES

* Values reported are the mean of three independent determinations. Standard deviation was within 5%.
** n.d. = not detectable.

Being that the Cathepsin G activity levels were lower than the LOD of the procedure, they could be estimated only in three samples (samples 5, 8 and 9).

As shown in Figure 26, a reasonable correlation was observed between the specific activity of HNE and the number of neutrophils determined in all samples (Fig. 27).

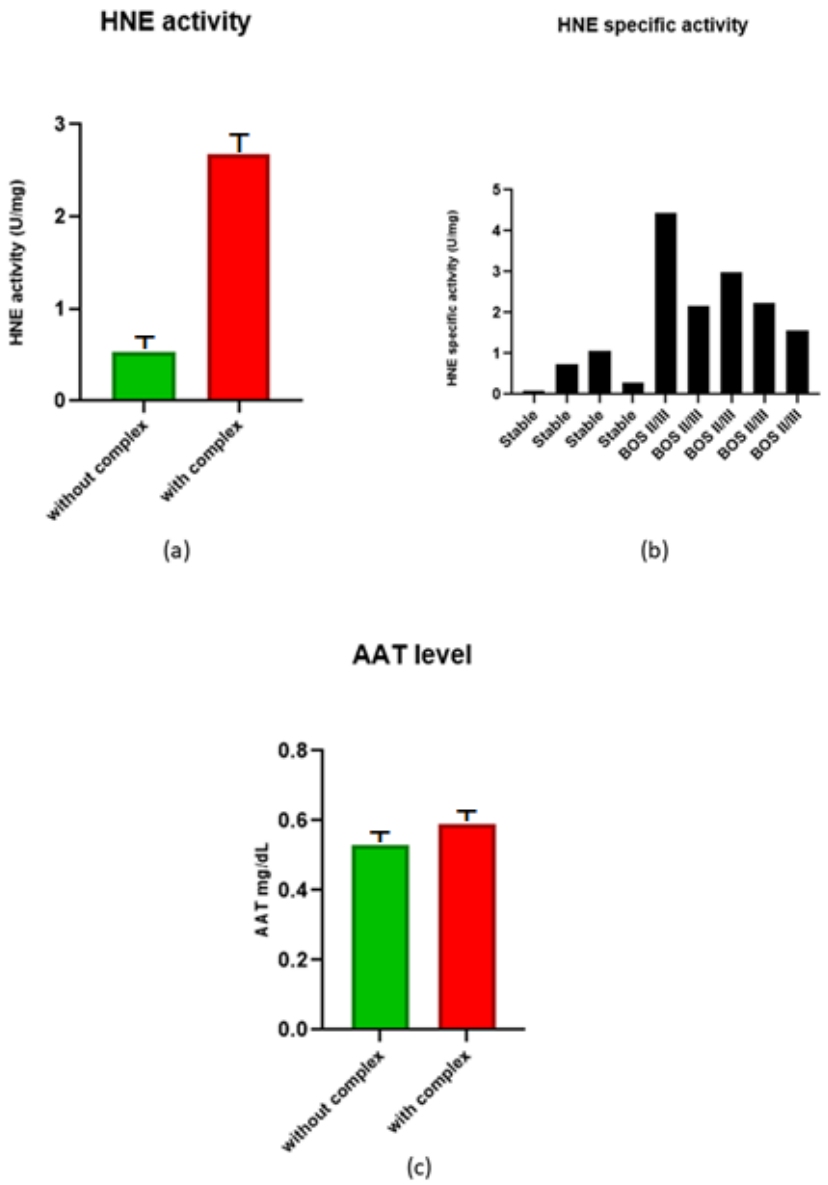

Figure 26. HNE activity level (a) with HNE specific activity of samples (b) and AAT average level (c).

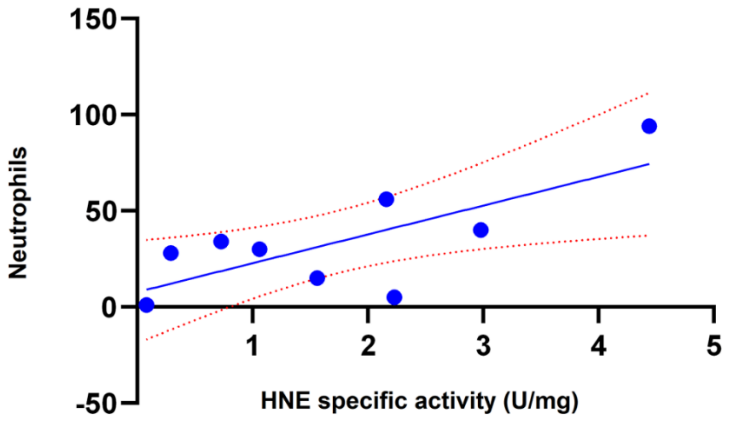

Figure 27. Correlation between the specific activity of HNE and the count of neutrophils in samples analyzed

3) Use of Western Blotting for HNE Detection

The presence/absence of HNE in the BALfs of subjects investigated was checked by running the samples on SDS-PAGE and blotting the bands on a PVDF membrane that was incubated with anti-HNE antibody (Fig. 28). The absence of immune reactive bands in BALfs lacking the 80 kDa band (lanes 1 to 3) unambiguously demonstrated that these samples did not contain HNE. Conversely, the specimens that formed the complex showed the presence of two bands (lanes 4 to 13). Based on their migration on the gel, these bands were assigned to free and complexed HNE. Following the LC–MS procedure described above, HNE was identified in both bands (data not shown).

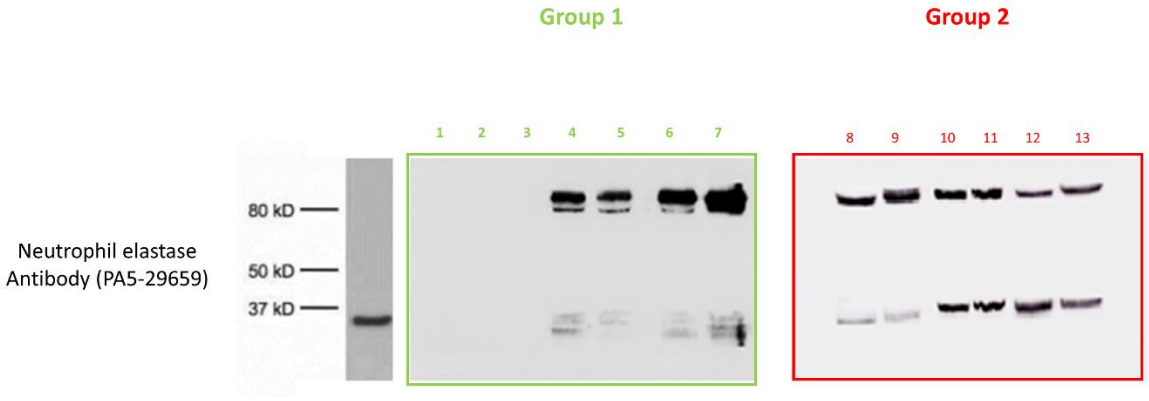

Figure 28. Western blotting profile obtained upon incubation of all BALfs with the anti-HNE antibody. Lanes 1–3: samples not showing the 80 kDa band when incubated with anti-AAT. Lanes 4–13: sample showing the 80 kDa band.

4) Inhibitory Capacity of AAT

The inflammation-mediated cell oxidative stress was previously observed to inactivate *in vitro* AAT through a sort of oxidative cascade [146, 147]. This would prevent (partially or totally) its capacity to inhibit HNE. The efficiency of AAT towards HNE was checked in BALfs from subjects who did not show the HNE-AAT complex by adding exogenous HNE (2 µL; 0,2 mg/mL) to samples. After 15 min of incubation at 37 °C, an aliquot was submitted to SDS-PAGE and gels blotted on a PVDF membrane which was incubated with the anti-AAT antibody. Figure 29 illustrates the results relative to these samples before (lanes 1; 2 and 3) and after incubation (lanes 1 *; 2 * and 3 *). The formation of the 80 kDa band clearly indicated that the BALf sample was able to capture the "excess" of HNE thus suggesting that an amount of functional AAT was still present in these samples.

When the same amount of exogenous HNE was added to samples which presented the complex, the 80 kDa band was seen to increase considerably. Figure 29 shows the results relative to a sample chosen at random among all available (sample #12). The results relative to other samples are shown in Figure S2 in the Supplementary Material. These data further support the hypothesis that AAT was functional in these samples.

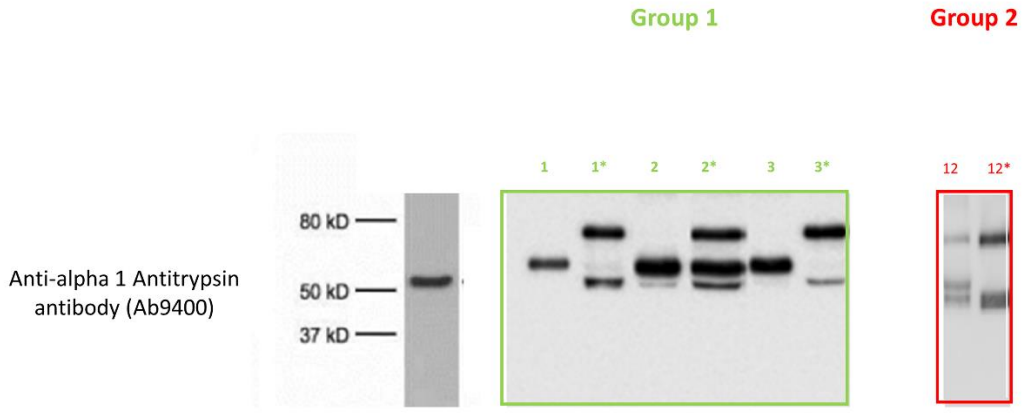

Figure 29. Western blotting of BALfs from the three patients without the 80 kDa band, before (1; 2 and 3) and after incubation with exogenous HNE (1 *; 2 * and 3 *). Western blotting of BALf from a patient with the 80 kDa band, before (12) and after incubation with exogenous HNE (12 *).

Since the mere assay of HNE and AAT is not able to provide information on the level of activity of these proteins, we explored their capacity to interact. Given the inhibitory role of AAT and being neutrophil elastase

its main physiological target, the formation of a complex between them must be interpreted as the result of the protective effect of this inhibitor against the proteolytic action of the protease.

The finding that a few samples of stable post-transplant subjects lacked this inhibitory complex was unexpected and opened the door to a series of questions. In fact, although the Western Blot analysis clearly indicated that all samples contained AAT, it did not provide information about the ability of this inhibitor to bind HNE in whole or in part. Thus, whether the lack of such complex in the BALf of the mentioned subjects should be ascribed to their pathological state, i.e., the low level of pulmonary inflammation, remained a speculation. In fact, while protease activity was undetectable in patients with a low level of lung inflammation, the formation of the complex could also have been prevented by possible inactivation processes at the expense of AAT occurring in the lungs of these individuals. This latter hypothesis was denied by the addition to the above samples of exogenous HNE, which lead to the formation of the complex. Instead, our findings supported the assumption that AAT was, at least in part, functional.

This result arouses a major question. On the assumption that any pathological condition leads to a number of pulmonary physiological changes, could this complex be considered a biomarker of lung status? It seems logical to argue that free HNE would be a marker of the degree of injury more relevant than the complex. In fact, if the rate of formation of AAT–HNE complexes is limited by the amount of available AAT, then it would be easier to measure NE in excess in the lung. The fact that free elastase in inflamed tissues can only be detected if it is present in excess over AAT activity or if this anti-elastolytic function has been somehow modified, was previously observed by other authors [151, 152]. This is not the case of the patients under investigation. In fact, given that both the initial lack of the complex and its formation by addition of exogenous HNE cannot reflect with certainty an excess of the protease, our results point to a different conclusion. The unifying view that apparently emerges from these data is that not necessarily all recipients classified as “stable” based on their clinical/functional status, display the same conditions at a molecular level.

The neutrophil count and detection of active HNE in tissues and fluids recovered from inflammatory sites might represent a critical step in tissue pathogenesis. In fact, significantly lower neutrophil levels in BALf from healthy subjects compared to BOS patients and the tendency of both HNE activity and the concentration of HNE-AAT complex to increase in these latter, had been previously observed [152]. Neutrophils produce antioxidants and are indispensable in forming the first line of defense during infection.

Knowledge about the complications of high neutrophil recruitment is still poor and bronchoscopy with bronchoalveolar lavage seems to be the best diagnostic approach to investigate the local alterations at bronchial and alveolar levels. As shown in Table 7, while the number of neutrophils was very low in the BALf of the three stable individuals who did not present free elastase activity or complex formation, these numbers and the HNE activity were increasing along with the severity of the disease.

Obviously, these data do not allow us to exclude that the lack of formation of the complex in some of our BALf samples was due to AAT modifications that made it unable to completely inhibit neutrophil elastase

activity. However, the addition of exogenous HNE to samples not showing the 80 kDa band and the consequent formation of this complex seemed to show the functionality of AAT present in these samples. The great increase observed in the 80 kDa band by addition of exogenous HNE was a further evidence that this hypothesis was most likely correct.

The results of our study allowed us to demonstrate, for the first time, that not all BALf samples contain the complex between HNE and its specific inhibitor AAT. This could indeed represent a new frontier in the field of biomarker discovery of lung inflammation in subjects with HNE/AAT unbalance.

While being obtained on a small number of samples, these results are indeed intriguing. If confirmed on a larger cohort of individuals, they would allow us to consider the AAT-HNE complex a reliable marker of pulmonary inflammation.

CHAPTER 4

Current Studies

Aα(Val360) – A Fibrinogen-Derived Neoepitope Marker of Human Neutrophil Elastase Activity

Alpha-1-antitrypsin deficiency is the only recognized genetic risk factor for chronic obstructive pulmonary disease, a leading cause of morbidity and mortality worldwide. The development of this lung disease is driven by a proteinase/anti-proteinase imbalance, in particular neutrophil elastase is considered to play an important role in disease pathogenesis. However, since its activity is inhibited within the neutrophil microenvironment, the direct confirmation of its role is difficult.

The direct measurement of extracellular elastase activity is difficult due to the following reasons:

- The released enzyme binds to substrate and to plasma proteinase inhibitors almost immediately upon its release from neutrophils
- Detection by immunoassays is not able to distinguish between free enzyme and enzyme bound to inhibitors
- Analysis of enzyme-inhibitor levels has the disadvantage to detect only the inactivated enzyme

Alternative assay procedures dependent upon the detection of specific HNE cleavage products have thus been pursued.

While the main target for extracellular elastase is elastin**, t**he main intercellular physiological function of neutrophil elastase is the degradation of foreign organic molecules phagocytosed by neutrophils. By degrading almost all extracellular matrix and key plasma proteins, HNE is the most destructive enzyme. In addition to elastin and extra-cellular matrix proteins, neutrophil elastase is known to degrade types I–IV collagen, proteoglycan, fibronectin, platelet IIb/IIIa receptor, complement receptor, thrombomodulin, lung surfactant, and cadherins. [153, 154]. Moreover, it possesses fibrinogenolytic capacity, with a high susceptibility towards degradation of the Aα-chain. [155].

Human fibrinogen (FBN) is a heterodimeric glycoprotein consisting of 3 non-identical chains, Aα, Bβ and γ. It has been recognized as a COPD biomarker [156]. As shown in Fig.30, elastase cleaves human fibrinogen at multiple sites: Aa (Val^{21}), Aa (Val^{360}), Aa (Thr^{568}). The Aa (Val^{360}) signal is present in all normal human plasma samples assayed to date and is elevated in cystic fibrosis plasma samples.

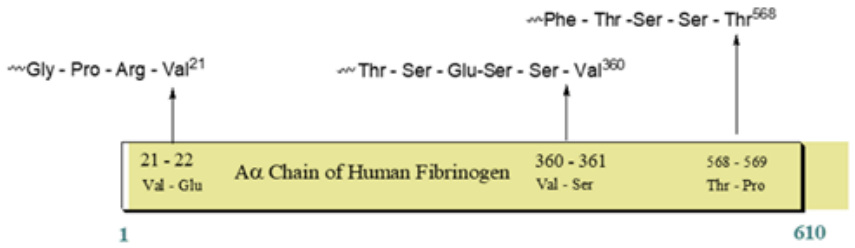

Figure 30. Cleavage sites of Human fibrinogen Aα Chain

Cartel et al. have developed a unique assay based on the detection of HNE-specific fibrinogen degradation product (Aα-Val360) [157]. They have demonstrated that the amount of this fragment is significantly greater in plasma of subjects with AAT deficiency than in healthy controls, indicating an imbalance *in vivo* in the protease/antiprotease ratio at sites of inflammation where fibrinogen is deposited. Therefore, Aα(Val360) may be considered a tool for identifying subjects with progressive disease at an early stage and as a measurement of the emphysematous status.

To generate this cleavage product, FBN (200 nmol) was incubated with HNE (1 nmol) for 1 h at 37ºC. From among the several fractions separated by HPLC (Fig. 31), the Aα(Val360) fraction was collected and its purity demonstrated by chromatography [158].

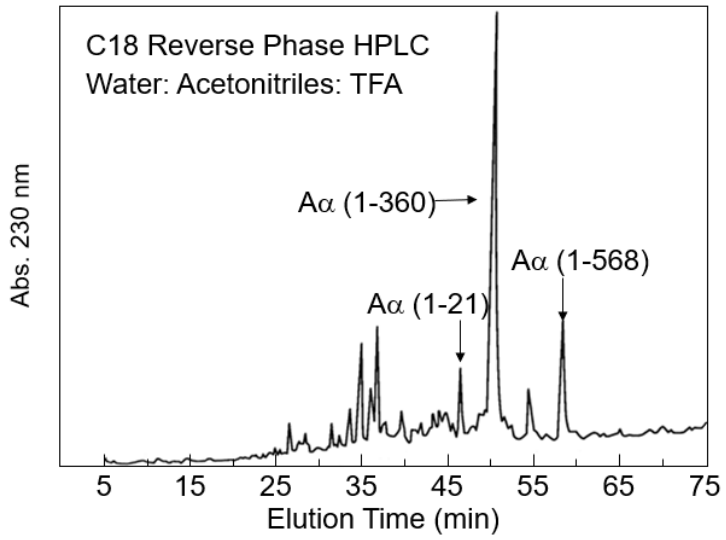

Figure 31. Generation of Multiple Cleavage Products from Human Fibrinogen by HNE

There is evidence that the Aa (Val^{360}) Neoepitope is a time dependent product of the HNE-FBN incubation (Fig. 32).

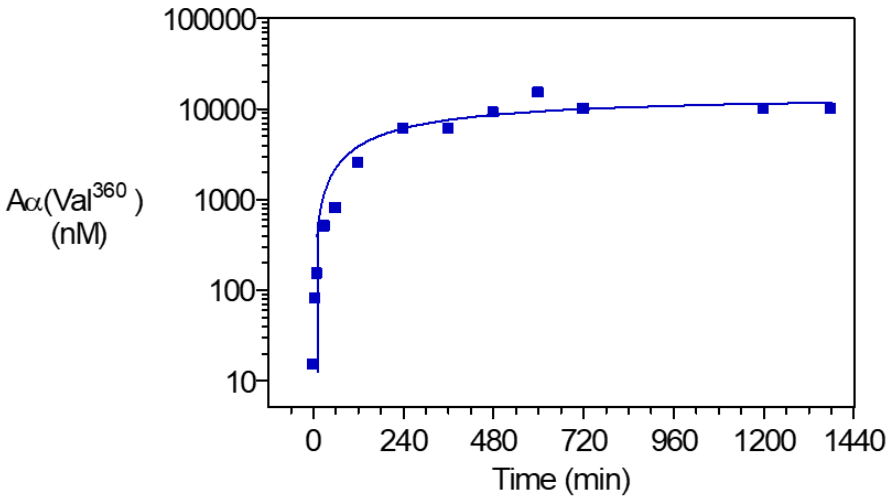

Figure 32. Incubation of human fibrinogen and HNE as a function of time at an enzyme ratio of 1:250

To detect Aα-Val360 in biological fluids Cartel et al developed an antiserum against this specific FBN neoepitope. To this purpose they submitted rabbits to an immunization protocol with Thyroglobulin-CJTSESSV (Fig. 33) to produce specific Ab against Aα-Val360 on the Aα chain of fibrinogen.

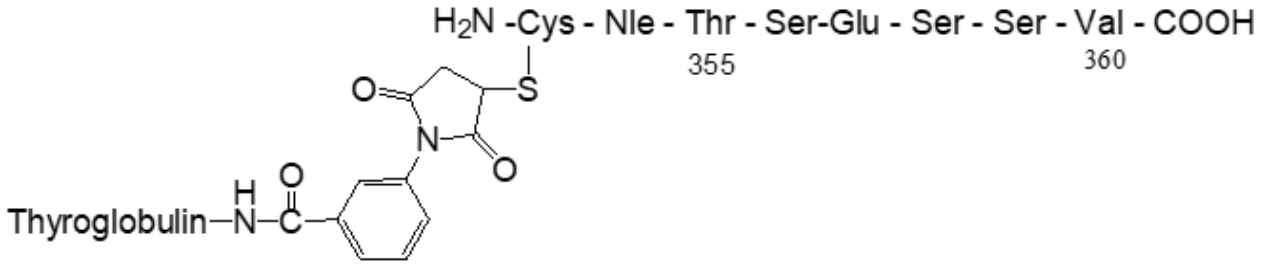

Figure 33. Thyroglobulin-CJTSESSV employed to develop the specific Ab against Aα-Val360

The results of this experiment are shown in the western blotting of Figure 34.

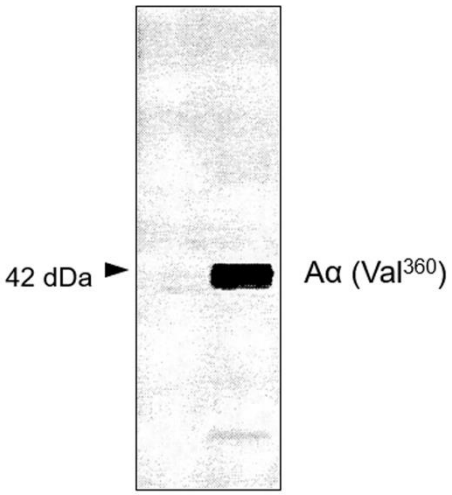

Figure 34. Western Blotting to confirm the production of the specific Ab against Aα-Val360

A specific and sensitive assay is crucial to detect the low levels of Aα-Val360.

To this purpose, I have spent three months at the laboratory of Dr. Stolk, head of the Department of Pulmonology, Leiden University Medical Center (NL) to use a DELFIA® immunoassay, a suitable alternative to traditional ELISA, in which the use of an enzyme is not required.

The technical procedure is shown in Figure 35:

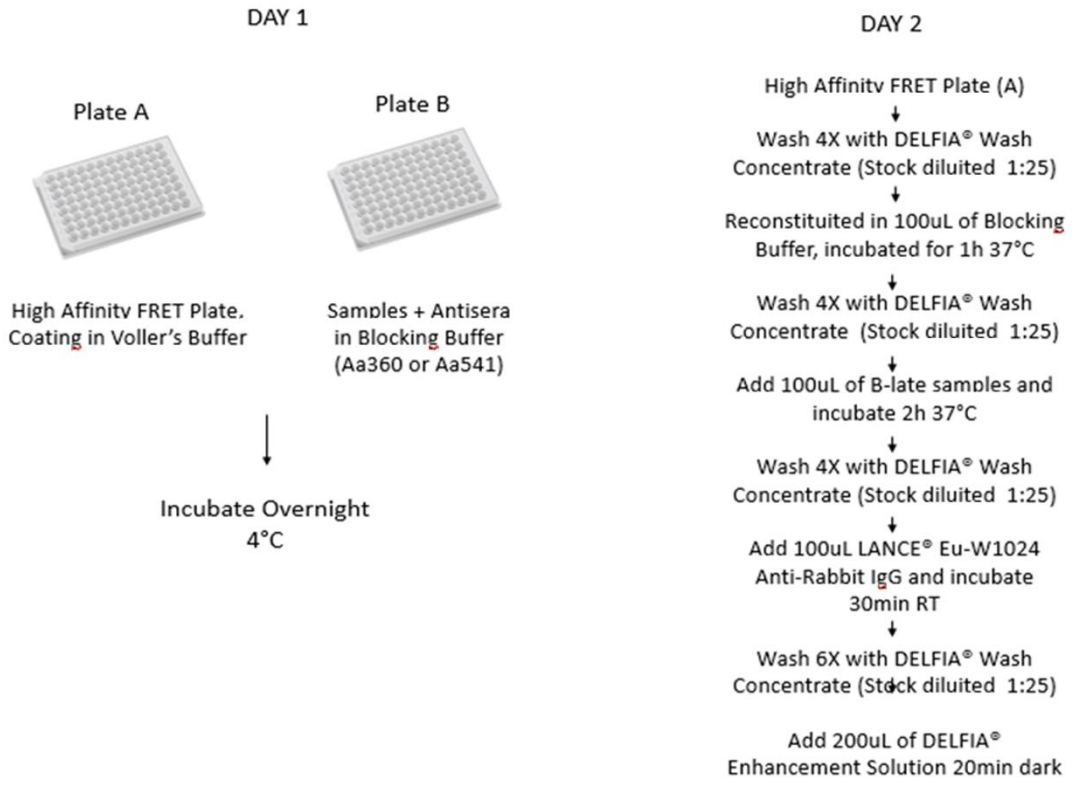

Figure 35. Technical protocol of DELFIA assay

DELFIA® Enhancement Solution is used to create a fluorescent Europium chelate for measuring DELFIA time-resolved fluorescence (TRF) assays as show in Fig. 36. The chelates have been developed from three lanthanides with spectra clearly distinguishable based on decay time and wavelength. The narrow emission peak is 613 nm for Europium (Eu).

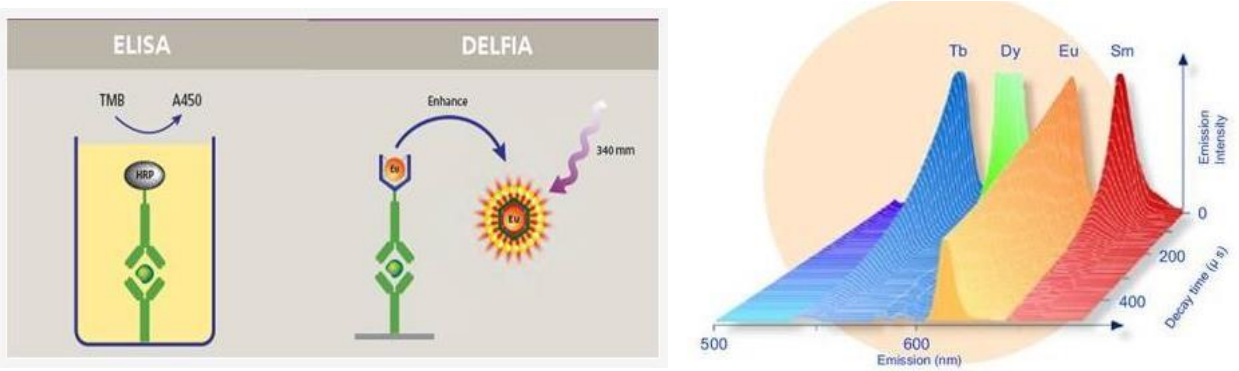

Figure 36. comparison between DELFIA and ELISA assays

These preliminary experiments were aimed to develop the appropriate experimental conditions for measuring Aα-Val360 in plasma samples obtained from healthy controls (n=10) and AATD patients (n=23). The results shown in Figure 37 evidence that significant differences between the two cohorts could be identified.

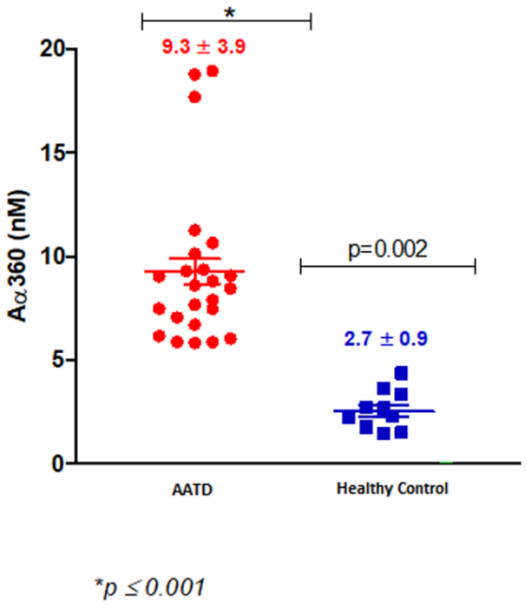

Figure 37. Aα360 Levels in Human Plasma

Based on these encouraging results, the intention would be to apply the same approach on BALf samples from lung transplant patients to detect Aα-Val360 as a new biomarker of HNE activity and to perform new western blotting to validate the procedure.

As compared to colorimetric ELISA, the DELFIA has a 10-fold enhancement of sensitivity and this increase allows for the use of lower sample volumes per well and will certainly be useful for those researchers who need to quantitate low levels of this fibrinopeptide.

AAT augmentation therapy

Although currently BOS has no effective therapies, what matters to patients (and doctors) is to stop or slow down the decline of FEV1 [94, 159, 160]. To this purpose, future treatments will have to make use of combinations of drugs and treatments that, as much as possible, prevent the onset of the disease or stabilize it once established. Current therapies are aimed at reducing exposure to risk factors such as infection and production of autoantibodies and anti-HLA antibodies.

Alpha-1 antitrypsin augmentation therapy (<11 µmol/L) was developed, since the late nineties, originally for patients with chronic obstructive pulmonary disease associated with AAT deficiency (161, 162). Cost effectiveness of intravenous augmentation therapy needs to be improved and, to slow down the FEV1 decline, aerosol administration is the most suitable candidate to counteract proteolytic tissue damage. Inhalation therapy is painless and relatively convenient and offers the opportunity for easier and more efficient delivery of AAT directly to the respiratory system [163].

As known, AAT deficiency is not the only condition characterized by neutrophilic inflammation and increased proteolytic activity. This was the rationale for hypothesizing that inhaled AAT in the airspaces could improve, slow or stop the progression of bronchiectasis in BOS patients.

Our proposal is that the “best” BOS stage should be selected to start with the administration of Alpha-1 antitrypsin. Obviously, only an appropriate longitudinal analysis of patients that develop BOS disease could answer this question.

A preliminary longitudinal study on 14 patients confirmed that the formation of AAT-HNE complex was concomitant with the level of severity of BOS. Based on these data, it can be speculated that BOS I is the most appropriate stage for Alpha-1 antitrypsin administration. Being this stage characterized by possible reversibility of pulmonary alterations, it could represent a good starting point for treatment of patients.

REFERENCES

[1] Chambers DC, Yusen RD, Cherikh WS, Goldfarb SB, Kucheryavaya AY, Khusch K, Levvey BJ, Lund LH, Meiser B, Rossano JW, et al. The Registry of the International Society for Heart and Lung Transplantation: Thirty-fourth Adult Lung And Heart-Lung Transplantation Report-2017; Focus Theme: Allograft ischemic time. **J Heart Lung Transplant**. 2017; 36(10):1047–59. DOI: 10.1016/j.healun.2017.07.016.

[2] Hardy JD, Araslan S, Webb WR. Transplantation of the lung. **Ann Surg** 1964;160: 440-448.

[3] Wolfe RA, Roys EC, Merion RM. Trends in organ donation and transplantation in the United States, 1999-2008. **Am J Transplant**. 2010; 10:961–972. DOI: 10.2215/CJN.09300913.

[4] Lehmann S, Uhlemann M, Leontyev S, Seeburger J, Garbade J, Merk DR, Bittner HB, Mohr FW. Bilateral versus single lung transplant for idiopathic pulmonary fibrosis. **Exp Clin Transplant.** 2014;12(5):443-7.

[5] Thabut G, Christie JD, Ravaud P, et al. Survival after bilateral versus single-lung transplantation for idiopathic pulmonary fibrosis. **Ann Intern Med**. 2009; 151(11): 767-74. DOI: 10.7326/0003-4819-151-11-200912010-00004.

[6] Weiss ES, Allen JG, Merlo CA, et al. Survival after single versus bilateral lung transplantation for high-risk patients with pulmonary fibrosis. **Ann Thorac Surg**. 2009;88(5):161625.

[7] Le Moine A, Goldman M, Abramowicz D. Multiple pathways to allograft rejection. **Transplantation**. 2002; 73(9):1373–1381.

[8] Gorer PA. The genetic and antigenic basis of tumor transplantation. **J Pathol Bacteriol**. 2005; 1937; 44:691–7. DOI: 10.1002/path.1700440313.

[9] Snyder LD, Palmer SM. Immune mechanisms of lung allograft rejection. **Semin Respir Crit Care Med**. 2006; 27: 534-43. DOI: 10.1055/s-2006-954610.

[10] Inaba K, Turley S, Yamaide F, Iyoda T, Mahnke K, Inaba M, et al. Efficient presentation of phagocytosed cellular fragments on the major histocompatibility complex class II products of dendritic cells. **J Exp Med**. 1998; 188: 2163–73. DOI: 10.1084/jem.188.11.2163.

[11] Lechler RI, Batchelor JR. Immunogenicity of retransplanted rat kidney allografts. Effect of inducing chimerism in the first recipient and quantitative studies of immunosuppression of the second recipient. **J Exp Med**. 1982; 156:1835–41.

[12] Martinu T, Chen Dong-Feng and Palmer Scott M. Acute Rejection and Humoral Sensitization in Lung Transplant Recipients. **Proc Am Thorac Soc**. 2009; 6(1): 54-65. DOI:10.1513/pats.200808-080GO.

[13] Vanaudenaerde BM, Dupont LJ, Wuyts WA, Verbeken EK, Meyts I, Bullens DM, Dilissen E, Luyts L, Van Raemdonck DE, Verleden GM. The role of interleukin-17 during acute rejection after lung transplantation. **Eur Respir J**. 2006; 27:779–787. DOI: 10.1164/rccm.200601-071OC.

[14] Linden A, Laan M, Anderson G.P. Neutrophils, interleukin- 17A and lung disease. **Eur Respir J** 2005; 25: 159–172. DOI: 10.1183/09031936.06.00019405.

[15] Gauthier JM, Hachem RR, Kreisel D. Update on Chronic Lung Allograft Dysfunction. **Curr Transplant Rep**. 2016; 3(3): 185–191. doi: 10.1007/s40472-016-0112-y.

[16] Hsiao HM, Scozzi D, Gauthier JM, Kreisel D. Mechanisms of Graft Rejection after Lung Transplantation. **Curr Opin Organ Transplant**. 2017; 22(1): 29–35.

[17] Verleden SE, Todd JL, Sato M, Palmer SM, Martinu T, Pavlisko EN, Vos R, Neyrinck A, Van Raemdonck D, Saito T, Oishi H, Keshavjee S, Greer M, Warnecke G, Gottlieb J, Haverich A. Impact of CLAD Phenotype on Survival After Lung Retransplantation: A Multicenter Study. **Am J Transplant**. 2015;15(8):2223-30. doi: 10.1111/ajt.13281.

[18] Royer PJ, Olivera-Botello G, Koutsokera A, Aubert JD, Bernasconi E, Tissot A, Pison C, Nicod L, Boissel JP, Magnan A, et al. Chronic Lung Allograft Dysfunction: A Systematic Review of Mechanisms. **Transplantation.** 2016; 100(9):1803–14. DOI: 10.1097/TP.0000000000001215.

[19] Sato M, Waddell TK, Wagnetz U, et al. Restrictive allograft syndrome (RAS): a novel form of chronic lung allograft dysfunction. J Heart Lung Transplant. **2011**; 30:735–742. DOI: 10.1016/j.healun.2011.01.712.

[20] Hinz B, Phan SH, Thannickal VJ, Galli A, Bochaton-Piallat ML, Gabbiani G. The myofibroblast. One function, multiple origins. **Am J Pathol**. 2007; 170:1807-16. DOI: 10.12691/ajmsm-1-6-4.

[21] Finlen Copeland CA, Snyder LD, Zaas DW, et al. Survival after bronchiolitis obliterans syndrome among bilateral lung transplant recipients. **Am J Respir Crit Care Med**. 2010; 182:784-9. DOI:10.1164/rccm.201002-0211OC.

[22] Heng D, Sharples LD, McNeil K, et al. Bronchiolitis obliterans syndrome: incidence, natural history, prognosis, and risk factors**. J Heart Lung Transplant**. 1998; 17(12):1255-63.

[23] Stewart S, Fishbein MC, Snell GI, et al. Revision of the 1996 working formulation for the standardization of nomenclature in the diagnosis of lung rejection. **J Heart Lung Transplant**. 2007; 26(12):1229–1242. DOI: 10.1016/j.healun.2007.10.017.

[24] Yousem SA, Berry GJ, Cagle PT, et al. Revision of the 1990 working formulation for the classification of pulmonary allograft rejection: Lung Rejection Study Group. **J Heart Lung Transplant**. 1996; 15(1Pt1):1–15.

[25] Palmer SM, Burch LH, Trindade AJ, et al. Innate immunity influences long-term outcomes after human lung transplant. **Am J Respir Crit Care Med**. 2005; :780–785. DOI:10.1164/rccm.200408- 1129OC.

[26] Grossman EJ, Shilling R. Bronchiolitis obliterans in lung transplantation: the good, the bad, and the future. **Translational Research.** 2009; 153: 153-165.

[27] Hayes D Jr. A review of bronchiolitis obliterans syndrome and therapeutic strategies. **J Cardiothorac Surg.** 2011 Jul 18;6:92. doi: 10.1186/1749-8090-6-92.

[28] Sharples LD, McNeil K, Stewart S, Wallwork J. Risk factors for bronchiolitis obliterans: a systematic review of recent publications. **J Heart Lung Transplant**. 2002 Feb;21(2):271-81.

[29] Scozzi D, Ibrahim M, Menna C, Krupnick AS, Kreisel D, Gelman AE. The Role of Neutrophils in Transplanted Organs**. Am J Transpla**nt. 2017 Feb;17(2):328-335. doi: 10.1111/ajt.13940

[30] Madill J, Aghdassi E, Arendt B, Hartman-Craven B, Gutierrez C, Chow CW, Allard J. Lung transplantation: does oxidative stress contribute to the development of bronchiolitis obliterans syndrome? **Transplant Rev** (Orlando). 2009;23(2):103-10. doi: 10.1016/j.trre.2009.01.003.

[31] Weigt SS, DerHovanessian A, Wallace WD, Lynch JP 3rd, Belperio JA. Bronchiolitis obliterans syndrome: the Achilles' heel of lung transplantation. **Semin Respir Crit Care Med**. 2013 Jun;34(3):336-51. doi: 10.1055/s-0033-1348467.

[32] Kinoshita T, Goto T. Molecular Mechanisms of Pulmonary Fibrogenesis and Its Progression to Lung Cancer: A Review. **Int J Mol Sci.** 2019;20(6). pii: E1461. doi: 10.3390/ijms20061461.

[33] Park JE, Kim CY, Park MS, Song JH, Kim YS, Lee JG, Paik HC, Kim SY. Prevalence of pre-transplant anti-HLA antibodies and their impact on outcomes in lung transplant recipients. **BMC Pulm Med**. 2018;18(1):45. doi: 10.1186/s12890-018-0606-8.

[34] Smith MA, Sundaresan S, Mohanakumar T, Trulock EP, Lynch JP, Phelan DL, Cooper JD, Patterson GA. Effect of development of antibodies to HLA and cytomegalovirus mismatch on lung transplantation survival and development of bronchiolitis obliteranssyndrome. **J Thorac Cardiovasc Surg**. 1998; 116:812–820. DOI: 10.1016/S0022-5223(98)00444-9.

[35] Luckraz H, Sharples L, McNeil K, Wreghitt T, Wallwork J. Cytomegalovirus antibody status of donor/recipient does not influence the incidence of bronchiolitis obliterans syndrome in lung transplantation**. J Heart Lung Transplant**. 2003; 22: 287–291. DOI: 10.1016/S1053- 2498(02)00471-0.

[36] Fisichella PM, Davis CS, Kovacs EJ. A review of the role of GERD-induced aspiration after lung transplantation. **Surg Endosc**. 2012 May;26(5):1201-4. doi: 10.1007/s00464-011-2037-y.

[37] Todd JL, Palmer SM. Bronchiolitis obliterans syndrome: the final frontier for lung transplantation. **Chest.** 2011;140(2):502-508. doi: 10.1378/chest.10-2838.

[38] Oikonomopoulou K, Hansen KK, Saifeddine M, Vergnolle N, Tea I, Diamandis EP, Hollenberg MD. Proteinase-mediated cell signalling: targeting proteinase-activated receptors (PARs) by kallikreins and more. **Biol Chem**. 2006;387(6):677-85.

[39] López-Otín C, Bond JS. Proteases: multifunctional enzymes in life and disease. **J Biol Chem**. 2008;283(45):30433-7. doi: 10.1074/jbc.R800035200.

[40] Chillappagari S, Preuss J, Licht S, Müller C, Mahavadi P, Sarode G, Vogelmeier C, Guenther A, Nahrlich L, Rubin BK, Henke MO. Altered protease and antiprotease balance during a COPD exacerbation contributes to mucus obstruction. **Respir Res**. 2015; 16:85. doi: 10.1186/s12931-015-0247-x.

[41] Menou A, Duitman J, Crestani B. The impaired proteases and anti-proteases balance in Idiopathic Pulmonary Fibrosis. **Matrix Biol**. 2018;68-69:382-403. doi: 10.1016/j.matbio.2018.03.001.

[42] Korkmaz B, Moreau T, Gauthier F. Neutrophil elastase, proteinase 3 and cathepsin G: physicochemical properties, activity and physiopathological functions. **Biochimie**. 2008;90(2):227-42. Epub 2007 Oct 25.

[43] Borregaard, N. Neutrophils, from marrow to microbes. **Immunit.** 2010; 33, 657–670. DOI 10.1016/j.immuni.2010.11.011.

[44] Nathan, C. Neutrophils and immunity: challenges and opportunities. **Nature Rev. Immunol.** 2006; 6, 173–182. DOI: 10.1038/nri178.

[45] Mantovani A, Cassatella MA, Costantini C, Jaillon S. Neutrophils in the activation and regulation of innate and adaptive immunity. **Nat Rev Immunol**. 2011;11(8):519–31. DOI: 10.1038/nri3024.

[46] Page, M.J., Di Cera, E. Serine peptidases: classification, structure and function. **Cell Mol. Life Sci**. 2008; 65, 1220–1236. DOI: 10.1007/s00018-008-7565-9.

[47] Hedstrom L. Serine protease mechanism and specificity. **Chem. Rev** 2002; 102:4501–4524. DOI: 10.1021/cr000033x.

[48] Blow DM, Birktoft JJ, Hartley BS. Role of a buried acid group in the mechanism of action of chymotrypsin. **Nature.** 1969; 221:337–340.

[49] Fujinaga M, Chernaia MM, Halenbeck R, Koths K, and James MN (1996) The crystal structure of PR3, a neutrophil serine proteinase antigen of Wegener's granulomatosis antibodies. **J Mol Biol**. 1996. 261:267–278. DOI: 10.1006/jmbi.1996.0458.

[50] Hof P, Mayr I, Huber R, Korzus E, Potempa J, Travis J, Powers JC, and Bode W. The 1.8 A crystal structure of human cathepsin G in complex with Suc-Val-Pro-PheP-(OPh)2: a Janus-faced proteinase with two opposite specificities. **EMBO J.** 1996; 15:5481–5491. DOI: 10.1002/j.1460- 2075.1996.tb00933.x.

[51] Heutinck KM, ten Berge IJ, Hack CE, Hamann J, Rowshani AT. Serine proteases of the human immune system in health and disease. **Mol Immunol**. 2010 DOI: 10.1016/j.molimm.2010.04.020.

[52] Rothman SS. The digestive enzymes of the pancreas: a mixture of inconstant proportions. **Annu. Rev. Physiol.** 1977; 39:373–389. DOI: 10.1146/annurev.ph.39.030177.002105.

[53] Huntington, J.A., Read, R.J., Carrell, R.W. Structure of a serpin-protease complex shows inhibition by deformation**. Nature**. 2000; 407, 923–926. DOI: 10.1038/35038119.

[54] Irving, J. A., Pike, R. N., Lesk, A. M., Whisstock, J. C. Phylogeny of the serpin superfamily: implications of patterns of amino acid conservation for structure and function. **Genome Res.** 2000; 10, 1845–1864. DOI: 10.1101/gr.GR-1478R.

[55] Irving, J. A., Steenbakkers, P. J., Lesk, A. M., Op den Camp, H. J., Pike, R. N., Whisstock, J. C. Serpins in prokaryotes. **Mol. Biol. Evol**. 2002; 19, 1881–1890. DOI: 10.1093/oxfordjournals.molbev.a004012.

[56] Silvestre-Roig C, Hidalgo A, Soehnlein O. Neutrophil heterogeneity: implications for homeostasis and pathogenesis. **Blood.** 2016;127(18): 2173–81. DOI: 10.1182/blood-2016-01-688887.

[57] Weissmann G, Smolen JE, Korchak HM. Release of inflammatory mediators from stimulated neutrophils. **N Engl J Med**. 1980; 303(1):27–34. DOI: 10.1056/NEJM198007033030109.

[58] Zimmer M, Medcalf RL, Fink TM, Mattmann C, Lichter P, and Jenne DE. Three human elastaselike genes coordinately expressed in the myelomonocyte lineage are organized as a single genetic locus on 19pter. **Proc Natl Acad Sci USA**. 1992; 89:8215–8219. DOI: 10.1073/pnas.89.17.8215.

[59] Caughey GH, Schaumberg TH, Zerweck EH, Butterfield JH, Hanson RD, Silverman GA, and Ley TJ. The human mast cell chymase gene (CMA1): mapping to the cathepsin G/granzyme gene cluster and lineage-restricted expression. Genomics. 1993; 15:614–620. DOI: 10.1006/geno.1993.1115.

[60] Bode W, Wei AZ, Huber R, Meyer E, Travis J, and Neumann S (1986) X-ray crystal structure of the complex of human leukocyte elastase (PMN elastase) and the third domain of the turkey ovomucoid inhibitor. **EMBO J** 1986; 5:2453–2458.

[61] Weinrauch Y, Drujan D, Shapiro SD, Weiss J, and Zychlinsky A. Neutrophil elastase targets virulence factors of enterobacteria. **Nature.** 2002; 417:91–94. DOI: 10.1038/417091a.

[62] Stockley, R. A. Neutrophils and the pathogenesis of COPD. **Chest.** 2002. DOI: 10.1378/chest.121.5.

[63] Liou, T. G.; Campbell, E. J. Nonisotropic enzyme-inhibitor interactions: A novel nonoxidative mechanism for quantum proteolysis by human neutrophils. **Biochemistry**. 1995; 34, 16171. DOI: 10.1021/bi00049a032.

[64] Liou, T. G.; Campbell, E. J. J. Quantum proteolysis resulting from release of single granules by human neutrophils: a novel, nonoxidative mechanism of extracellular proteolytic activity. **Immunol.** 1996, 157, 2624.

[65] Sandhaus RA, Turino G. Neutrophil elastase-mediated lung disease. **COPD**. 2013;10: 60–3. DOI: https://doi.org/10.3109/15412555.2013.764403

[66] Silverman GA, Bird PI, Carrell RW, Church FC, Coughlin PB, Gettins PG, Irving JA, Lomas DA, Luke CJ, Moyer RW, et al. The serpins are an expanding superfamily of structurally similar but functionally diverse proteins. Evolution, mechanism of inhibition, novel functions, and a revised nomenclature. **J Biol Chem** 2001 276:33293–33296. DOI: 10.1074/jbc.R100016200.

[67] Mangan MS, Kaiserman D, and Bird PI. The role of serpins in vertebrate immunity. **Tissue Antigens**. 2008; 72:1–10. DOI: 10.1111/j.1399-0039.2008.01059. x.

[68] Hunt, L. T., Dayhoff, M. O. A surprising new protein superfamily containing ovalbumin, antithrombin-III, and 1-proteinase inhibitor. **Biochem. Biophys. Res. Commun.** 1980; 95, 864–871. DOI: 10.1016/0006-291X(80)90867-0.

[69] Potempa J, Korzus E, and Travis J. The serpin superfamily of proteinase inhibitors: structure, function, and regulation**. J Biol Chem**. 1994; 269:15957–15960.

[70] Carrell RW, Mushunje A, Zhou A. Serpins show structural basis for oligomer toxicity and amyloid ubiquity. **FEBS Lett**. 2008 Jul 23;582(17):2537-41. doi: 10.1016/j.febslet.2008.06.021.

[71] Lucas A, Yaron JR, Zhang L, Ambadapadi S. Overview of Serpins and Their Roles in Biological Systems. **Methods Mol Biol**. 2018;1826:1-7. doi: 10.1007/978-1-4939-8645-3_1.

[72] Gettins, P. G. Serpin structure, mechanism, and function. **Chem. Rev**. 2002; 102, 4751–4804. DOI: 10.1021/cr010170.

[73] Whisstock, J. C., Bottomley, S. P. Molecular gymnastics: serpin structure, folding and misfolding. **Curr. Opin. Struct. Biol**. 2006; 16, 761–768. DOI: 10.1016/j.sbi.2006.10.005.

[74] Sun, J., Whisstock, J. C., Harriott, P., Walker, B., Novak, A., Thompson, P. E., Smith, A. I., Bird, P. I. Importance of the P4_ residue in human granzyme B inhibitors and substrates revealed by scanning mutagenesis of the proteinase inhibitor 9 reactive center loop. **J. Biol. Chem**. 2001; 276, 15177–15184. DOI: 10.1074/jbc.M006645200.

[75] Calugaru SV, Swanson R, Olson ST. The pH dependence of serpinproteinase complex dissociation reveals a mechanism of complex stabilization involving inactive and active conformational states of the proteinase which are perturbable by calcium. **J Biol Chem**. 2001; 276: 32446–55. DOI: 10.1074/jbc.M104731200.

[76] Tew DJ, Bottomley SP: Intrinsic fluorescence changes and rapid kinetics of proteinase deformation during serpin inhibition. **FEBS Lett**. 2001, 494:30-33. DOI: 10.1016/S0014-5793(01)02305-5.

[77] Dementiev, A., Dobo, J., Gettins, P. G. Active site distortion is sufficient for proteinase inhibition by serpins: structure of the covalent complex of 1-proteinase inhibitor with porcine pancreatic elastase. **J. Biol. Chem**. 2006; 281, 3452–3457.

[78] Lomas DA, Parfrey H. Alpha1-antitrypsin deficiency: Molecular pathophysiology. **Thorax**. 2004 Jun;59(6):529 35.

[79] Karadagi A, Johansson H, Zemack H, Salipalli S, Mörk LM, Kannisto K, Jorns C, Gramignoli R, Strom S, Stokkeland K, Ericzon BG, Jonigk D, Janciauskiene S, Nowak G, Ellis ECS. Exogenous alpha 1-antitrypsin down-regulates SERPINA1 expression. **PLoS One**. 2017 May 9;12(5):e0177279. doi: 10.1371/journal.pone.0177279.

[80] Calabrese F, Giacometti C, Beghe B, Rea F, Loy M, Zuin R, Marulli G, Baraldo S, Saetta M, Valente M. Marked alveolar apoptosis/proliferation imbalance in end-stage emphysema. **Respir Res**. 2005; 6:14.

[81] Petrache I, Fijalkowska I, Medler TR, Skirball J, Cruz P, Zhen L, Petrache HI, Flotte TR, Tuder RM. Alpha-1 antitrypsin inhibits caspase-3 activity, preventing lung endothelial cell apoptosis. **Am J Pathol**. 2006;169(4):1155-66.

[82] Stoller JK, Aboussouan LS. A review of a1-antitrypsin deficiency. **Am J Respir Crit Care Med.** 2012; 185: 246–59. DOI: 10.1164/rccm.201108-1428CI.

[83] Janciauskiene SM, Bals R, Koczulla R, Vogelmeier C, Köhnlein T, Welte T. The discovery of a1-antitrypsin and its role in health and disease. **Respir Med.** 2011; 105: 1129–39. DOI: 10.1016/j.rmed.2011.02.002.

[84] Kalsheker N, Morley S, Morgan K. Gene regulation of the serine proteinase inhibitors α1-antitrypsin and α1-antichymotrypsin. **Biochem. Soc. Trans**. 2002; 30, 93–98. DOI: 10.1042/0300-5127:0300093.

[85] Johnson D, Travis J: The oxidative inactivation of human alpha1-proteinase inhibitor: furthernevidence for the methionine at the active center. **J Biol Chem**. 1979; 254:4022-4026.

[86] Ciliberto, G., Dente, L. & Cortese, R. Cell-specific expression of a transfected human α1-antitrypsin gene. **Cell.** 1985; 41, 531–540. DOI: 10.1016/S0092-8674(85)80026-X.

[87] Rollini, P., Fournier, R. E. Differential regulation of gene activity and chromatin structure within the human serpin gene cluster at 14q32.1 in macrophage microcell hybrids. **Nucleic Acids Res**. 2000; 28, 1767–1777. DOI: 10.1093/nar/28.8.1767.

[88] Boutten A, Venembre P, Seta N: Oncostatin M is a potent stimulator of alpha1-antitrypsin secretion in lung epithelial cells: modulation by transforming growth factor-beta and interferon-gamma. **Am J Respir Cell Mol Biol**. 1998; 18:511-520. DOI: 10.1165/ajrcmb.18.4.2772.

[89] Zhou L, Twinning SS, Yue BY: Involvement of Sp1 elements in the promoter activity of alpha1- proteinase inhibitor gene. **J Biol Chem**. 1998; 273:9959-9965.

[90] DeMeo DL and Silverman EK. Alpha1-antitrypsin deficiency, 2: genetic aspects of alpha1-antitrypsin deficiency: phenotypes and genetic modifiers of emphysema risk. **Thorax**. 2004; 59: 259-64. DOI: 10.1136/thx.2003.006502.

[91] Luisetti M, Seersholm N. Alpha1-antitrypsin deficiency. 1: epidemiology of alpha1-antitrypsin deficiency. **Thorax**. 2004; 59:164-169. DOI: 10.1136/thorax.2003.006494.

[92] Curiel DT, Holmes MD, Okayama H, et al. Molecular basis of the liver and lung disease associated with the alpha 1-antitrypsin deficiency allele M malton. **J Biol Chem**. 1989; 264:13938–45.

[93] Laurell CB, Eriksson S: The electrophoretic pattern alpha1- globulin pattern of serum in alpha1-antitrypsin deficiency. **Scan J Clin Lab Invest**. 1963, 15:132-140. DOI: 10.3109/15412555.2013.771956.

[94] Stockley RA, Miravitlles M, Vogelmeier C. Augmentation therapy for alpha-1 antitrypsin deficiency: towards a personalised approach. **Orphanet J Rare Dis**. 2013;8:149. doi: 10.1186/1750-1172-8-149.

[95] Piloni D, Morosini M, Magni S, Balderacchi A, Scudeller L, Cova E, et al. Analysis of long term CD4+CD25highCD127- T-reg cells kinetics in peripheral blood of lung transplant recipients. **BMC Pulm Med.** 2017; 17: 102. DOI: 10.1186/s12890-017-0446-y.

[96] Meloni F, Solari N, Miserere S, Morosini M, Cascina A, Klersy C, et al. Chemokine redundancy in BOS pathogenesis. A possible role also for the CC chemokines: MIP3-beta, MIP3-alpha, MDC and their specific receptors. **Transpl Immunol**. 2008; 18: 275–280. DOI: 10.1016/j.trim.2007.08.004.

[97] Estenne M, Hertz MI. Bronchiolitis obliterans after human lung transplantation**. Am J Respir Crit Care Med.** 2002; 166: 440–444.

[98] Verleden GM, Vos R, Vanaudenaerde B, Dupont L, Yserbyt J, Van Raemdonck D, et al. Current views on chronic rejection after lung transplantation. **Transpl Int.** 2015; 28: 1131-1139. DOI: 10.1111/tri.12579.

[99] Del Fante C, Scudeller L, Oggionni T, Viarengo G, Cemmi F, Morosini M, et al. Long-Term Off-Line Extracorporeal Photochemotherapy in Patients with Chronic Lung Allograft Rejection Not Responsive to Conventional Treatment: A 10-Year Single-Centre Analysis. **Respiration**. 2015; 90: 118-128. DOI: 10.1159/000431382.

[100] Lilleri D, Gerna G, Bruno F, Draghi P, Gabanti E, Fornara C, et al: Systemic and local human cytomegalovirus-specific T-cell response in lung transplant recipients. **New Microbiol**. 2013; 36: 267–277.

[101] Smith PK, Krohn RI, Hermanson GT, Mallia AK, Gartner FH, Provenzano MD, et al. Measurement of protein using bicinchoninic acid. **Anal Biochem.** 1985; 150, 76-85. DOI: 10.1016/0003-2697(85)90442-7.

[102] Candiano G., Bruschi M, Musante L, Santucci L, Ghiggeri GM, Carnemolla B. Blue silver: a very sensitive colloidal coomassie G-250 staining for proteome analysis. **Electrophoresis.** 2004; 25:1327-1333. DOI: 10.1002/elps.200305844.

[103] Di Venere M, Fumagalli M, Cafiso A, De Marco L, Epis S, Plantard O, et al. Ixodes ricinus and Its Endosymbiont Midichloria mitochondrii: A Comparative Proteomic Analysis of Salivary Glands and Ovaries. **PLoS One.** 2015; 10: e0138842. 10.1371/journal.pone.0138842.

[104] Di Silvestre D, Brambilla F, Scardoni G, Brunetti P, Motta S, Matteucci M, Laudanna C, Recchia FA, Lionetti V, Mauri P. Proteomics-based network analysis characterizes biological processes and pathways activated by preconditioned mesenchymal stem cells in cardiac repair mechanisms. **Biochim Biophys Acta Gen Subj**. 2017; 1861(5 Pt A):1190-1199. doi: 10.1016/j.bbagen.2017.02.006.

[105] Carvalho PC1, Hewel J, Barbosa VC, Yates JR 3rd. Identifying differences in protein expression levels by spectral counting and feature selection. **Genet Mol Res.** 2008 Apr 15;7(2):342-56.

[106] Hilario M, Kalousis A. Approaches to dimensionality reduction in proteomic biomarker studies. **Brief Bioinform.** 2008 Mar;9(2):102-18. doi: 10.1093/bib/bbn005.

[107] Mauri P, Dehò G. A proteomic approach to the analysis of RNA degradosome composition in Escherichia coli. **Methods Enzymol**. 2008;447:99-117. doi: 10.1016/S0076-6879(08)02206-4.

[108] Pain M, Royer PJ, Loy J, Girardeau A, Tissot A, Lacoste P, Roux A, Reynaud-Gaubert M, Kessler R, Mussot S, Dromer C, Brugière O, Mornex JF, Guillemain R, Dahan M, Knoop C, Botturi K, Pison C, Danger R, Brouard S, Magnan A. T Cells Promote Bronchial Epithelial Cell Secretion of Matrix Metalloproteinase-9 via a C-C Chemokine Receptor Type 2 Pathway: Implications for Chronic Lung Allograft Dysfunction. **Am J Transplant.** 2017;17(6):1502-1514. doi: 10.1111/ajt.14166.

[109] Pugh C1, Hathwar V, Richards JH, Stonehuerner J, Ghio AJ. Disruption of iron homeostasis in the lungs of transplant patients. **J Heart Lung Transplant**. 2005 Nov;24(11):1821-7.

[110] Ohshimo S, Bonella F, Sommerwerck U, Teschler H, Kamler M, Jakob HG, Kohno N, Guzman J, Costabel U. Comparison of serum KL-6 versus bronchoalveolar lavage neutrophilia for the diagnosis of bronchiolitis obliterans in lung transplantation. **J Heart Lung Transplant**. 2011 Dec;30(12):1374-80. doi: 10.1016/j.healun.2011.07.010.

[111] Gudmann NS, Manon-Jensen T, Sand JMB, Diefenbach C, Sun S, Danielsen A, Karsdal MA, Leeming DJ2. Lung tissue destruction by proteinase 3 and cathepsin G mediated elastin degradation is elevated in chronic obstructive pulmonary disease. **Biochem Biophys Res Commun**. 2018;503(3):1284-1290. doi: 10.1016/j.bbrc.2018.07.038.

[112] Lai T, Li Y, Mai Z, Wen X, Lv Y, Xie Z, Lv Q, Chen M, Wu D, Wu B. Annexin A1 is elevated in patients with COPD and affects lung fibroblast function. **Int J Chron Obstruct Pulmon Dis**. 2018; 13:473-486. doi: 10.2147/COPD.S149766.

[113] Wang Y, Jia M, Yan X, Cao L, Barnes PJ, Adcock IM, Huang M, Yao X. Increased neutrophil gelatinase-associated lipocalin (NGAL) promotes airway remodelling in chronic obstructive pulmonary disease. **Clin Sci**. 2017 May 22;131(11):1147-1159. doi: 10.1042/CS20170096.

[114] Siqueiros-Cendón T1, Arévalo-Gallegos S2, Iglesias-Figueroa BF2, García-Montoya IA2, Salazar-Martínez J3, Rascón-Cruz Q2. Immunomodulatory effects of lactoferrin. **Acta Pharmacol Sin**. 2014 May;35(5):557-66. doi: 10.1038/aps.2013.200.

[115] Kawamata T, Tooyama I, Yamada T, Walker DG, McGeer PL. Lactotransferrin immunocytochemistry in Alzheimer and normal human brain. **Am J Pathol.** 1993; 142: 1574–85.

[116] Uchida K, Matsuse R, Tomita S. Immunochemical detection of human lactoferrin in feces as a new marker for inflammatory gastrointestinal disorders and colon cancer**. Clin Biochem.** 1994; 27: 259–64.

[117] Van de Graaf EA, Out TA, Kobesen A, Jansen HM. Lactoferrin and secretory IgA in the bronchoalveolar lavage fluid from patients with a stable asthma. **Lung** 1991; 169: 275–83.

[118] Barroso B, Abello N, Bischoff R. Study of human lung elastin degradation by different elastases using high-performance liquid chromatography/mass spectrometry. **Anal. Biochem**. 2006; 35:216-22

[119] Houghto AM, Quintero PA, Perkins DL, Kobayashi DK, Kelley DG, Marconcini LA. Elastin fragments drive disease progression in a murine model of emphysema. **J. Clin. Invest**. 2006; 116: 753-759

[120] Wu N1, Liu S, Guo C, Hou Z, Sun MZ. The role of annexin A3 playing in cancers. **Clin Transl Oncol.** 2013;15(2):106-10. doi: 10.1007/s12094-012-0928-6.

[121] Grzela K, Litwiniuk M, Zagorska W, Grzela T. Airway Remodeling in Chronic Obstructive Pulmonary Disease and Asthma: the Role of Matrix Metalloproteinase-9. **Arch Immunol Ther Exp (Warsz**). 2016;64(1):47-55. doi: 10.1007/s00005-015-0345-y.

[122] Linder R, Rönmark E, Pourazar J, Behndig A, Blomberg A, Lindberg A. Serum metalloproteinase-9 is related to COPD severity and symptoms - cross-sectional data from a population based cohort-study. **Respir Res**. 2015; 21; 16:28. doi: 10.1186/s12931-015-0188-4.

[123] Kesimer M, Ford AA, Ceppe A, Radicioni G, Cao R, Davis CW, Doerschuk CM, Alexis NE, Anderson WH, Henderson AG, Barr RG, Bleecker ER, Christenson SA, Cooper CB, Han MK, Hansel NN, Hastie AT, Hoffman EA, Kanner RE, Martinez F, Paine R 3rd, Woodruff PG, O'Neal WK, Boucher RC. Airway Mucin Concentration as a Marker of Chronic Bronchitis. **N Engl J Med**. 2017;377(10):911-922. doi: 10.1056/NEJMoa1701632.

[124] De Torre C, Ying SX, Munson PJ, Meduri GU, Suffredini AF. Proteomic analysis of inflammatory biomarkers in bronchoalveolar lavage. **Proteomics**. 2006 Jul;6(13):3949-57.

[125] Fischer BM, Pavlisko E, Voynow JA. Pathogenic triad in COPD: oxidative stress, protease-antiprotease imbalance, and inflammation**. Int J Chron Obstruct Pulmon Dis**. 2011; 6:413-21. doi: 10.2147/COPD.S10770

[126] Hatipoğlu U, Stoller JK. α1-antitrypsin deficiency. **Clinics in Chest Medicine**. 2016;37(3):487–504. doi: 10.1016/j.ccm.2016.04.011.

[127] King MB, Campbell EJ, Gray BH, Hertz MI. The proteinase-antiproteinase balance in alpha-1-proteinase inhibitor-deficient lung transplant recipients. **Am J Respir Crit Care Med**. 1994 Apr;149(4 Pt 1):966-71.

[128] Markley JL, Dashti H, Wedell JR, Westler WM, Eghbalnia HR. Tools for Enhanced NMR-Based Metabolomics Analysis. **Methods Mol Biol**. 2019; 2037:413-427. doi: 10.1007/978-1-4939-9690-2_23.

[129] Huang D, Hudson BC, Gao Y, Roberts EK, Paravastu AK. Solid-State NMR Structural Characterization of Self-Assembled Peptides with Selective 13C and 15N Isotopic Labels. **Methods Mol Biol**. 2018;1777:23-68. doi: 10.1007/978-1-4939-7811-3_2.

[130] Ciaramelli C, Fumagalli M, Viglio S, Bardoni AM, Piloni D, Meloni F, Iadarola P, Airoldi C. 1H NMR To Evaluate the Metabolome of Bronchoalveolar Lavage Fluid (BALf) in Bronchiolitis Obliterans Syndrome (BOS): Toward the Development of a New Approach for Biomarker Identification. **J Proteome Res**. 2017;16(4):1669-1682. doi: 10.1021/acs.jproteome.6b01038.

[131] Wolak JE, Esther CR, O'Connell TM. Metabolomic analysis of bronchoalveolar lavage fluid from cystic fibrosis patients. **Biomarkers.** 2009, 14 (1), 55−60

[132] De Backer D, Creteur J, Zhang H, Norrenberg M, Vincent JL. Lactate production by the lungs in acute lung injury. **Am J Respir Crit Care Med**. 1997;156(4 Pt 1):1099-104.

[133] Freund HR, Ryan JA Jr, Fischer JE**.** Amino acid derangements in patients with sepsis: treatment with branched chain amino acid rich infusions. **Ann Surg**. 1978;188(3):423-30.

[134] Lambert IH. Regulation of the cellular content of the organic osmolyte taurine in mammalian cells. **Neurochem Res**. 2004 Jan;29(1):27-63.

[135] Lambert IH, Hoffmann EK, Pedersen SF. Cell volume regulation: physiology and pathophysiology. **Acta Physiol (Oxf).** 2008 Dec;194(4):255-82. doi: 10.1111/j.1748-1716.2008.01910.x.

[136] Lambert IH, Kristensen DM, Holm JB, Mortensen OH. Physiological role of taurine--from organism to organelle. **Acta Physiol (Oxf).** 2015 Jan;213(1):191-212. doi: 10.1111/apha.12365.

[137] Yvon M, Chabanet C, Pélissier JP. Solubility of peptides in trichloroacetic acid (TCA) solutions. Hypothesis on the precipitation mechanism. **Int J Pept Protein Res**. 1989; 34: 166-176.

[138] Laemmli UK. Cleavage of structural proteins during the assembly of the head of bacteriophage T4. **Nature.** 1970; 227: 680-685.

[139] Iskender I, Sakamoto J, Nakajima D, Lin H, Chen M, Kim H, Guan Z, Del Sorbo L, Hwang D, Waddell TK, Cypel M, Keshavjee S, Liu M. Human α1-antitrypsin improves early post-transplant lung function: Pre-clinical studies in a pig lung transplant model. **J. Heart Lung Transplant**. 2016; 35, 913–921. doi: 10.1016/j.healun.2016.03.006

[140] Fisichella PM, Davis CS, Lowery E, Ramirez L, Gamelli RL, Kovacs EJ. Aspiration, localized pulmonary inflammation, and predictors of early-onset bronchiolitis obliterans syndrome after lung transplantation. **J Am Coll Surg**. 2013 Jul;217(1):90-100; discussion 100-1. doi: 10.1016/j.jamcollsurg.2013.03.008.

[141] Gao W, Zhao J, Kim H, Xu S, Chen M, Bai X, Toba H, Cho HR, Zhang H, Keshavjeel S, Liu M. α1-Antitrypsin inhibits ischemia reperfusion-induced lung injury by reducing inflammatory response and cell death. **J Heart Lung Transplant**. 2014;33(3):309-15. doi: 10.1016/j.healun.2013.10.031.

[142] Sundaresan S, Mohanakumar T, Smith MA, Trulock EP, Lynch J, Phelan D, Cooper JD, Patterson GA. HLA-A locus mismatches and development of antibodies to HLA after lung transplantation correlate with the development of bronchiolitis obliterans syndrome. **Transplantation.** 1998 Mar 15;65(5):648-53.

[143] Gerna G, Lilleri D, Furione M, Castiglioni, Meloni F, Rampino T, Agozzino M, Arbustini E. Human cytomegalovirus end-organ disease is associated with high or low systemic viral load in preemptively treated solid-organ transplant recipients. **New Microbiol**. 2012;35:279–287.

[144] Kotsimbos TC, Snell GI, Levvey B, Spelman DW, Fuller AJ, Wesselingh SL, Williams TJ, Ostergaard L. Chlamydia pneumoniae serology in donors and recipients and the risk of bronchiolitis obliterans syndrome after lung transplantation. **Transplantation**. 2005 Feb 15;79(3):269-75.

[145] Daud SA, Yusen RD, Meyers BF, Chakinala MM, Walter MJ, Aloush AA, Patterson GA, Trulock EP, Hachem RR. Impact of immediate primary lung allograft dysfunction on bronchiolitis obliterans syndrome. **Am J Respir Crit Care Med.** 2007 Mar 1;175(5):507-13

[165] Subramaniyam D, Virtala R, Pawłowski K, Clausen IG, Warkentin S, Stevens T, Janciauskiene S. TNF-alpha-induced self-expression in human lung endothelial cells is inhibited by native and oxidized alpha1-antitrypsin. **Int J Biochem Cell Biol.** 2008;40(2):258-71.

[147] Montecucco F, Bertolotto M, Ottonello L, Pende A, Dapino P, Quercioli A, Mach F, Dallegri F. Chlorhexidine prevents hypochlorous acid-induced inactivation of alpha1-antitrypsin**. Clin Exp Pharmacol Physiol**. 2009 Nov;36(11):e72-7. doi: 10.1111/j.1440-1681.2009.05270.x.

[148] Giuliano S, Agresta AM, De Palma A, Viglio S, Mauri P, Fumagalli M, et al. Proteomic analysis of lymphoblastoid cells from Nasu-Hakola patients: a step forward in our understanding of this neurodegenerative disorder. **PLoS One.** 2014; 9: e110073. DOI: 10.1371/journal.pone.0110073.

[149] Fietta AM, Bardoni AM, Salvini R, Passadore I, Morosini M, Cavagna L, et al. Analysis of bronchoalveolar lavage fluid proteome from systemic sclerosis patients with or without functional, clinical and radiological signs of lung fibrosis. **Arthritis Res Ther**. 2006; 8: R160. DOI: 10.1186/ar2067.

[150] Cagnone M, Piloni D, Ferrarotti I, Di Venere M, Viglio S, Magni S, Bardoni A, Salvini R, Fumagalli M, Iadarola P, Martinello S, Meloni F. A Pilot Study to Investigate the Balance between Proteases and α1-Antitrypsin in Bronchoalveolar Lavage Fluid of Lung Transplant Recipients. **High Throughput**. 2019 Feb 13;8(1). pii: E5. doi: 10.3390/ht8010005.

[151] Magi B, Bini L, Perari MG, Fossi A, Sanchez JC, Hochstrasser D. Bronchoalveolar lavage fluid protein composition in patients with sarcoidosis and idiopathic pulmonary fibrosis: a two-dimensional electrophoretic study. **Electrophoresis.** 2002; 23: 3434-3444. DOI: 10.1002/1522-2683(200210)23:19<3434:AID-ELPS3434>3.0.CO;2-R.

[152] Hirsch J, Elssner A, Mazur G, Maier KL, Bittmann I, Behr J, Schwaiblmair M, Reichenspurner H, Fürst H, Briegel J, Vogelmeier C. Bronchiolitis obliterans syndrome after (heart-)lung transplantation. Impaired antiprotease defense and increased oxidant activity. **Am J Respir Crit Care Med**. 1999; 160: 1640–1646. DOI: 10.1164/ajrccm.160.5.9902012.

[153] Kawabata K, Hagio T, Matsuoka S. The role of neutrophil elastase in acute lung injury. **Eur J Pharmacol.** 2002;451(1):1-10.

[154] Lee WL, Downey GP. Leukocyte elastase: physiological functions and role in acute lung injury. **Am J Respir Crit Care Med.** 2001;164(5):896-904.

[155] Bach-Gansmo ET, Godal HC, Skjønsberg OH. Degradation of fibrinogen and cross-linked fibrin by human neutrophil elastase generates D-like fragments detected by ELISA but not latex D-dimer test. **Thromb Res.** 1998;92(3):125-34.

[156] Duvoix A, Dickens J, Haq I, Mannino D, Miller B, Tal-Singer R, Lomas DA. Blood fibrinogen as a biomarker of chronic obstructive pulmonary disease**. Thorax**. 2013 Jul;68(7):670-6. doi: 10.1136/thoraxjnl-2012-201871.

[157] Carter RI, Ungurs MJ, Mumford RA, Stockley RA. Aα-Val360: a marker of neutrophil elastase and COPD disease activity. **Eur Respir J.** 2013;41(1):31-8. doi: 10.1183/09031936.00197411.

[158] Carter RI, Ungurs MJ, Pillai , Mumford RA, Stockley RA. The Relationship of the Fibrinogen Cleavage Biomarker Aα-Val360 With Disease Severity and Activity in α1-Antitrypsin Deficiency. **Chest.** 2015;148(2):382-388. doi: 10.1378/chest.14-0520.

[159] Seersholm N, Wencker M, Banik N, Viskum K, Dirksen A, Kok-Jensen A, Konietzko N. Does alpha1-antitrypsin augmentation therapy slow the annual decline in FEV1 in patients with severe hereditary alpha1-antitrypsin deficiency? Wissenschaftliche Arbeitsgemeinschaft zur Therapie von Lungenerkrankungen (WATL) alpha1-AT study group. **Eur Respir J.** 1997;10(10):2260-3.

[160] Wewers MD, Casolaro MA, Sellers SE, Swayze SC, McPhaul KM, Wittes JT, Crystal RG. Replacement therapy for alpha 1-antitrypsin deficiency associated with emphysema. **N Engl J Med**. 1987;316(17):1055-62.

[161] Gadek JE, Pacht ER. Pathogenesis of hereditary emphysema and replacement therapy for alpha 1-antitrypsin deficiency. Insight into the more common forms of emphysema**. Chest**. 1996 Dec;110(6 Suppl):248S-250S.

[162] Silverman EK, Sandhaus RA. Clinical practice. Alpha1-antitrypsin deficiency. **New England Journal of Medicine.** 2009;360(26):2749-57.

[163] Griese M, Scheuch G. Delivery of Alpha-1 Antitrypsin to Airways. **Ann Am Thorac Soc**. 2016;13 Suppl 4:S346-51. doi: 10.1513/AnnalsATS.201507-469KV.

SUPPLEMENTARY MATERIAL

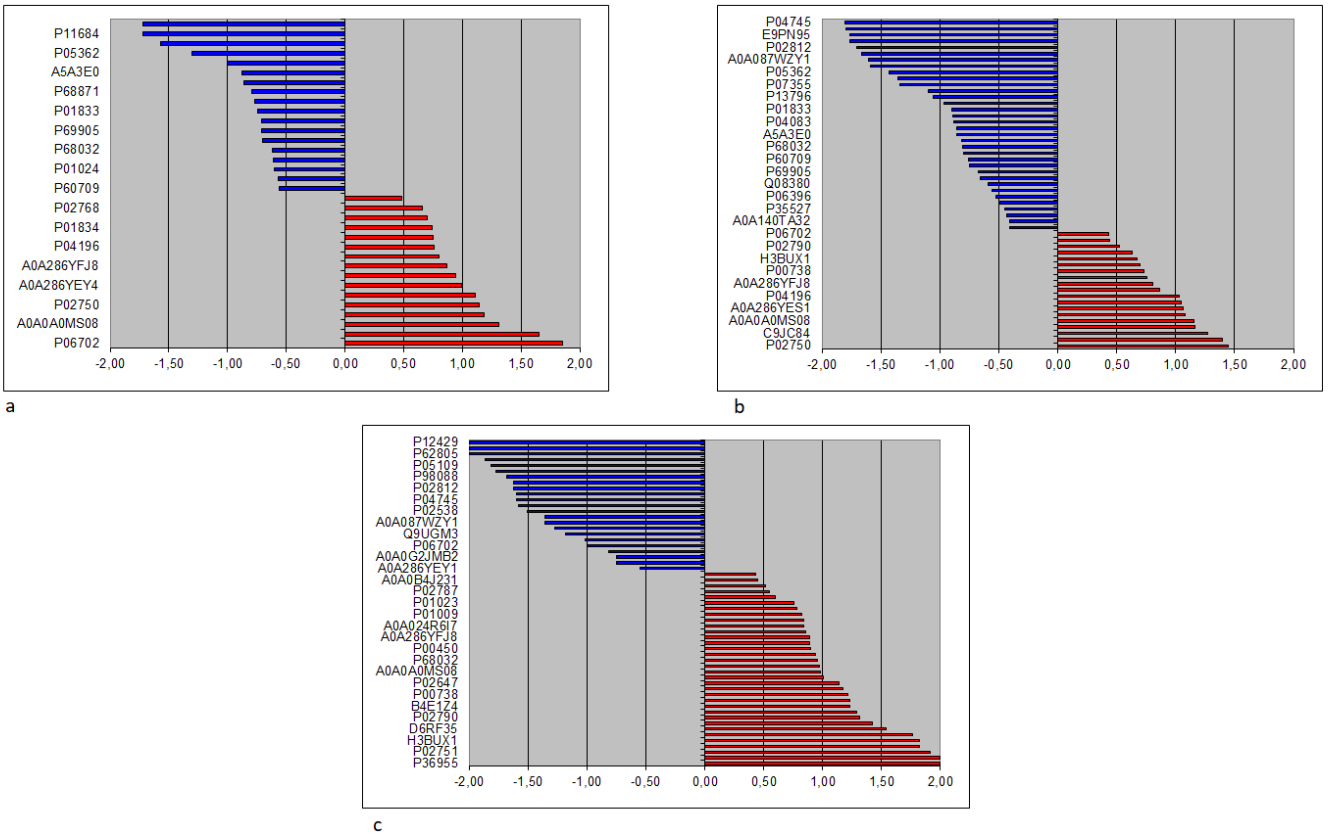

Figure S1. 147 differentially expressed proteins: 35 were the distinct proteins that resulted differentially expressed between stable and BOS 0p subjects (figure S1 panel a); 54 between Stable and BOS1 (figure S1 panel b); 58 between stable and BOS II + BOS III (figure S1 panel c).

Table S1. Distinct proteins that resulted differentially expressed between stable and BOS 0p subjects

Reference	Accession	DAVE_	DCI_
Protein S100-A9 OS=Homo sapiens OX=9606 GN=S100A9 PE=1 SV=1	P06702	1,86	27
Immunoglobulin heavy constant mu (Fragment) OS=Homo sapiens OX=9606 GN=IGHM PE=1 SV=1	A0A1B0GUU9	1,65	37
Immunoglobulin heavy constant gamma 1 (Fragment) OS=Homo sapiens OX=9606 GN=IGHG1 PE=1 SV=1	A0A0A0MS08	1,31	6775
Keratin, type I cytoskeletal 9 OS=Homo sapiens OX=9606 GN=KRT9 PE=1 SV=3	P35527	1,19	13
Leucine-rich alpha-2-glycoprotein OS=Homo sapiens OX=9606 GN=LRG1 PE=1 SV=2	P02750	1,14	30
Immunoglobulin heavy constant gamma 3 (Fragment) OS=Homo sapiens OX=9606 GN=IGHG3 PE=1 SV=1	A0A286YES1	1,11	**302**
Immunoglobulin heavy constant gamma 2 (Fragment) OS=Homo sapiens OX=9606 GN=IGHG2 PE=1 SV=1	A0A286YEY4	0,99	**381**
Fibrinogen gamma chain OS=Homo sapiens OX=9606 GN=FGG PE=1 SV=1	C9JC84	0,95	12
Immunoglobulin heavy constant gamma 4 (Fragment) OS=Homo sapiens OX=9606 GN=IGHG4 PE=1 SV=1	A0A286YFJ8	0,87	87
Mesothelin (Fragment) OS=Homo sapiens OX=9606 GN=MSLN PE=1 SV=1	H3BUX1	0,80	12
Histidine-rich glycoprotein OS=Homo sapiens OX=9606 GN=HRG PE=1 SV=1	P04196	0,76	13
Fibrinogen beta chain OS=Homo sapiens OX=9606 GN=FGB PE=1 SV=2	P02675	0,75	19
Immunoglobulin kappa constant OS=Homo sapiens OX=9606 GN=IGKC PE=1 SV=2	P01834	0,74	2087
Galectin-3-binding protein OS=Homo sapiens OX=9606 GN=LGALS3BP PE=1 SV=1	Q08380	0,70	12
Serum albumin OS=Homo sapiens OX=9606 GN=ALB PE=1 SV=2	P02768	0,66	16321
Hemopexin OS=Homo sapiens OX=9606 GN=HPX PE=1 SV=2	P02790	0,48	445
Actin, cytoplasmic 1 OS=Homo sapiens OX=9606 GN=ACTB PE=1 SV=1	P60709	-0,56	-131
Beta-actin-like protein 2 OS=Homo sapiens OX=9606 GN=ACTBL2 PE=1 SV=2	Q562R1	-0,57	-28
Complement C3 OS=Homo sapiens OX=9606 GN=C3 PE=1 SV=2	P01024	-0,60	-1407
Alpha-1-antitrypsin OS=Homo sapiens OX=9606 GN=SERPINA1 PE=1 SV=3	P01009	-0,61	-1759
Actin, alpha cardiac muscle 1 OS=Homo sapiens OX=9606 GN=ACTC1 PE=1 SV=1	P68032	-0,62	-41
ITIH4 protein OS=Homo sapiens OX=9606 GN=ITIH4 PE=1 SV=1	B7ZKJ8	-0,70	-18
Hemoglobin subunit alpha OS=Homo sapiens OX=9606 GN=HBA1 PE=1 SV=2	P69905	-0,71	-42
Plasma protease C1 inhibitor OS=Homo sapiens OX=9606 GN=SERPING1 PE=1 SV=2	P05155	-0,71	-42
Polymeric immunoglobulin receptor OS=Homo sapiens OX=9606 GN=PIGR PE=1 SV=4	P01833	-0,74	-225
Transthyretin OS=Homo sapiens OX=9606 GN=TTR PE=1 SV=1	P02766	-0,77	-38
Hemoglobin subunit beta OS=Homo sapiens OX=9606 GN=HBB PE=1 SV=2	P68871	-0,80	-205
Hemoglobin subunit delta (Fragment) OS=Homo sapiens OX=9606 GN=HBD PE=1 SV=1	E9PEW8	-0,86	-49
POTE ankyrin domain family member F OS=Homo sapiens OX=9606 GN=POTEF PE=1 SV=2	A5A3E0	-0,88	-20
Annexin A2 OS=Homo sapiens OX=9606 GN=ANXA2 PE=1 SV=2	P07355	-1,00	-11
Intercellular adhesion molecule 1 OS=Homo sapiens OX=9606 GN=ICAM1 PE=1 SV=2	P05362	-1,30	-19
BPI fold-containing family B member 1 OS=Homo sapiens OX=9606 GN=BPIFB1 PE=1 SV=1	Q8TDL5	-1,57	-62
Uteroglobin OS=Homo sapiens OX=9606 GN=SCGB1A1 PE=1 SV=1	P11684	-1,72	-247
Uteroglobin OS=Homo sapiens OX=9606 GN=SCGB1A1 PE=1 SV=1	E9PN95	-1,72	-159

Table S2. Distinct proteins that resulted differentially expressed between stable and BOS I

Reference	Accession	DAVE_	DCI_
Leucine-rich alpha-2-glycoprotein OS=Homo sapiens OX=9606 GN=LRG1 PE=1 SV=2	P02750	1,45	31
Immunoglobulin heavy constant mu (Fragment) OS=Homo sapiens OX=9606 GN=IGHM PE=1 SV=1	A0A1B0GU	1,39	36
Fibrinogen gamma chain OS=Homo sapiens OX=9606 GN=FGG PE=1 SV=1	C9JC84	1,27	14
Fibronectin OS=Homo sapiens OX=9606 GN=FN1 PE=1 SV=4	P02751	1,16	63
Immunoglobulin heavy constant gamma 1 (Fragment) OS=Homo sapiens OX=9606 GN=IGHG1 PE=1 SV=1	A0A0A0M	1,16	6577
Fibrinogen beta chain OS=Homo sapiens OX=9606 GN=FGB PE=1 SV=2	P02675	1,08	22
Immunoglobulin heavy constant gamma 3 (Fragment) OS=Homo sapiens OX=9606 GN=IGHG3 PE=1 SV=1	A0A286YE	1,07	**299**
Alpha-2-macroglobulin OS=Homo sapiens OX=9606 GN=A2M PE=1 SV=3	P01023	1,04	180
Histidine-rich glycoprotein OS=Homo sapiens OX=9606 GN=HRG PE=1 SV=1	P04196	1,03	14
Alpha-1B-glycoprotein OS=Homo sapiens OX=9606 GN=A1BG PE=1 SV=4	P04217	0,87	45
Immunoglobulin heavy constant gamma 4 (Fragment) OS=Homo sapiens OX=9606 GN=IGHG4 PE=1 SV=1	A0A286YF	0,81	84
Immunoglobulin heavy constant gamma 2 (Fragment) OS=Homo sapiens OX=9606 GN=IGHG2 PE=1 SV=1	A0A286YE	0,76	**343**
Haptoglobin OS=Homo sapiens OX=9606 GN=HP PE=1 SV=1	P00738	0,73	184
Immunoglobulin kappa constant OS=Homo sapiens OX=9606 GN=IGKC PE=1 SV=2	P01834	0,70	2028
Mesothelin (Fragment) OS=Homo sapiens OX=9606 GN=MSLN PE=1 SV=1	H3BUX1	0,68	11
Alpha-1-antichymotrypsin OS=Homo sapiens OX=9606 GN=SERPINA3 PE=1 SV=2	P01011	0,63	20
Hemopexin OS=Homo sapiens OX=9606 GN=HPX PE=1 SV=2	P02790	0,53	467
Apolipoprotein A-I OS=Homo sapiens OX=9606 GN=APOA1 PE=1 SV=1	P02647	0,44	**303**
Protein S100-A9 OS=Homo sapiens OX=9606 GN=S100A9 PE=1 SV=1	P06702	0,43	16
Alpha-1-antitrypsin OS=Homo sapiens OX=9606 GN=SERPINA1 PE=1 SV=1	A0A024R6	-0,41	-934
Complement C4-A OS=Homo sapiens OX=9606 GN=C4A PE=1 SV=1	A0A140TA	-0,41	-167
Pulmonary surfactant-associated protein A2 OS=Homo sapiens OX=9606 GN=SFTPA2 PE=1 SV=1	Q8IWL1	-0,43	-331
Keratin, type I cytoskeletal 9 OS=Homo sapiens OX=9606 GN=KRT9 PE=1 SV=3	P35527	-0,45	-22
Complement C4-B OS=Homo sapiens OX=9606 GN=C4B PE=1 SV=2	P0C0L5	-0,49	-222
Gelsolin OS=Homo sapiens OX=9606 GN=GSN PE=1 SV=1	P06396	-0,52	-13
Alpha-1-antitrypsin OS=Homo sapiens OX=9606 GN=SERPINA1 PE=1 SV=3	P01009	-0,55	-1481
Galectin-3-binding protein OS=Homo sapiens OX=9606 GN=LGALS3BP PE=1 SV=1	Q08380	-0,59	-39
Beta-actin-like protein 2 OS=Homo sapiens OX=9606 GN=ACTBL2 PE=1 SV=2	Q562R1	-0,66	-37
Hemoglobin subunit alpha OS=Homo sapiens OX=9606 GN=HBA1 PE=1 SV=2	P69905	-0,67	-38
Complement C3 OS=Homo sapiens OX=9606 GN=C3 PE=1 SV=2	P01024	-0,75	-2201
Actin, cytoplasmic 1 OS=Homo sapiens OX=9606 GN=ACTB PE=1 SV=1	P60709	-0,76	-239
Hemoglobin subunit beta OS=Homo sapiens OX=9606 GN=HBB PE=1 SV=2	P68871	-0,80	-205
Actin, alpha cardiac muscle 1 OS=Homo sapiens OX=9606 GN=ACTC1 PE=1 SV=1	P68032	-0,80	-72
Keratin, type II cytoskeletal 1 OS=Homo sapiens OX=9606 GN=KRT1 PE=1 SV=6	P04264	-0,81	-92
POTE ankyrin domain family member F OS=Homo sapiens OX=9606 GN=POTEF PE=1 SV=2	A5A3E0	-0,85	-18
Hemoglobin subunit delta (Fragment) OS=Homo sapiens OX=9606 GN=HBD PE=1 SV=1	E9PEW8	-0,86	-49
Annexin A1 OS=Homo sapiens OX=9606 GN=ANXA1 PE=1 SV=2	P04083	-0,88	-70
CD44 antigen OS=Homo sapiens OX=9606 GN=CD44 PE=1 SV=3	P16070	-0,89	-11
Polymeric immunoglobulin receptor OS=Homo sapiens OX=9606 GN=PIGR PE=1 SV=4	P01833	-0,89	-355
Transthyretin OS=Homo sapiens OX=9606 GN=TTR PE=1 SV=1	P02766	-0,96	-67
Plastin-2 OS=Homo sapiens OX=9606 GN=LCP1 PE=1 SV=6	P13796	-1,05	-19
Plasma protease C1 inhibitor OS=Homo sapiens OX=9606 GN=SERPING1 PE=1 SV=2	P05155	-1,09	-134
Annexin A2 OS=Homo sapiens OX=9606 GN=ANXA2 PE=1 SV=2	P07355	-1,34	-34
Annexin A5 OS=Homo sapiens OX=9606 GN=ANXA5 PE=1 SV=2	P08758	-1,35	-36
Intercellular adhesion molecule 1 OS=Homo sapiens OX=9606 GN=ICAM1 PE=1 SV=2	P05362	-1,43	-32
Vimentin OS=Homo sapiens OX=9606 GN=VIM PE=1 SV=4	P08670	-1,59	-68
Uncharacterized protein OS=Homo sapiens OX=9606 PE=4 SV=1	A0A087W	-1,60	-72
BPI fold-containing family B member 1 OS=Homo sapiens OX=9606 GN=BPIFB1 PE=1 SV=1	Q8TDL5	-1,66	-104
Basic salivary proline-rich protein 2 OS=Homo sapiens OX=9606 GN=PRB2 PE=1 SV=3	P02812	-1,70	-35
Uteroglobin OS=Homo sapiens OX=9606 GN=SCGB1A1 PE=1 SV=1	P11684	-1,76	-344
Uteroglobin OS=Homo sapiens OX=9606 GN=SCGB1A1 PE=1 SV=1	E9PN95	-1,77	-227
Alpha-amylase 2B OS=Homo sapiens OX=9606 GN=AMY2B PE=1 SV=1	P19961	-1,80	-309
Alpha-amylase 1 OS=Homo sapiens OX=9606 GN=AMY1A PE=1 SV=2	P04745	-1,80	-522

Table S3. Distinct proteins that resulted differentially expressed between stable and BOS II/III

Reference	Accession	DAVE_	DCI_
Pigment epithelium-derived factor OS=Homo sapiens OX=9606 GN=SERPINF1 PE=1 SV=4	P36955	2,00	11
Histidine-rich glycoprotein OS=Homo sapiens OX=9606 GN=HRG PE=1 SV=1	P04196	2,00	16
Fibronectin OS=Homo sapiens OX=9606 GN=FN1 PE=1 SV=4	P02751	1,92	68
Fibrinogen gamma chain OS=Homo sapiens OX=9606 GN=FGG PE=1 SV=1	C9JC84	1,82	14
Mesothelin (Fragment) OS=Homo sapiens OX=9606 GN=MSLN PE=1 SV=1	H3BUX1	1,82	14
Leucine-rich alpha-2-glycoprotein OS=Homo sapiens OX=9606 GN=LRG1 PE=1 SV=2	P02750	1,76	32
Vitamin D-binding protein OS=Homo sapiens OX=9606 GN=GC PE=1 SV=1	D6RF35	1,54	29
Alpha-1B-glycoprotein OS=Homo sapiens OX=9606 GN=A1BG PE=1 SV=4	P04217	1,42	52
Hemopexin OS=Homo sapiens OX=9606 GN=HPX PE=1 SV=2	P02790	1,32	679
Fibrinogen beta chain OS=Homo sapiens OX=9606 GN=FGB PE=1 SV=2	P02675	1,29	23
cDNA FLJ55673, highly similar to Complement factor B (EC 3.4.21.47) OS=Homo sapiens OX=9606 PE=1 SV=1	B4E1Z4	1,23	88
Alpha-1-antichymotrypsin OS=Homo sapiens OX=9606 GN=SERPINA3 PE=1 SV=2	P01011	1,23	25
Haptoglobin OS=Homo sapiens OX=9606 GN=HP PE=1 SV=1	P00738	1,22	**221**
Immunoglobulin heavy constant mu (Fragment) OS=Homo sapiens OX=9606 GN=IGHM PE=1 SV=1	A0A1B0GU	1,18	35
Apolipoprotein A-I OS=Homo sapiens OX=9606 GN=APOA1 PE=1 SV=1	P02647	1,14	474
Complement C4-A OS=Homo sapiens OX=9606 GN=C4A PE=1 SV=1	A0A140TA	1,01	114
Immunoglobulin heavy constant gamma 1 (Fragment) OS=Homo sapiens OX=9606 GN=IGHG1 PE=1 SV=1	A0A0A0M	0,98	6250
Complement C4-B OS=Homo sapiens OX=9606 GN=C4B PE=1 SV=2	P0C0L5	0,98	113
Actin, alpha cardiac muscle 1 OS=Homo sapiens OX=9606 GN=ACTC1 PE=1 SV=1	P68032	0,96	14
Immunoglobulin heavy constant gamma 3 (Fragment) OS=Homo sapiens OX=9606 GN=IGHG3 PE=1 SV=1	A0A286YE	0,94	**287**
Ceruloplasmin OS=Homo sapiens OX=9606 GN=CP PE=1 SV=1	P00450	0,90	**213**
Immunoglobulin heavy constant gamma 2 (Fragment) OS=Homo sapiens OX=9606 GN=IGHG2 PE=1 SV=1	A0A286YE	0,89	**367**
Immunoglobulin heavy constant gamma 4 (Fragment) OS=Homo sapiens OX=9606 GN=IGHG4 PE=1 SV=1	A0A286YF	0,89	88
Beta-actin-like protein 2 OS=Homo sapiens OX=9606 GN=ACTBL2 PE=1 SV=2	Q562R1	0,86	11
Alpha-1-antitrypsin OS=Homo sapiens OX=9606 GN=SERPINA1 PE=1 SV=1	A0A024R6	0,84	602
Actin, cytoplasmic 1 OS=Homo sapiens OX=9606 GN=ACTB PE=1 SV=1	P60709	0,84	50
Alpha-1-antitrypsin OS=Homo sapiens OX=9606 GN=SERPINA1 PE=1 SV=3	P01009	0,83	577
Serum albumin OS=Homo sapiens OX=9606 GN=ALB PE=1 SV=2	P02768	0,78	17724
Alpha-2-macroglobulin OS=Homo sapiens OX=9606 GN=A2M PE=1 SV=3	P01023	0,76	160
Immunoglobulin kappa constant OS=Homo sapiens OX=9606 GN=IGKC PE=1 SV=2	P01834	0,60	1880
Serotransferrin OS=Homo sapiens OX=9606 GN=TF PE=1 SV=3	P02787	0,55	**362**
Complement C3 OS=Homo sapiens OX=9606 GN=C3 PE=1 SV=2	P01024	0,52	**378**
Immunoglobulin lambda-like polypeptide 5 OS=Homo sapiens OX=9606 GN=IGLL5 PE=1 SV=1	A0A0B4J2	0,45	22
Hemoglobin subunit beta OS=Homo sapiens OX=9606 GN=HBB PE=1 SV=2	P68871	0,43	27
Immunoglobulin heavy constant alpha 1 (Fragment) OS=Homo sapiens OX=9606 GN=IGHA1 PE=1 SV=1	A0A286YE	-0,55	-315
Transthyretin OS=Homo sapiens OX=9606 GN=TTR PE=1 SV=1	P02766	-0,75	-36
Immunoglobulin heavy constant alpha 2 (Fragment) OS=Homo sapiens OX=9606 GN=IGHA2 PE=1 SV=1	A0A0G2JM	-0,75	-279
Keratin, type II cytoskeletal 1 OS=Homo sapiens OX=9606 GN=KRT1 PE=1 SV=6	P04264	-0,81	-92
Protein S100-A9 OS=Homo sapiens OX=9606 GN=S100A9 PE=1 SV=1	P06702	-1,00	-215
Annexin A1 OS=Homo sapiens OX=9606 GN=ANXA1 PE=1 SV=2	P04083	-1,01	-104
Deleted in malignant brain tumors 1 protein OS=Homo sapiens OX=9606 GN=DMBT1 PE=1 SV=2	Q9UGM3	-1,18	-20
Uteroglobin OS=Homo sapiens OX=9606 GN=SCGB1A1 PE=1 SV=1	P11684	-1,27	-27
Uncharacterized protein OS=Homo sapiens OX=9606 PE=4 SV=1	A0A087W	-1,36	-24
Uteroglobin OS=Homo sapiens OX=9606 GN=SCGB1A1 PE=1 SV=1	E9PN95	-1,36	-24
Keratin, type II cytoskeletal 6A OS=Homo sapiens OX=9606 GN=KRT6A PE=1 SV=3	P02538	-1,51	-11
Mucin-5B OS=Homo sapiens OX=9606 GN=MUC5B PE=1 SV=3	Q9HC84	-1,58	-147
Alpha-amylase 1 OS=Homo sapiens OX=9606 GN=AMY1A PE=1 SV=2	P04745	-1,60	-111
Alpha-amylase 2B OS=Homo sapiens OX=9606 GN=AMY2B PE=1 SV=1	P19961	-1,60	-71
Basic salivary proline-rich protein 2 OS=Homo sapiens OX=9606 GN=PRB2 PE=1 SV=3	P02812	-1,63	-21
Myeloperoxidase OS=Homo sapiens OX=9606 GN=MPO PE=1 SV=1	P05164	-1,63	-47
Mucin-5AC OS=Homo sapiens OX=9606 GN=MUC5AC PE=1 SV=4	P98088	-1,69	-189
BPI fold-containing family B member 1 OS=Homo sapiens OX=9606 GN=BPIFB1 PE=1 SV=1	Q8TDL5	-1,78	-252
Protein S100-A8 OS=Homo sapiens OX=9606 GN=S100A8 PE=1 SV=1	P05109	-1,82	-94
Lactotransferrin OS=Homo sapiens OX=9606 GN=LTF PE=1 SV=6	P02788	-1,87	-47
Histone H4 OS=Homo sapiens OX=9606 GN=HIST1H4A PE=1 SV=2	P62805	-2,00	-11
Keratin, type II cytoskeletal 4 OS=Homo sapiens OX=9606 GN=KRT4 PE=1 SV=4	P19013	-2,00	-10
Annexin A3 OS=Homo sapiens OX=9606 GN=ANXA3 PE=1 SV=3	P12429	-2,00	-14

Table S4. Primary sequence of all peptides identified for each protein

ACCESSION	MASS	SCORE(%)	COVERAGE(%)	DESCRIPTION	M/Z	Z	PEPTIDE
sp|P01009|	46,737	99	14,83%	Alpha-1-antitrypsin OS=Homo sapiens			
	1345,9855				674	2	RLGMFNIQHCK
	920,99274				922	1	FLENEDR
	1777,9855				890	2	TDTSHHDQDHPTFNK
	1331,9783				445	3	LVDKFLEDVKK
	1077,9855				540	2	FLENEDRR
	1544,9783				516	3	SPLFMGKVVNPTQK
	851,9855				427	2	SASLHLPK
	1317,9855				660	2	LGMFNIQHCKK
sp|P08246|	28,518	62	4,87%	Neutrophil elastase OS=Homo sapiens			
	1545,9855				774	2	AVRVVLGAHNLSRR
	1389,9855				696	2	AVRVVLGAHNLSR

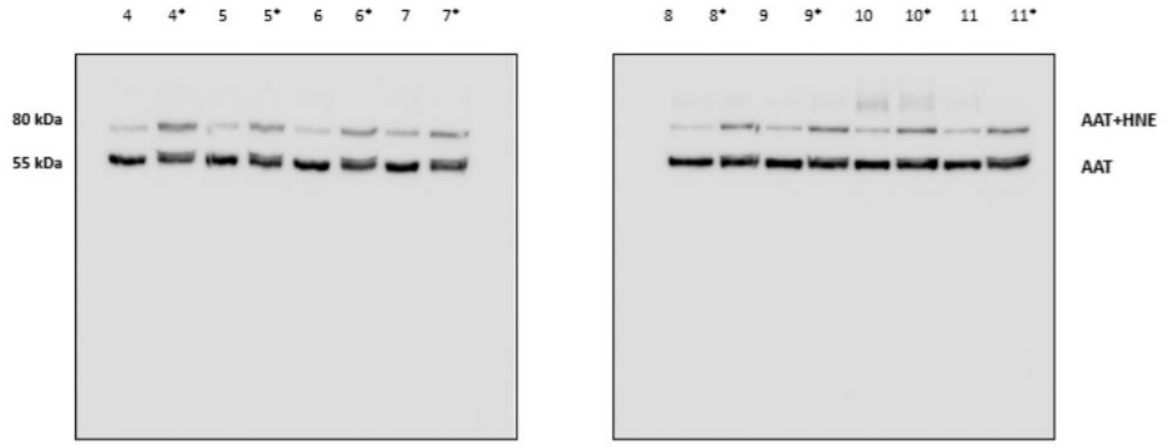

Figure S2. Western blotting of BALf from patients with the 80 kDa band before and after incubation with exogenous HNE* (left to right in both panels).

Related Articles

Maddalena Cagnone[1]
Roberta Salvini[1]
Anna Bardoni[1]
Marco Fumagalli[2]
Paolo Iadarola[2]
Simona Viglio[1]

[1]Department of Molecular Medicine, Biochemistry Unit, University of Pavia, Italy
[2]Department of Biology and Biotechnologies "L.Spallanzani", Biochemistry Unit, University of Pavia, Italy

Received July 19, 2018
Revised September 10, 2018
Accepted September 10, 2018

Review

Searching for biomarkers of chronic obstructive pulmonary disease using proteomics: The current state

Detection of proteins which may be potential biomarkers of disorders represents a big step forward in understanding the molecular mechanisms that underlie pathological processes. In this context proteomics plays the important role of opening a path for the identification of molecular signatures that can potentially assist in early diagnosis of several clinical disturbances. Aim of this report is to provide an overview of the wide variety of proteomic strategies that have been applied to the investigation of chronic obstructive pulmonary disease (COPD), a severe disorder that causes an irreversible damage to the lungs and for which there is no cure yet. The results in this area published over the past decade show that proteomics indeed has the ability of monitoring alterations in expression profiles of proteins from fluids/tissues of patients affected by COPD and healthy controls. However, these data also suggest that proteomics, while being an attractive tool for the identification of novel pathological mediators of COPD, remains a technique mainly generated and developed in research laboratories. Great efforts dedicated to the validation of these biological signatures will result in the proof of their clinical utility.

Keywords:
Biomarkers / Biological fluids / Chronic obstructive pulmonary disease / Liquid chromatography / Mass spectrometry / Proteomics
DOI 10.1002/elps.201800305

1 Introduction

Chronic obstructive pulmonary disease (COPD), an inflammatory respiratory disorder characterized by a progressive and not-reversible airflow obstruction, is one of the top five causes of death and disability worldwide [1]. Rather than a specific disease, the term COPD describes a group of lung conditions among which persistent bronchitis and emphysema are the most representative. These processes (which can also occur together) cause airway narrowing with consequent damage of lung tissue and difficulty in breathing [1–4]. While cigarette smoking is the primary risk agent for COPD, numerous other factors share the responsibility for the onset of the disease. For instance, a family history of COPD, the chronic exposure to environmental/occupational pollutants (as well as to second-hand smoke), the deficiency of alpha1-antitrypsin may be triggering factors that contribute to the development of the pathology [1, 2].

Although quantifying the economic and monetary consequences of the illness is not easy, the impact it has on single individuals and the society is enormous. The reduced/loss of productivity due to absence or premature retirement from work (together with possible costs of hospitalization) are disease-attributable direct and indirect costs of particular importance [1, 2, 5]. From a clinical point of view, while the treatments currently available may slow the progression of the disease and help patients feel better and breathe more easily, they cannot reverse the damage to the lungs. Thus, as a matter of fact, COPD has no cure yet and an important key towards a more successful treatment of the disorder would be its early detection. The first diagnosis of COPD is currently based on the observation of peculiar signs and symptoms which include breathing difficulty, cough, production of mucus and wheezing. However, it is not unusual that people do not experience symptoms until later stages of the disease or that symptoms are un-/under-recognized even by physicians [1–4, 6, 7]. Under this scenario it appears obvious that the identification of molecular signatures, referred to as "biomarkers", that may display the presence of the disease (or its level of severity) and reflect either its progression or the response to treatment would provide a novel context for

Correspondence: Professor Paolo Iadarola, Dept. of Biology and Biotechnologies "L.Spallanzani", University of Pavia, Via Ferrata 9, 27100 Pavia, Italy
Fax: +39-0382-423108
E-mail: piadarol@unipv.it

Abbreviations: 1DE, mono-dimensional electrophoresis; **2D-DIGE**, two-dimensional difference gel electrophoresis; **2DE**, two-dimensional electrophoresis; **BALf**, Broncho Alveolar Lavage fluid; **CE**, capillary electrophoresis; **COPD**, chronic obstructive pulmonary disease; **EBC**, exhaled breath condensate; **HPLC**, high performance liquid chromatography; **IEF**, isoelectrofocusing; **IS**, induced Sputum; **iTRAQ**, isobaric tag for relative and absolute quantitation; **MS**, mass spectrometry

the precise interpretation of symptoms. A plethora of compounds which include specific cells, genes, gene products or other molecules meet these requirements. In the wake of these considerations, the number of articles which describe well-characterized biomarkers for a myriad of pathologies, including COPD, has constantly increased over the last decade [8–14]. In particular, with the advent of proteomics, the screening of proteins aimed at the identification of potential biomarkers of disorders has become a hot topic in both basic and clinical research. Proteomic analyses may indeed reveal meaningful patterns and often yield trustworthy views of complex biological systems. In addition, they have the potential to reveal disease mechanisms that cannot be identified at the genomic level and offer the great advantage of direct clinical relevance. Thanks to these advantages, detection and identification of proteins in different fluids/tissues is currently an area of increasing interest for understanding whether they are attractive tools for monitoring alterations in bodily districts or surrogate endpoints of the disease [10, 11, 13, 14]. In terms of experimental procedures, the basic options available for proteomic investigations are sophisticated on-gel and gel-free approaches coupled to mass spectrometry (MS) for the identification of proteins is [15].

Despite proteomics in the pulmonary area has not been used yet as extensively as in other fields, the depth of analysis ultimately reached by several studies of different lung fluids and tissues has never been reported before [15–20]. In particular, over the last decade, a progressive increase has been observed in the number of proteomic publications dedicated to COPD [21–24]. This proves illuminating about the contribution of these approaches in the generation of comprehensive protein profiles that could be useful for exploring protein-based pathological mechanisms of the disorder.

Aim of the current report is to provide an update on the status of proteome research in the field of COPD by presenting specific applications of this procedure to the investigation of fluids/tissues from different cohorts of individuals diagnosed with this pathological condition.

2 Experimental procedures currently applied to proteomic studies

Briefly, identification of proteins in proteomics occurs through the analysis of (i) intact proteins or (ii) protein fragments. The first procedure (referred to as "top-down" proteomics) consists in the separation of intact proteins by gel-based 1DE or 2DE or gel-free 1D or 2D-HPLC) and CE techniques. Proteins are subsequently extracted/recovered, digested (usually with trypsin) and analyzed by MS.

With the second procedure ("bottom-up" proteomics), the whole mixture of proteins in the sample is fragmented (usually with trypsin), the huge number of peptides separated by gel-free techniques (CE or 1D/2D/3D-HPLC) and finally analyzed by MS. The two approaches are schematized in Fig. 1.

The top-down approach has a variety of advantages which include the ability to detect degradation products, sequence variants, and combinations of post-translational modifications (PTMs). The other side of the coin is represented by the amount of material required that is 10 to 100 folds higher than that required for the bottom-up procedure.

Another major limitation of the top-down approach is the bad identification of hydrophobic membrane proteins or proteins that are too basic/acidic and too large/small. Finally, a limited number of bioinformatic tools for data interpretation is available. As far as the bottom-up analysis is concerned, it is able to identify more proteins in more-complex samples. However, this may be also seen as a limitation given the extended run times required for the analysis. Other practical limitations include the loss of information about

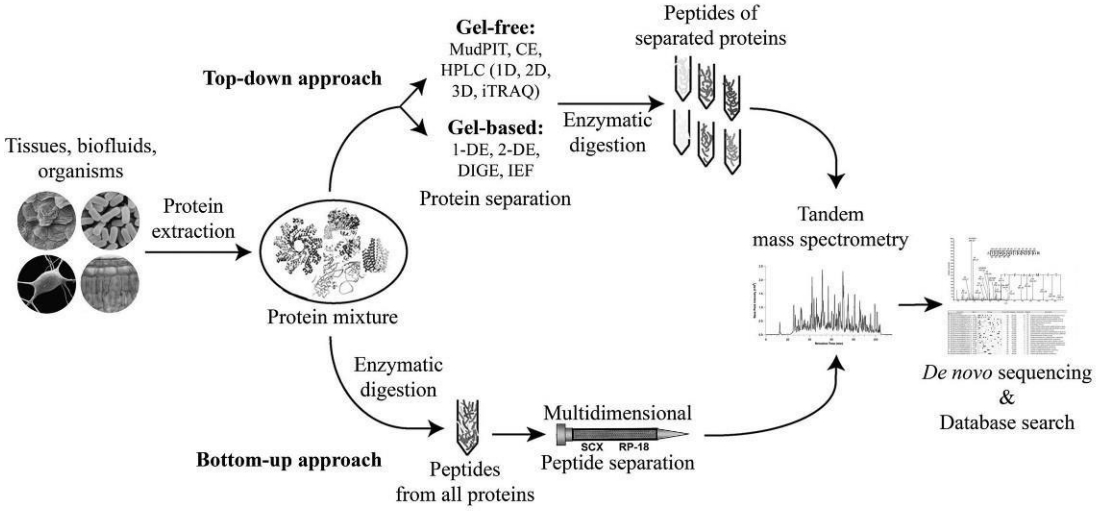

Figure 1. Scheme of "top-down" and "bottom-up" proteomic approaches.

low-abundant peptides in mass spectra dominated by high-abundant species and the loss of much information about PTMs.

Nevertheless, taking advantage of their synergy /complementarity, these techniques are often combined to generate a very efficient analytical tool for large scale profiling of complex proteomes and for studying particular sub-proteomes [25].

By scrolling the next paragraphs, the reader will realize that two techniques prevail over others mentioned in articles considered. One of these is two-dimensional difference gel electrophoresis (2D-DIGE), an in-gel approach that uses covalent labeling of proteins with fluorescent spectrally resolvable cyanine dyes (Cy2, Cy3, and Cy5) prior to isoelectrofocusing (IEF). The advantage of this technology over other electrophoretic approaches is that two or more samples are labeled with different dyes and separated on the same gel. This eliminates gel-to-gel variability and makes spot matching and quantitation much simpler and more accurate. The dyes are compatible with MS and comparable in sensitivity to silver staining methods.

One of the most commonly used procedures in the field of gel-free techniques cited in this report is the isobaric tags for relative and absolute quantitation (iTRAQ). This technology utilizes isobaric reagents (usually consisting of an N-methyl piperazine reporter group, a balance group and an N-hydroxy succinimide ester group) to label the primary amines of peptides and proteins. The function of the balance groups is to make the labeled peptides from each sample isobaric. The quantification is facilitated through the analysis of reporter groups that are generated upon fragmentation in the tandem mass spectrometer (MS/MS) system.

A careful reading of the articles contained in this report reveals that iTRAQ is ideally suited for comparing normal, diseased, and drug-treated samples, for time course studies and biological replicates.

3 Biological fluids

Blood serum or plasma are traditionally used for a myriad of tests in humans with different medical conditions and, as such, are also predominant in clinical proteomic studies. Plasma/serum are, in fact, the most used biological matrices cited in articles discussed in this report. The rationale for this choice is that changes in serum/plasma proteins that signal pathological states may be used for the diagnosis and prognosis of disorders. However, the large dynamic concentration range of these macromolecules in blood makes their analysis extremely challenging. In fact, the content of high-abundant proteins (i.e. human serum albumin and immunoglobulin) makes it difficult to detect the less abundant ones, which could be potential markers for various diseases. Depletion of these abundant proteins not always is the safest shrewdness as this process also involves the sacrifice of other potentially interesting proteins which are usually removed as well, at least partially [26]. In spite of these problems, the fact that lung cells release part of their contents into the bloodstream upon damage or death, makes human plasma one of the most important sources of information also for COPD proteomics.

Bronchoalveolar lavage fluid (BALF), induced sputum (IS) and exhaled breath condensate (EBC) may appear more suitable matrices to monitor the respiratory tract for various compounds [27]. The choice of a fluid is strongly influenced by the invasiveness degree of the methods of collection with respect to the clinical condition of patients. Working on individuals with poor lung function, sampling procedures particularly safe and easy to perform would obviously be preferred.

For instance, BAL/BALF collection, that is achieved after liquid instillation through a fibro bronchoscope and recovery of the fluid by aspiration, is a rather invasive procedure. Another limitation is represented by the close relationship between some proteins in BAL and serum that raises an issue about the strict specificity of the BALF proteome to lung.

Strictly connected with BALF is epithelial lining fluid (ELF), a thin fluid layer that covers the mucosa of the large and small airways and lung alveoli. Being the first barrier between the lung and the outside, it is seen as an intriguing target for proteomic studies focused on lung diseases. Proteomic studies on ELF are usually carried out on BALF because several concerns limit its use. First, this procedure entails the dilution of ELF by a factor ranging between 60 and 120-fold. This would, obviously, prevent the detection of less-abundant proteins. Second, different lavages may involve great variability of dilution that cannot be corrected. To overcome these limitations, an alternative method of sampling has been recently developed. It consists in the use of small probes (bronchoscopic microprobe, BMP) containing an absorptive tip that is placed on the mucosal layer of the bronchial wall under visual control during bronchoscopy [28].

Sputum and EBC are perhaps the fluids collected by the mildest processing. Sputum can be either spontaneous or induced by inhalation of nebulized hypertonic saline solution which liquefies airway secretions and promotes coughing. This allows any patient to expectorate small amounts of sample effortlessly [29]. The addition of bronchodilators, to decrease even the minimal risk associated with induction, makes sputum readily accessible. This minimal discomfort to the patient is particularly appreciated when repeated evaluation of airway inflammation in longitudinal follow-up studies must be performed. The presence in sputum of several components (mucus, cells resident within either the tissue or the airways lumen, externally derived particulate/ inhaled matter from the environment, microbial products from any colonizing bacteria or viruses, cellular debris from all of these compartments) makes it a wealth of information on lung conditions [18].

Variable amounts of EBC may be obtained, without any discomfort or risk (for both children and adults), by cooling exhaled air from spontaneous breathing in commercially

available equipments. The volatile and nonvolatile substances from the central airways contained in this water vapor are likely to reflect the composition of the airway-lining fluid. By providing an information complementary to that of BALF and induced sputum, it is potentially very helpful in proteomic/metabolomic studies on COPD as an attractive alternative to these fluids.

While the number of articles which mention the use of urine for proteomic studies on COPD is very limited, also this fluid may have significant clinical advantages. It is available in large quantities, is collected in a non-invasive and unrestricted way and its composition in terms of proteins (and fragments) is relatively stable compared to other biofluids. The protein content, while being less complex, is not very dissimilar from that of blood. Due to the filtering action of the kidneys, many of the proteins commonly detected in blood may also be detected in urine.

3.1 Plasma/serum

As stated above, a good number of authors have used plasma/serum as the source of proteomic information on COPD. Being smoking one of the main causes that leads to the development of COPD, several studies were focused on the finding of proteins differentially expressed between smokers and nonsmokers or between healthy smokers and smokers with COPD. Aim of this search was the identification of signatures that could serve as an early marker of the disorder. Using both in-gel and gel-free procedures, these investigations resulted in the identification of interesting potential biomarkers [30–35].

The analysis of plasma samples from 24 healthy smokers with COPD (stage 2a) and 24 smokers without COPD allowed Bandow et al [30] to identify candidate biomarkers of COPD and verify whether their concentration would revert to normal levels in individuals submitted to drug treatment in clinical trials. The attention of the authors was focused on the down-regulation, in smokers with COPD, of plasma retinal-binding protein and glutathione peroxidase. Other proteins were up-regulated.

The increase in these subjects of the so-called fragment D forming the D-dimer, a degradation product of fibrinogen which is used as an indicator for significant clot formation and breakdown, was also underlined. The same finding had been previously reported by other authors in patients with COPD exacerbation [31].

The plasma proteome of 38 middle-aged or older adult smokers with mild to moderate COPD investigated by Rana et al [32] by means of a sophisticated procedure allowed them to identify twelve proteins (from among thirty-three unique proteins) that have known roles in the coagulation and complement cascades. In the belief of the authors, these proteins were potential mechanistic biomarkers associated with the rate of lung function decline in COPD.

Plasma proteins differentially expressed between healthy smokers and non-smokers have also been identified by Bortner et al [33]. Several of these proteins were associated with immunity and inflammatory responses and were linked to COPD and lung cancer. Based on these findings they could demonstrate, for the first time, that the expression profile of the human plasma proteome is influenced by chronic cigarette smoking. In particular, the authors hypothesized that the increased expression of gelsolin could be connected with the necrosis of vascular endothelial cells induced by cigarette smoking. By playing a key role as an actin scavenger in plasma, this protein provides protection against actin accumulation.

A discovery panel of eight plasma samples from male subjects (four smokers without COPD and four with COPD) was analyzed by Diao et al [34, 35] to identify new biomarkers of the disease. An ELISA approach was used by the same authors on another verification panel consisting in eighty-six male subjects (thirty-three smokers without COPD and fifty-three with COPD) to verify and explore the clinical value of biomarkers. The analysis of samples from the discovery panel revealed that thirteen proteins were up-regulated and twenty-eight were down-regulated in COPD patients compared to controls. The liver-derived plasma proteins (influencing glucose metabolism [34] or functioning as T3 and T4 carrier in circulation [35]) identified and verified in the verification panel had a role in the progression of COPD. According to authors these proteins could be reliable biomarkers for predicting the occurrence of acute exacerbations.

Another current proteomic research in the COPD area is the comparison of serum/plasma protein profiles from patients with different lung disorders with the aim to identify over- or under-expressed proteins peculiar of COPD.

This was the rationale of the work by Gomes-Alves et al [36] who established the protein profiles of serum and nasal epithelial cells from healthy controls versus cystic fibrosis (CF), asthma and COPD patients. Several specific signatures that differentiated (with statistical significance) patients from controls and, in particular, CF from asthma and COPD patients were identified. These findings demonstrated that, rather than individual components, it is the combination of markers that has a better predictive value. The data generated with this work could provide the basis for future development of assays that allow prediction of lung disease progression and optimization of therapeutic intervention in CF, asthma and COPD.

The plasma protein profiles from healthy controls, stable patients with asthma and patients with COPD were compared by Verrils et al [37]. Among the 58 differentially expressed proteins identified by MALDI-TOF, the authors reported a panel of four biomarkers that can be used in combination for a careful identification of asthma and COPD patients. The panel included three positive acute-phase proteins (α2-macroglobulin, ceruloplasmin, and haptoglobin) and one type II acute-phase protein (hemopexin) that have important anti-inflammatory and anti-microbial activity through the inhibition of oxidative stress and iron sequestration. These markers have been also validated by immunoassays in a

second clinical population of older adults with obstructive airway diseases [37].

A few studies have been focused on the identification of biomarkers of acute COPD exacerbations (AECOPD). One of these was carried out by Chen et al [38] who aimed at integrating proteomic profiles of inflammatory mediators with clinical and biological informatics. The analysis of plasma samples from six healthy controls and twelve patients with stable COPD or AECOPD allowed to measure five hundred inflammatory mediators using antibody microarrays and to assess the severity of disorders by applying a Digital Evaluation Score System (DESS). Twenty mediators were significantly down-regulated in patients with AECOPD compared to stable controls. The fact that selected mediators were involved in innate immune progression, inflammatory injury, or tissue repair processes suggested an impaired regulation of systemic inflammatory responses in AECOPD.

Based on the assumption that the discovery of new biomarkers could potentially revolutionize the diagnosis and management of AECOPD, Leung et al [39] analyzed the plasma protein profiles from seventy-two AECOPD patients at both exacerbation and convalescent time points by using a Multiple Reaction Monitoring (MRM)-MS approach. Seven proteins resulted differentially expressed between the two time points selected for analysis. Given the association between AECOPD and cardiovascular co-morbidities, the attention of the authors was focused on two down-regulated proteins from the cholesterol pathway (i.e. APOA4 and APOC2) whose specific role in the AECOPD development has not been established yet. While connections between APOC2 and COPD pathogenesis have not been demonstrated by the authors, the involvement of APOA4 in anti-oxidant and anti-inflammatory responses, suggested a protective role of this protein in the lung.

Proteomic profiles of plasma and peripheral blood mononuclear cells from healthy controls, AECOPD patients on day 1, 3 and 10 after admission and patients with stable COPD have been evaluated by Shi et al [40] using an antibody-based membrane array in a study aimed at identifying AECOPD-specific inflammatory and immune modulatory mediators. This approach allowed to identify several differentially expressed proteins, among which four immune modulatory mediator candidates (haptoglobin, HP, alpha1-acid glycoprotein 1, SERPING1, and complement C3) were significantly up-regulated in patients with AECOPD (on days indicated above) compared to stable COPD or healthy controls. The authors hypothesized that the synthesis and over-expression of HP in the human lung alveolar epithelial cells during inflammation could be the rationale for understanding its involvement in lung injury and repair. Conversely, alpha1-acid glycoprotein 1 seems to modulate the activity of the immune system during the acute-phase reaction and complement C3 plays a significant role in the activation of the complement system. The role of the protein expressed by the gene SERPING 1 has not been established yet. According to authors, a complete understanding of the AECOPD-specific immune modulatory mediators' complex network will help the development of precision or personalized medicine strategies for prevention and treatment of the disorder.

The molecular mechanisms underlying COPD were investigated by Merali et al [41] who focused their attention on the identification of novel, low abundant plasma proteins which could serve as potential biomarkers of the disorder. Plasma samples in the discovery group (ten COPD patients and ten healthy controls) were stringently immunodepleted with a tandem, antibody-affinity resin column approach [42] to remove as many of the high abundant proteins as possible. Samples from each group were pooled and proteins fractionated by 1DE prior to ESI-MS/MS analysis. Thirty-one proteins, including coagulation factors, adhesion molecules and acute phase response proteins were up-regulated in COPD patients compared to controls. By contrast, molecules involved in protease-induced lung tissue injury and repair were down-regulated. Proteins that play a role in oxidative stress, protein metabolism and alveolar macrophage activation, were chosen for immunoassay validation.

Based on the assumption that an aberrant glycosylation is closely associated with the pathogenesis of various human diseases, the role played by the N-glycosylation of surfactant protein D (SP-D), a lung-specific glycoprotein, was investigated by Ito et al [43]. To determine whether changes in N-glycosylation patterns of serum SP-D could have a diagnostic value suggestive of COPD development, enriched SP-D serum samples from healthy never-smokers, smokers and stable COPD patients were submitted to proteomic analysis based on MALDI-Qit-TOF MS. The fucosylation levels of serum SP-D were found significantly higher in COPD patients compared to healthy smokers and, in turn, in these latter compared to subjects who were never-smokers. A correlation between the levels of fucosylation in serum SP-D and the severity of emphysema was also drawn. These findings strongly suggested that fucosylated SP-D may represents a potential biomarker of COPD development.

The most recent article on proteomics of COPD deals with the identification of novel biomarkers of early-stage COPD that could be helpful in terms of treatment selection and patient monitoring. Blood samples from 29 mild and 14 moderate COPD patients were analyzed by Baralla et al [44] using 2DE followed by MALDI-TOF MS. Among the differentially expressed proteins identified, those involved in inflammation were up-regulated while proteins with antioxidant properties were down-regulated. The finding that Vitamin D binding protein, apolipoprotein H and prothrombin were up-regulated in mild COPD patients and down-regulated in the group of moderate COPD could suggest that their increase in response to inflammation processes and oxidative stress burden is a temporary phenomenon that is overcome as a result of the chronic exposure of airways and lungs to oxidative stress and inflammation.

3.2 Induced sputum

Analysis of sputum to study respiratory diseases has a long pedigree. Since the early 80s, sputum induction by inhalation of hypertonic saline has been successfully used not only for the diagnosis of *Pneumocystis carinii* pneumonia in patients infected by HIV but also for examining the inflammatory response in asthmatic subjects [45]. The recent improvement of sputum induction and its subsequent processing have provided valuable information about inflammatory events in various illnesses such as tuberculosis, cystic fibrosis, lung cancer, chronic cough and COPD [46].

The first comprehensive proteomic analysis of sputum was proposed by Casado et al [47] who investigated in depth the profiles exhibited by different cohorts of patients, namely healthy nonsmokers ($n = 7$), healthy smokers ($n = 13$), smokers with chronic bronchitis ($n = 11$), COPD patients with airflow obstruction ($n = 15$) and COPD patients with airflow obstruction and emphysema ($n = 10$). In an effort to draw a profile of proteins relevant to the clinical status of each cohort, more than two hundred proteins were identified in total. The finding that immune globulins were present in larger number in healthy smokers compared to non-smokers allowed to speculate that one of the effects of smoking was the stimulation of the humoral immunity, with the consequent increase of local immunoglobulin production. Glandular proteins were up-regulated in the group of healthy smokers compared to non-smokers. The up-regulation of cytoskeletal actin in lungs of smokers was a clear sign that cellular destruction was taking place in these individuals.

The bioinformatic analysis of these data, performed by Baraniuk et al [48], allowed to deepen the information they contained. It was observed that epithelial proteins were significantly up-regulated in non-smokers compared to the other groups and that, in agreement with goblet-cell hyperplasia and mucus hypersecretion, MUC5AC was up-regulated in healthy smokers and chronic bronchitis patients compared to nonsmokers and COPD patients. An up-regulation of glandular proteins and a down-regulation of Ig joining chain in patients with airflow limitations compared to other groups was also evidenced. Particular emphasis was also given to the unique proteomic profile exhibited by subjects with emphysema that was characterized by a heavy up-regulation of both plasma proteins and components of neutrophil extracellular traps, such as histones and defensins. In conclusion, the proteomic profiles generated, peculiar for each group, were considered as complex "biosignatures" suggesting distinct pathophysiological mechanisms for MUC5AC hypersecretion, airflow obstruction, and inflammatory emphysema phenotypes.

More recently, the proteomics of IS from nonsmokers, smokers and individuals with COPD was investigated also by other research teams [49–51]. The analysis of sputa from forty-four COPD patients and twenty healthy smokers performed by Nicholas et al [49] resulted in the identification of fifteen differentially expressed proteins, mostly belonging to three major groups: acute-phase proteins, innate defense proteins and transport proteins. In particular, two proteins (lipocalin and apolipoprotein A1) were significantly reduced in COPD patients compared to healthy smokers. The correlation of their levels with FEV1/FVC ratio was the proof of their relationship with disease severity. The fact that these results were in good agreement with previously published data [47, 48] confirmed that a few of proteins identified could actually be considered reliable biomarkers of the disease.

The cysteine-specific 2D-DIGE coupled with MS was the peculiar approach applied by Ohlmeier et al [50] to analyze IS of nonsmokers, smokers, and smokers with moderate COPD. The apparent up-regulation in smokers and subjects with COPD of polymeric immunoglobulin receptor, a protein involved in specific immune defense and inflammation attracted their attention as this finding suggested a possible role of this protein in the r–egulation of inflammation during COPD pathogenesis.

To investigate how changes in the IS proteome may reflect different conditions such as cigarette smoke exposure, smoking cessation or the presence of early-stage COPD, Titz et al [51] analyzed the protein profiles of IS from current asymptomatic smokers, smokers with early stage COPD, former smokers, and never smokers. The proteome of current smokers clearly reflected the common physiological responses to smoke exposure, including the xenobiotic and oxidative stress response, changes in mucin production and alterations in the protease balance. By contrast, the former smoker group showed nearly complete attenuation of these biological effects. This study was a good model for studying the ability of sputum profiling to capture the complex and reversible physiological response to cigarette smoke exposure. It is worth pointing out that, also in this case, several of the differentially expressed proteins identified were the same previously indicated as potential signatures of COPD [47–49].

The work of Terracciano et al [52] pointed to a different goal. They were interested in the characterization of the low-molecular weight proteome of IS from healthy controls and patients affected by COPD and asthma. To reach this goal, an intriguing proteomic approach based on a solid phase extraction step (with mesoporous silica beads, MSBs) coupled to MALDI-TOF MS was applied. Briefly, after incubating (for 1 h at room temperature) MSBs with IS samples, the bound peptides were eluted, analyzed by MS and differentially expressed proteins identified. The interest of the authors was focused on human α-defensins, antimicrobic peptides produced by neutrophils whose levels were significantly increased in COPD patients compared to healthy controls. Beside their role as important components of the innate and adaptive immune response pathways, α-defensins are known for their cytotoxic effects on cells. These peptides also compete with neutrophil elastase (NE) for the binding with α-1-antitrypsin, the NE inhibitor. Based on these considerations, the authors suggested that increased α-defensin levels may directly contribute to lung

tissue damage and may also affect the protease/antiprotease balance, thus contributing to COPD exacerbation.

Aim of the study by Gray et al [53] was to identify potential biomarkers of suppurative and inflammatory lung diseases by analyzing IS from twenty healthy controls, twenty-four patients with asthma, twenty-four COPD patients, twenty-eight subjects affected by CF, and nineteen bronchiectasis patients. Calgranulins A, B and C, while being up-regulated in all disease groups compared to controls, were particularly high in CF and bronchiectasis patients. Conversely, very low levels of Clara cell secretory proteins were found in these groups. Finally, a separate form of calgranulin A (whose functional significance remains unclear), originated by a theoretical removal of two residues (glutamic acid and lysine) from the N-terminus of this protein, was identified in the same groups.

To evaluate the association of sputum bactericidal/permeability-increasing fold containing protein B1 (BPIFB1) levels with smoking and longitudinal changes in lung function of smokers with COPD, Gao et al [54] investigated the proteomics of IS from thirty-one non-smokers, one hundred and sixty-nine smokers and fifty-two patients with COPD. They found a significant up-regulation of BPIFB1 (also known as LPLUNC1) in smokers with COPD compared to non-smokers and smokers without COPD. This protein is expressed in the airway epithelium, in a population of goblet cells in the nasal passage and within the serous cells of the airway submucosal glands. The protein is among the most abundant polypeptides secreted into the respiratory tract and is thought to have a significant role in airway defense. These results were in perfect agreement with the role of BPIFB1 in pulmonary immunity and the levels of this protein in sputum were significantly correlated to longitudinal declines of lung function in patients with COPD.

Scrolling through this paragraph the reader can observe that, despite the obvious differences among laboratories, patients and applied techniques, a core of proteins (LPLUNC1, lipocalins, mucins, calgranulins) is steadily identified. Since this does not happen by chance, it could be the proof of principle that one of these proteins or a cluster of them is actually involved in the mechanisms underlying the disorder. No wonder whether further studies recognize these proteins as reliable biomarkers of COPD.

Taken together, these results also confirm that the sophisticated techniques presently available may foster a big step forward in the search for disease markers.

3.3 Bronchoalveolar lavage fluid

Given that proteins detected in BALF are secreted by epithelial and inflammatory cells or derive from plasma exudation, the study of this proteome in patients affected by COPD may help to gain critical insights into pathogenesis and lung defense mechanisms. The results discussed in the current paragraph show that the analysis of this fluid may provide data alternative/complementary to those of IS and/or serum.

The global proteome of BALF from twenty-nine light and heavy smokers and eighteen never-smokers in a six to seven years follow-up study was investigated by Plymoth et al [55]. Briefly, by applying a technology toolbox (consisting of replicate 2DE separations, image annotation and mass spectrometry identification), the authors identified a global set of proteins differentially expressed by presence/absence and intensity scores. In particular they observed that inflammatory and redox proteins were unambiguously up-regulated in smokers compared to never-smokers. This finding was intriguing as it suggested that certain patterns of proteins could be representative of COPD progression even before the disease becomes clinically evident.

The involvement of redox processes in the development of COPD was confirmed by Pastor et al [56,57] who evidenced a distinct proteomic reactive oxygen species (ROS) protein signature in BALF from COPD and lung cancer patients. The fifteen differentially expressed proteins associated with ROS metabolism identified in this study highlighted the role of ROS proteins in the pathogenic pathways of lung cancer and COPD. These findings provide a new and larger context for future studies on the pathological mechanisms of COPD and support the view of BALF as an important source of information of lung status.

The intent of the work by Kohler et al [58] was to elucidate putative molecular mechanisms underlying gender-based differences in the pathophysiology of COPD. From the analysis of the proteome of non-symptomatic smokers and smokers with COPD significant gender differences could be observed. A subset of nineteen proteins provided a highly predictive model for classification of female non-symptomatic smokers from female smokers with COPD. Subsequent pathway analyses correlated the observed alterations to down-regulation of the lysosomal pathway and up-regulation of the oxidative phosphorylation pathway. Cathepsin B (down-regulated), ATP synthase and chaperonin (both up-regulated) were the most prominent disease marker candidates. No altered proteins were found in the corresponding male classification model.

The strategy followed by Tu et al [59] to analyze the BALF proteome from healthy controls and patients with moderate and stable COPD (ten subjects/group) included an efficient preparation procedure that normalized the variable protein concentration in BALF and provided quantitative recovery. In addition, the nano-LC/MS analysis was performed with a long, heated column. Seventy-six proteins were determined as significantly altered in COPD. The biological processes involved in this diversity were alcohol metabolic process, gluconeogenesis/glycolysis, inflammatory response, proteolysis, and oxidation/reduction. In particular, the authors' attention was focused on the significant up-regulation of key enzymes involved in alcohol metabolism whose presence in BALF has never been reported by other authors. The alteration of these enzymes could be considered a new mechanism of response to oxidative stress in COPD which has critical implications in its pathogenesis. Thus, these findings provide new insights

for identifying novel biomarkers and pathological mediators in clinical studies.

3.4 Epithelial lining fluid

The use of ELF in the COPD area was mainly promoted by Franciosi's team [60–62] to investigate the proteomics of healthy subjects and COPD patients.

The initial work consisted in the comparison of the pattern of proteins in ELF of a single control versus that of a COPD patient [60]. This work allowed them to identify more than three hundred proteins related to inflammation, oxidative stress, bacterial infection and protease/anti-protease balance. Among the inflammatory proteins, a polypeptide belonging to the PLUNC family which can be involved in the airway inflammatory response upon exposure to irritants and can also be associated with tumor progression is worth of mention. In addition, the up-regulation in the COPD patient of two proteins of the S100 family, expressed in epithelial cells, macrophages and phagocytes during chronic inflammations, suggested their correlation to COPD progression. The presence of proteins related to oxidative stress, i.e. manganese superoxide dismutase (MnSOD), an enzyme involved in the removal of reactive oxygen species, confirmed the previously discussed (see [55–57]) importance of oxidative stress in the development of COPD. Other proteins, i.e. proteasome-related proteins are thought to contribute to the proteolytic degradation of alveolar walls.

Proteins belonging to the PLUNC and the redox family had been previously discussed in paragraphs dedicated to sputum and BALf, respectively (see above paragraphs). Detection of these proteins also in ELF provides evidence of the proximity of this matrix to both sputum and BALF and confirms that its analysis can be very helpful for integrating the information collected from the other fluids.

To further evaluate the presence of putative COPD biomarkers in ELF, the same authors performed two comparative studies on a larger number of COPD and control samples (four samples/group) [61]. They focused their attention on four proteins (lactotransferrin, α1-anti-chymotrypsin, cofilin-1 and HMGB1) that were significantly over expressed in COPD patients compared to controls. Given the increase of secretion of antimicrobial proteins by epithelial cells upon airway inflammation, the up-regulation of lactotransferrin could be related to its antimicrobial properties. Due to its anti-inflammatory activity, the over-expression of α1-anti-chymotrypsin and the simultaneous decreased levels of HMGB1 are suggestive of a necrotic state of the epithelial cells covering airways. Finally, the increase in cofilin-1 concentration is, most likely, a dramatic response to oxidative stress due to elevated levels of ROS.

In the last article of this series [62], these authors assessed whether members of a family with severe early-onset COPD are "susceptible individuals" with an increased risk to develop COPD. ELF from young individuals susceptible or non-susceptible to develop COPD and older subjects with established COPD was collected at baseline and 24 h after smoking three cigarettes. Controls at baseline were older healthy smoking and non-smoking individuals. The intriguing results in terms of differentially expressed proteins allowed the authors to deduce that, unlike patients with established COPD, smoking induces a differential protein response in susceptible and non-susceptible young individuals.

3.5 Exhaled breath condensate

The properties of EBC mentioned above make it a useful tool for epidemiological investigation, in particular for an early diagnosis of COPD and other lung diseases such as asthma, bronchiectasis, cystic fibrosis and adult respiratory distress syndrome.

Two studies concerning the proteomic profiles of EBC from COPD patients have been carried out in our own laboratory [8, 63]. In both cases aim of the study was obtaining a global picture of the EBC proteome in patients with α1-antitrypsin deficiency (AATD) and pulmonary emphysema. The two studies differed either for the number of patients involved and for the methodological approach applied.

In the first study [63] EBCs from healthy controls and patients (twenty subjects/group) were analyzed in parallel by a combination of 1DE, 2DE, μ-HPLC and SELDI-TOF MS. The results evidenced the up-regulation in AATD patients of a few inflammatory proteins. The identification in patients of a good number of cytokeratins allowed to speculate that these molecules were clinically relevant endpoints of pulmonary damage. This conclusion was in contrast with the hypothesis of other investigators [64, 65] who suggested an environmental origin for a large fraction of EBC proteins.

The cohort considered in the second study [8] consisted of eighty-three individuals. Forty-five were non-smokers and healthy smokers (NS/HS); fifteen were COPD patients without emphysema (COPD) and twenty-three were subjects with pulmonary emphysema associated with AATD (AATD). Among the proteins identified by LC-MS/MS, also in this case several inflammatory cytokines were over expressed in patients compared to NS/HS. The same behavior was observed for type I and II cytokeratins; two SP-A isoforms, calgranulin A and B and α1-antitrypsin. Of great interest was the identification of IL-1α in EBC of AATD and not in that of COPD patients. This allowed to speculate that this molecule could discriminate the two groups of patients.

Another study in this area was carried out by Kononikhin et al [66] who investigated the protein composition of EBC from patients with different respiratory diseases (seventeen COPD patients, thirteen patients with pneumonia and twenty-three healthy non-smokers). Three differentially expressed proteins (dermcidin,DCD; α1-microglobulin/bikunin precursor and SHROOM3) attracted authors' attention. DCD, an antimicrobial protein with proteolytic activity, was down-regulated in patients with pneumonia compared to other groups. This finding was of great interest as it suggested that the attenuation of antibacterial

protection could be one of the key factors responsible for the disease onset. The α1-microglobulin/bikunin precursor is proteolytically processed into two distinct proteins i.e. α1-microglobulin, which may play a role in the inflammatory processes regulation and bikunin, a urinary trypsin inhibitor with an important role in many physiological and pathological processes. The down-regulation of α1-microglobulin/bikunin precursor in patients with COPD and pneumonia could be due to the acute inflammation that distinguishes these two groups from others. Conversely, the increased expression levels of SHROOM3 (a protein involved in regulating cell shape) in subjects with COPD and pneumonia could be related to lung tissue degradation.

3.6 Urine

The only article dealing with the proteomics of urine in the field of COPD is that from Carleo et al [67]. Based on the evidence that urinary proteome can be highly informative also in non-urogenital diseases, they investigated (by capillary electrophoresis coupled to MS) the urinary peptidome of nineteen patients with normal (PiMM; n = 7) and deficient (PiZZ; n = 12) α1-antitrypsin (AAT) variants. They identified sixty-six peptides from the collagen family that were distributed unevenly between the two phenotypes, some being more frequent in the PiMM phenotype and others in the PiZZ phenotype. This latter was also characterized by low levels of urinary peptides involved in lipoprotein/lipid and retinoic acid metabolism. Conversely, gelsolin and hemoglobin alpha were identified in urine of PiZZ individuals but not of PiMM. Of great interest was also the finding of two AAT peptides in 43% of PiMM cases and their total absence in the PiZZ phenotype.

These results could be helpful not only for a better understanding of the pathobiology of disease progression but also for improving therapies personalized according to patients' phenotype.

4 Lung tissue

It has been previously emphasized that the best option for diagnosing pulmonary disorders causing minimal discomfort to the patient is the use of biological fluids collected through little- or non-invasive methods. However, to obtain an accurate diagnosis of the disorder under investigation, in some cases more invasive approaches are strictly necessary. Transbronchial lung biopsies (performed using a bronchoscope inserted through the main airways of the lungs) or open lung biopsies (performed by making an incision in the chest between the ribs) are typical surgical procedures. The recovered tissue is a source of information alternative/complementary to that held by fluids.

A comprehensive analysis of lung tissues (and IS) from healthy controls and patients affected by COPD (at different stages), idiopathic pulmonary fibrosis (IPF) and AATD was performed by Ohlmeier et al [68–70] with the purpose to identify novel biomarkers for an early diagnosis of COPD. They observed that SP-A was up-regulated in lungs of COPD patients compared to those of healthy and fibrotic patients. These results were confirmed by immune-histochemical, morphometric and western blotting analyses. Increased SP-A levels were also detected in IS from COPD patients. Being SP-A the major pulmonary surfactant-associated protein with multiple functions in the regulation of inflammatory processes and in innate host defense, it could be considered a promising candidate for early detection of COPD [68].

In another comparative study performed on lung tissues of the same patients [69], these authors identified eighty-two differentially expressed proteins among which COPD-specific proteins. The finding that transglutaminase 2 (TGM2), a multifunctional enzyme associated with other pathologies (including autoimmune, inflammatory and neurodegenerative diseases), was up-regulated in severe to very severe COPD correlated this enzyme to COPD severity. An upgrade of this research consisted in the investigation of the content of different receptors for advanced glycation end product (RAGE) isoforms in lung tissues of patients mentioned above [70]. They identified three RAGE variants (full-length RAGE, FLRAGE, C-terminal processed full-length RAGE, cRAGE and the alternatively spliced endogenous secretory RAGE, esRAGE). Based on previous findings that RAGE interacts with a series of ligands and with bacteria and prion surface molecules [71], the current results suggest that FLRAGE in healthy lungs could act as a sensor for infections or other cellular signals mediated by specific ligands. Interestingly, all these variants were down-regulated in IPF compared to other cohorts whereas their levels were not reduced in AATD. Conversely, while both FLRAGE and esRAGE remained unchanged in COPD patients, the levels of cRAGE were down-regulated, this decrease being more pronounced in severe COPD. As above underlined for TGM2, also this finding was of great interest as it revealed that the cRAGE level could be correlated to the disease severity. Furthermore, since IPF is characterized by pure fibrosis and COPD lungs contain fibrotic lesions, the loss of FLRAGE and cRAGE could be considered a marker of fibrosis and/or tissue damage. However, being RAGE levels unchanged in AATD patients compared to controls, its down-regulation could not be directly associated to pure pulmonary emphysema.

The protein profiles of lung tissue from non-smokers, smokers without COPD and smokers with COPD have been investigated by 2DE and MALDI-TOF/MS also by Lee et al [72]. Not surprisingly, differentially expressed proteins were found between the different cohorts of individuals analyzed. Among the up-regulated proteins in COPD patients, of particular interest were matrix metalloproteinase MMP-13 (an extracellular zinc-dependent endopeptidase involved in the degradation and remodeling of extracellular matrix in physiological and pathological processes [72]) and thioredoxin-like protein 2 (predominantly expressed in the cilia of lung airway epithelium). Based on these findings, the authors suggested that gaining further insights into

the above mentioned proteins could lead to a better understanding of the pathophysiologic mechanism underlying COPD.

Healthy lungs and lung specimens from IPF and COPD patients were used by Ishikawa et al [73] to study in more details the expression of hemoglobin α (Hbα) and β (Hbβ) monomers in the human lung, according to their data, both Hb monomers were regularly expressed in the alveolar epithelial cells of normal and COPD lung. By contrast, their levels were very low or undetectable in IPF lungs, in which the alveolar epithelium is replaced by a thick fibrotic barrier. In addition, the modification of a thiol group (Cys105) in the Hbα monomer, prevented the formation in these lungs of the Hbα complexes. Even though the authors assessed that the loss of Hbα complex warrants further investigation, they pointed to this event as a IPF-specific modification.

A sequential tissue extraction strategy based on quantitative comparison of the proteome of lung tissue from COPD and IPF patients was applied by Åhrman et al [74] to describe the disease-specific remodeling of human lung tissue, with specific focus on the extracellular matrix (ECM) proteome. Metalloproteinase inhibitor 3 (TIMP3) and matrix metalloproteinase 28 (MMP-28), two important extracellular matrix regulators; serine protease HTRA1 and macrophage metalloelastase (MMP-12), involved in tissue homeostasis, were up-regulated in COPD patients compared to IPF and controls. Conversely, cell adhesion laminins LAMB1 and LAMC1 were down-regulated in IPF.

Taken together, these findings suggested an impaired cell-ECM communication. In addition, imbalances in the protease/protease inhibitor ratio were detected in both COPD and IPF groups.

5 Cell culture

It has been previously reported that the imbalance of redox status of red blood cells due to extensive oxidative stress induced by COPD causes structural and functional changes of these cells in patients affected by this pathology [75]. In an effort to identify these changes in the sub-proteome of erythrocyte's membrane, Alexandre et al [76] compared a cohort of COPD patients versus healthy controls (about twenty-five subjects each group). The erythrocyte membrane fraction was isolated by carbonate treatment and ultracentrifugation and its quantitative protein profiling was obtained by using differential stable isotope ($^{16}O/^{18}O$) labelling and multidimensional shotgun proteomics with SCX/RPLC-MS. The number of proteins identified was large (more than one thousand) and many of these (around two hundred) showed significant changes in their relative abundance between groups. This effect was particularly evident in proteins associated with COPD erythrocyte deformation and dysfunction. It must be acknowledged that, while not being exploited for diagnostics, detection of these changes at the proteome level may be helpful to gain a better understanding of COPD.

To evaluate whether investigation on cytokine expression could be a suitable approach to measure systemic inflammation in forty-one COPD patients (and seven healthy controls), Loi et al. [77] used peripheral blood neutrophils. The labeling of protein extracts with fluorescent cyanine dyes (Cy2/Cy3/Cy5) and the separation by 2D-DIGE resulted in the identification of 1200–2400 protein spots, twenty-one of which were differentially expressed.

The release of damage-associated molecular patterns (DAMPs) by airway epithelial cells is believed to play a crucial role in the initiation of COPD. High-mobility group box-1 (HMGB1) is the classical DAMP that functions as "alarmin" by acting on local immune cells to evoke the activation of innate and adaptive immune responses. The profiling of HMGB1 in the culture supernatant of un-stimulated airway epithelial cells was performed by Wong et al [78] with high-resolution clear native electrophoresis (hrCNE) immune precipitation and LC−MS/MS. This study allowed identification of one hundred eighty-five proteins among which fourteen aroused considerable interest being identified as primary interactors of HMGB1. These findings provided a new starting point for future investigations on possible extracellular functions of HMGB1 in epithelial cell homeostasis at the airway mucosal surface.

To investigate the impact of long-term habitual smoking on the immune cell proteome of BAL, Yang et al [79] applied the iTRAQ (4-plexed labelling) procedure to BAL cells from never-smokers ($n = 17$) and smokers with normal lung function ($n = 25$). The pathway enrichment analyses performed by the authors revealed that the significantly ($p < 0.05$) altered proteins (five hundred) were associated with fifteen molecular pathways. Two of these pathways, i.e. the phagosome and leukocyte trans endothelial migration, significantly correlated with the proportion of CD8+ T-cell in BAL, as well as with the level of airway obstruction (FEV1/FVC) in the group of smokers. These findings stress the importance these pathways may play both in the protection against, as well as in the early pathophysiology, of smoking-induced inflammatory lung disorders such as COPD.

This shotgun proteomic method was subsequently applied (on BAL cells from smokers with normal lung function and early stage COPD patients) by the same research group to demonstrate gender differences in respiratory symptoms, lung function and molecular markers of inflammation in COPD [80]. While in females one hundred sixty-four proteins were significantly altered in smokers versus COPD, only twenty four proteins were altered in the corresponding males. This approach revealed that the gender specific dysregulation of the phagocytosis-lysosomal axis and T-cell polarization may provide mechanistic clues to the faster decline of lung function and higher risk of hospitalization observed in female COPD patients.

A schematic summary of fluids/tissues considered in this report together with the methodological approaches applied for their investigation, the number of patients analyzed, of proteins identified and the reference number of the original article is shown in Table 1.

Table 1. Schematic summary of fluids/tissues with methodological approaches, patients analyzed, proteins identified and the reference number

Source	Proteomic approach	Number of subjects analyzed	Number of proteins identified	Reference
Plasma/serum	2DE, MALDI-TOF, nano-LC-MS/MS	48	5298	[30]
	AMT, PMT, FT-ICR MS	38	533	[31]
	iTRAQ	451	100	[32]
	iTRAQ-labeling	95	830	[33]
	iTRAQ-labeling	94	n.r.	[34]
	SELDI-TOF-MS	125	n.r.	[35]
	2D-DIGE, MALDI-TOF	43	58	[36]
	Microarray Assay	18	507	[37]
	(MRM)-MS	72	55	[38]
	Microarray Assay	220	507	[39]
	1DE, ESI-MS/MS	80	31	[40]
	MALDI-QIT-TOF	53	n.r.	[42]
	2DE, MALDI-TOF MS	43	20	[43]
IS	LC-ESI-Q/TOF-MS	56	203	[46, 47]
	2DE, LC-ESI-MS	97	15	[48]
	2D-DIGE, MS	544	n.r.	[49]
	LC-MS/MS	240	n.r.	[50]
	SPE, MALDI-TOF MS	n.r.*	400	[51]
	SELDI-TOF/MS	115	976	[52]
	2DE, MS	252	n.r.	[53]
BALf	2DE, LC-MS/MS	47	481	[54]
	2DE, MALDI-TOF/TOF	60	123	[55, 56]
	2D DIGE, nano-LC-MS	77	n.r.	[57]
	nano LC/MS	20	423	[58]
ELF	nanoLC-MS/MS	25	134	[59]
	2D, LC-MS/MS, MALDI-TOF/TOF	8	300	[60, 61]
EBC	1DE, 2DE, μ-HPLC, SELDI-TOF MS	83	76	[8]
	LC-MS/MS, SELDI-TOF	45	n.r.	[62]
	LC-MS/MS	79	n.r.	[65]
Urine	CE, MS	19	66	[66]
Lung tissue	2DE, MS	8	n.r.	[67]
	2D-DIGE, MS	8	n.r.	[68]
	2DE, MS	51	82	[69]
	2DE, MALDI-TOF-MS	22	20	[71]
	2DE, MS	28	n.r.	[72]
	1DE, LC-MS/MS	11	3369	[73]
Cell culture	$^{16}O/^{18}O$ stable isotope labeling, LC-MS/MS	53	1083	[75]
	2D-DIGE	48	21	[76]
	LC-MS/MS	n.r.	n.r.	[77]
	iTRAQ, LTQ Orbitrap MS	42	506	[78]
	iTRAQ, LTQ Orbitrap MS			[79]

6 From laboratory research to a clinical setting: future perspectives

Not surprisingly, the commonly used on-gel and gel-free proteomic methods for the analysis of biofluids and tissues, which have been generated and developed in research laboratories, not always reflect the needs requested by a clinical setting. As a matter of fact, relatively few proteomic techniques are currently applied in routine diagnostic laboratories that continue to witness the prevalence of genetic and immune assays.

The difficulties encountered by proteomics to enter the routine clinical diagnostic laboratories have different technical and (bio)chemical motivations. These reasons have been comprehensively analyzed by Vogeser and Seger who addressed a variety of issues in an interesting review article [81]. They realized that the perception of expense, sensitivity, availability, as well as throughput and robustness could all be factors that limit the diffusion of LC-MS/MS in the setting of clinical laboratories. Indeed, the high costs of the purchase/maintenance of equipments are considerably increased by significant investments needed for experiencing technicians in method development/validation, daily operation and troubleshooting.

This analysis of strengths and weaknesses of LC-MS/MS systems was substantially in agreement with that performed

by van den Ouweland and Kema [82]. These latter authors, however, supported another interesting hypothesis i.e. that the implementation of proteomic approaches in clinical laboratories must proceed through the availability of ready-to-use reagent kits that eliminate method development and validation steps. The adoption of such strategy may probably arouse interest around LC-MS/MS and promote a wider acceptance of these procedures in routine laboratories.

In spite of this, all experimental results commented in this report, taken together, show at which extent the contribution offered by proteomic procedures may be important in deepening the mechanisms of COPD and provide a good picture of COPD proteomics to date. They emphasize that proteomics of COPD, while not being a current tool in clinical laboratories, has emerged at a research level over the past decade as an attractive analytical technique for investigating this severe respiratory disease. Several of the above reports demonstrate the suitability of working "in parallel" on healthy and diseased states. The rationale of this approach is that the comparison of the proteomic fingerprints of these two conditions may highlight perturbations from the healthy state phenotype before the disease can manifest. These data confirm that the progression from health to disease state always matches with significant changes of protein expression in both the circulation and affected tissues.

It can be inferred that proteomic techniques have the merit to produce profiles relevant for gaining insights into molecular events correlated with the onset/progression of COPD and also to provide qualitative/quantitative information on proteins directly involved in the disorder.

Finally, it should be underlined that the quality of data has witnessed a considerable improvement through the application of sophisticated technologies (i.e. the iTRAQ labeling, the MALDI-Qit TOF system) that couple accuracy of analysis with precision in the calculation of protein concentration. This progress resulted in the production of high-reliable data and in the possibility to determine the extent of post-translational modifications (phosphorylation, glycosylation and ubiquitination) that significantly contribute to protein function [38]. The prospective transfer of this biological knowledge into the clinic will hopefully allow understanding the role these proteins play in the pathogenesis of respiratory diseases. This obviously means finding the coveted link between basic medical research and clinical laboratory medicine.

Given these assumptions, this branch of respiratory proteomics will likely witness a considerable improvement in the future.

7 Concluding remarks

The significant advances in both procedures and instrumentation observed over the last decade pushed the boundaries of what is possible in proteomic research of human tissues and biofluids. The establishment of comprehensive protein maps creates optimism regarding the potential of proteins identified, as the sum of many mediators, to reveal disease-specific fingerprints thus being able to characterize a disease. The content of this report confirms that the research dealing with the use of proteomics for deciphering the protein profiles of fluids/tissues from individuals affected by chronic obstructive pulmonary disease (and other respiratory disorders) is very fruitful. The constant publication of good articles in this field witnesses the benefits that respiratory proteomics may contribute to the identification/characterization of COPD-associated proteins.

However, despite the number of proteins so far indicated as potential biomarkers of the disorder is high, validation of these findings still needs a great deal of work and novel platforms must be developed to demonstrate their clinical utility. Nevertheless, the current data are sufficiently encouraging to justify subsequent application of these technologies to other clinical specimens in the firm belief that proteomics could, in a near future, contribute to revolutionize the treatment of many diseases.

The authors have declared no conflict of interest.

8 References

[1] Lopez, A. D., Murray, C. C., *Nat. Med.* 1998, *4*,1241–1243.

[2] Barnes, P. J., *N. Engl. J. Med.* 2000, *343*, 269–280.

[3] Chapman, K. R., Mannino, D. M., Soriano, J.B., Vermeire, P. A., Buist, A.S., Thun, M. J., Connell, C., Jemal, A., Lee, T. A., Miravitlles, M., Aldington, S., Beasley, R., *Eur. Respir. J.* 2006, *27*, 188–207.

[4] Miravitlles, M., Roche, N., Cardoso, J., Halpin, D., Aisanov, Z., Kankaanranta, H., Kobližek, V., Śliwiński, P., Bjermer, L., Tamm, M., Blasi, F., Vogelmeier, C. F., *Respir. Res.* 2018, *19*, 11.

[5] Collins, P. F., Stratton, R. J., Kurukulaaratchy, R. J., Elia, M., *Int. J. Chron. Obstruct. Pulmon. Dis.*. 2018,*13*, 1289–1296.

[6] Fernández-Villar, A., Represas, C., Mouronte-Roibás, C., Ramos-Hernández, C., Priegue-Carrera, A., Fernández-García, S., López-Campos, J. L., *PLoS One*. 2018, *13*, e0194983.

[7] Amin, A. N., Bollu, V., Stensland, M. D., Netzer, L., Ganapathy, V., *Am. J. Health Syst. Pharm.* 2018, *75*, 359–366.

[8] Fumagalli, M., Ferrari, F., Luisetti, M., Stolk, J., Hiemstra, P. S., Capuano, D., Viglio, S., Fregonese, L., Cerveri, I., Corana, F., Tinelli, C., Iadarola, P., *Int. J. Mol. Sci.* 2012, *13*, 13894–910.

[9] Viglio, S., Stolk, J., Luisetti, M., Ferrari, F., Piccinini, P., Iadarola, P., *Electrophoresis*. 2014, *35*, 109–18.

[10] Brightling, C. E., *Allergy Asthma Proc.* 2016, *37*, 432–438.

[11] Ho, T., Dasgupta, A., Hargreave, F. E., Nair, P., *Expert Rev. Respir. Med.*. 2017, *11*, 403–411.

[12] Liu, X., Qu, J., Xue, W., He, L., Wang, J., Xi, X., Liu, X., Yin, Y., Qu, Y., *Int. J. Chron. Obstruct. Pulmon. Dis.*. 2018, *13*, 1217–1228.

[13] Salimian, J., Mirzaei, H., Moridikia, A., Harchegani, A. B., Sahebkar, A., Salehi, H., *J. Res. Med. Sci.*. 2018, *23*, 27.

[14] Linder, R., Rönmark, E., Pourazar, J., Behndig, A. F., Blomberg, A., Lindberg, A., *Respir. Res.* 2018, *19*, 64.

[15] Wheelock, C. E., Goss, V. M., Balgoma, D., Nicholas, B., Brandsma, J., Skipp, P. J., Snowden, S., Burg, D., D'Amico, A., Horvath, I., Chaiboonchoe, A., Ahmed, H., Ballereau, S., Rossios, C., Chung, K. F., Montuschi, P., Fowler, S. J., Adcock, I. M., Postle, A. D., Dahlén, S. E., Rowe, A., Sterk, P. J., Auffray, C., Djukanovic, R., *Eur. Respir. J.* 2013, *42*, 802–825.

[16] Pelaia, G., Terracciano, R., Vatrella, A., Gallelli, L., Busceti, M. T., Calabrese, C., Stellato, C., Savino, R., Maselli, R., *Biomed. Res. Int.*. 2014, *2014*, 764581.

[17] Stockley, R. A., *Int. J. Chron. Obstruct. Pulmon. Dis.*. 2014, *9*, 163–77.

[18] Terracciano, R., Pelaia, G., Preianò, M., Savino, R., *Proteomics. Clin. Appl.* 2015, *9*, 203–20.

[19] Teran, L.M., Montes-Vizuet, R., Li, X., Franz, T., *J. Proteome Res.* 2015, *14*, 38–50.

[20] Priyadharshini, V. S., Teran, L. M., *Adv. Protein Chem. Struct. Biol.*. 2016, *102*, 115–146.

[21] Paone, G., Leone, V., Conti, V., De Marchis, L., Ialleni, E., Graziani, C., Salducci, M., Ramaccia, M., Munafò, G., *Eur. Rev. Med. Pharmacol. Sci.*. 2016, *20*, 698–708.

[22] Ghosh, N., Dutta, M., Singh, B., Banerjee, R., Bhattacharyya, P., Chaudhury, K., *Expert Rev. Mol. Diagn.* 2016, *16*, 897–913.

[23] Kan, M., Shumyatcher, M., Himes, B. E., *Respir. Res.* 2017, *18*, 149.

[24] Fujii, K., Nakamura, H., Nishimura, T., *Expert Rev. Proteomics* 2017, *14*, 373–386.

[25] Yan, X., Sun, L., Zhu, G., Cox, O. F., Dovichi, N. J., *Proteomics* 2016, *16*, 2945–2952.

[26] Urbas, L., Brne, P., Gabor, B., Barut, M., Strlic, M., Petric, T. C., Strancar, A., *J. Chromatogr. A* 2009, *1216*, 2689–2694.

[27] Montuschi, P., Santini, G., Valente, S., Mondino, C., Macagno, F., Cattani, P., Zini, G., Mores, N., *J. Chromatogr. B AnalytTechnolBiomed Life Sci.* 2014, *964*, 12–25.

[28] Ishizaka, A., Watanabe, M., Yamashita, T., Ogawa, Y., Koh, H., Hasegawa, N., Nakamura, H., Asano, K., Yamaguchi, K., Kotani, M., Kotani, T., Morisaki, H., Takeda, J., Kobayashi, K., Ogawa, S. *Crit. Care Med.* 2001, *29*, 896–898.

[29] Iadarola, P., Viglio, S. *Expert Rev. Proteomics* 2017, *14*, 391–393.

[30] Bandow, J. E., Baker, J. D., Berth, M., Painter, C., Sepulveda, O. J., Clark, K. A., Kilty, I., VanBogelen, R. A., *Proteomics* 2008, *8*, 3030–41.

[31] Kunter, E., Ilvan, A., Ozmen, N., Demirer, E., Ozturk, A., Avsar, K., Sayan, O., Kartaloğlu. Z., *Respiration.* 2008, *75*, 145–54.

[32] Rana, G. S., York, T. P., Edmiston, J. S., Zedler, B. K., Pounds, J. G., Adkins, J. N., Varnum, S. M., Smith, R. D., Liu, Z., Li, G., Webb, B. T., Murrelle, E. L., Flora J. W., *Anal. Bioanal. Chem.* 2010, *397*, 1809–19.

[33] Bortner, J. D. Jr., Richie, J. P. Jr., Das, A., Liao, J., Umstead, T. M., Stanley, A., Stanley, B. A., Belani, C. P., El-Bayoumy, K., *J. Proteome Res.* 2011, *10*, 1151–9.

[34] Diao, W. Q., Shen, N., Du, Y. P., Liu, B. B., Sun, X. Y., Xu, M., He, B., *Sci. Rep.* 2016, *6*, 30045.

[35] Diao, W., Shen, N., Du, Y., Sun, X., Liu, B., Xu, M., He, B., *Int. J. Chron. Obstruct. Pulmon. Dis.*. 2017, *12*, 1549–1564.

[36] Gomes-Alves, P., Imrie, M., Gray, R. D., Nogueira, P., Ciordia, S., Pacheco, P., Azevedo, P., Lopes, C., De Almeida, A. B., Guardiano, M., Porteous, D. J., Albar, J. P., Boyd, A. C., Penque, D., *Clin. Biochem.* 2010, *43*, 168–77.

[37] Verrills, N. M., Irwin, J. A., He, X. Y., Wood, L.G., Powell, H., Simpson, J. L., McDonald, V.M., Sim, A., Gibson, P. G., *Am. J. Respir. Crit. Care Med.* 2011, *183*, 1633–43.

[38] Chen, H., Wang, Y., Bai, C., Wang, X., *J. Proteomics* 2012, *75*, 2835–43.

[39] Leung, J. M., Chen, V., Hollander, Z., Dai, D., Tebbutt, S. J., Aaron, S. D., Vandemheen, K. L., Rennard, S. I., FitzGerald, J. M., Woodruff, P. G., Lazarus, S. C., Connett, J. E., Coxson, H. O., Miller, B., Borchers, C., McManus, B. M., Ng, R. T., Sin, D. D. *PLoS One.* 2016, *11*, e0161129.

[40] Shi, L., Zhu, B., Xu, M., Wang, X., *Cell Biol. Toxicol.* 2018, *34*, 109–123.

[41] Merali, S., Barrero, C. A., Bowler, R. P., Chen, D. E., Criner, G., Braverman, A., Litwin, S., Yeung, A., Kelsen, S. G., *COPD.* 2014, *11*, 177–89.

[42] Patel, B. B., Barrero, C. A., Braverman, A., Kim, P. D., Jones, K. A., Chen, D. E., *J. Proteome Res.* 2012, *11*, 5947–5958.

[43] Ito., E., Oka, R., Ishii, T., Korekane, H., Kurimoto, A., Kizuka, Y., Kitazume, S., Ariki, S., Takahashi, M., Kuroki, Y., Kida, K., Taniguchi, N., *J. Proteomics.* 2015, *127*, 386–94.

[44] Baralla, A., Fois, A. G., Sotgiu, E., Zinellu, E., Mangoni, A. A., Sotgia, S., Zinellu, A., Pirina, P., Carru, C., *Proteomics Clin. Appl.* 2018, *12*, e1700088.

[45] Pitchenik, A. E., Ganjei, P., Torres, A., Evans, D. A., Rubin, E., Baier, H., *Am. Rev. Respir. Dis.* 1986, *133*, 226–229.

[46] Nicholas, B., Djukanović, R., *Biochem. Soc. Trans.* 2009 *37*, 868–872.

[47] Casado, B., Iadarola, P., Pannell, L.K., Luisetti, M., Corsico, A., Ansaldo, E., Ferrarotti, I., Boschetto, P., Baraniuk, J. N., *J. Proteome Res.* 2007, *6*, 4615–23.

[48] Baraniuk, J.N., Casado, B., Pannell, L.K., McGarvey, P. B., Boschetto, P., Luisetti, M., Iadarola, P., *Int. J. Chron. Obstruct. Pulmon Dis.* 2015, *10*, 1957–75.

[49] Nicholas, B. L., Skipp, P., Barton, S., Singh, D., Bagmane, D., Mould, R., Angco, G., Ward, J., Guha-Niyogi, B., Wilson, S., Howarth, P., Davies, D. E., Rennard, S., O'Connor, C. D., Djukanovic, R., *J. Respir. Crit. Care Med.* 2010, *18*, 1049–60.

[50] Ohlmeier, S., Mazur, W., Linja-Aho, A., Louhelainen, N., Rönty, M., Toljamo, T., Bergman, U., Kinnula, V. L., *J. Proteome Res.* 2012, *11*, 599–608.

[51] Titz. B., Sewer, A., Schneider, T., Elamin, A., Martin, F., Dijon, S., Luettich, K., Guedj, E., Vuillaume, G., Ivanov, N. V., Peck, M. J., Chaudhary, N. I., Hoeng, J., Peitsch, M. C., *J. Proteomics* 2015, *128*, 306–20.

[52] Terracciano, R., Preianò, M., Palladino, G. P., Carpagnano, G. E., Barbaro, M. P., Pelaia, G., Savino, R., Maselli, R., *Proteomics* 2011, *11*, 3402–14.

[53] Gray, R. D., MacGregor, G., Noble, D., Imrie, M., Dewar, M., Boyd, A. C., Innes, J.A., Porteous, D. J., Greening, A. P., *Am. J. Respir. Crit. Care Med.* 2008, *178*, 444–52.

[54] Gao, J., Ohlmeier, S., Nieminen, P., Toljamo, T., Tiitinen, S., Kanerva, T., Bingle, L., Araujo, B., Rönty, M., Höyhtyä, M., Bingle, C. D., Mazur, W., Pulkkinen, V., *Am. J. Physiol. Lung Cell. Mol. Physiol.* 2015, *309*, L17-26.

[55] Plymoth, A., Löfdahl, C. G., Ekberg-Jansson, A., Dahlbäck, M., Broberg, P., Foster, M., Fehniger, T. E., Marko-Varga, G., *Clin. Chem.* 2007, *53*, 636–644.

[56] Pastor, M. D., Nogal, A., Molina-Pinelo, S., Meléndez, R., Salinas, A., González De la Peña, M., Martín-Juan, J., Corral, J., García-Carbonero, R., Carnero, A., Paz-Ares, L., *J. Proteomics* 2013, *89*, 227–37.

[57] Pastor, M. D., Nogal, A., Molina-Pinelo, S., Meléndez, R., Romero-Romero, B., Mediano, M. D., López-Campos, J. L., García-Carbonero, R., Sanchez-Gastaldo, A., Carnero, A., Paz-Ares, L., *Int. J. Mol. Sci.* 2013, *14*, 3440–3455.

[58] Kohler, M., Sandberg, A., Kjellqvist, S., Thomas, A., Karimi, R., Nyrén, S., Eklund, A., Thevis, M., Sköld, C. M., Wheelock, Å. M., *J. Allergy Clin. Immunol.* 2013, *131*, 743–751.

[59] Tu, C., Mammen, M. J., Li, J., Shen, X., Jiang, X., Hu, Q., Wang, J., Sethi, S., Qu, J., *J. Proteome Res.* 2014 *13*, 627–639.

[60] Franciosi, L., Govorukhina, N., Ten-Hacken, N., Postma, D., Bischoff, R., *Methods Mol. Biol.* 2011, *790*, 17–28.

[61] Franciosi, L., Govorukhina, N., Fusetti, F., Poolman, B., Lodewijk, M. E., Timens, W., Postma, D., Ten Hacken, N., Bischoff, R., *Electrophoresis* 2013, *34*, 2683–94.

[62] Franciosi, L., Postma, D. S., van den Berge, M., Govorukhina, N., Horvatovich, P. L., Fusetti, F., Poolman, B., Lodewijk, M. E., Timens, W., Bischoff, R., ten Hacken, N. H., *PLoS One*. 2014 *9*, e102037.

[63] Fumagalli, M., Dolcini, L., Sala, A., Stolk, J., Fregonese, L., Ferrari, F., Viglio, S., Luisetti, M., Iadarola, P. *J. Proteomics* 2008, *71*, 211–21.

[64] Hoffmann, H., Tabaksblat, L., Enghild, J., Dahl, R. *Eur. Respir. J.* 2005 *26*, 231S.

[65] Hoffmann, H., Tabaksblat, L., Enghild, J., Dahl, R., *Eur. Respir. J.* 2008, *31*, 1–5.

[66] Kononikhin, A. S., Fedorchenko, K. Y., Ryabokon, A. M., Starodubtseva, N. L., Popov, I. A., Zavialova, M. G., Anaev, E. C., Chuchalin, A. G., Varfolomeev, S. D., Nikolaev, E. N., *Biomed. Khim.* 2015 *61*, 777–80.

[67] Carleo, A., Chorostowska-Wynimko, J., Koeck, T., Mischak, H., Czajkowska-Malinowska, M., Rozy, A., Welte, T., Janciauskiene, S. *Int. J. Chron. Obstruct. Pulmon Dis.* 2017, *12*, 829–837.

[68] Ohlmeier, S., Vuolanto, M., Toljamo, T., Vuopala, K., Salmenkivi, K., Myllärniemi, M., Kinnula, V. L., *J. Proteome Res.* 2008, *7*, 5125–32.

[69] Ohlmeier, S., Mazur, W., Salmenkivi, K., Myllärniemi, M., Bergmann, U., Kinnula, V. L., *Proteomics Clin. Appl.* 2010, 97–105.

[70] Ohlmeier, S., Nieminen, P., Gao, J., Kanerva, T., Rönty, M., Toljamo, T., Bergmann, U., Mazur, W., Pulkkinen, V., *Am. J. Physiol. Lung Cell. Mol. Physiol.* 2016, *310*, L1155-65.

[71] Hofmann, M. A., Drury, S., Fu, C., Qu, W., Taguchi, A., Lu, Y., Avila, C., Kambham, N., Bierhaus, A., Nawroth, P., Neurath, M. F., Slattery, T., Beach, D., McClary, J., Nagashima, M., Morser, J., Stern, D., Schmidt, A. M., *Cell* 1999, *97*, 889–901.

[72] Lee, E. J., In, K. H., Kim, J. H., Lee, S. Y., Shin, C., Shim, J. J., Kang, K. H., Yoo, S. H., Kim, C. H., Kim, H. K., Lee, S. H., Uhm, C. S., *Chest* 2009, *135*, 344–352.

[73] Ishikawa, N., Ohlmeier, S., Salmenkivi, K., Myllärniemi, M., Rahman, I., Mazur, W., Kinnula, V. L., *Respir. Res.* 2010, *11*, 123.

[74] Åhrman, E., Hallgren, O., Malmström, L., Hedström, U., Malmström, A., Bjermer, L., Zhou, X.H., Westergren-Thorsson, G., Malmström, J., *J. Proteomics* 2018, https://doi.org/10.1016/j.jprot.2018.02.027.

[75] Santini, M. T., Straface, E., Cipri, A., Peverini, M., Santulli, M., Malorni, W., *Haemostasis* 1997, *27*, 201–210.

[76] Alexandre, B. M., Charro, N., Blonder, J., Lopes, C., Azevedo, P., BugalhodeAlmeida, A., Chan, K. C., Prieto, D. A., Issaq, H., Veenstra, T. D., Penque, D., *J. Proteomics* 2012, *76*, 259–69.

[77] Loi, A. L. T., Hoonhorst, S., van Aalst, C., Langereis, J., Kamp, V., Sluis-Eising, S., Ten Hacken, N., Lammers, J. W., Koenderman, L., *Respir. Res.* 2017, *18*, 100.

[78] Wong, S. L., To, J., Santos, J., Allam, V. S. R. R., Dalton, J. P., Djordjevic, S. P., Donnelly, S., Padula, M. P., Sukkar, M. B., *J. Proteome Res.* 2018, *17*, 33–45.

[79] Yang, M., Kohler, M., Heyder, T., Forsslund, H., Garberg, H. K., Karimi, R., Grunewald, J., Berven, F. S., Magnus Sköld, C., Wheelock, Å. M., *Respir. Res.* 2018, *19*, 40.

[80] Yang, M., Kohler, M., Heyder, T., Forsslund, H., Garberg, H. K., Karimi, R., Grunewald, J., Berven, F. S., Nyrén, S., Magnus Sköld, C., Wheelock, Å. M., *Respir Res.* 2018, *19*, 39.

[81] Vogeser, M., Seger, C., *Clin. Biochem.* 2008, *41*, 649–662.

[82] van den Ouweland, J. M., Kema, I. P., *J. Chromatogr. B Analyt. Technol. Biomed. Life Sci.* 2012, *883*, 18–32.

International Journal of
Pulmonary & Respiratory Sciences
ISSN: 2573-2234

Juniper Publishers
key to the Researchers

Short Communication
Volume 3 Issue 3- May 2018
DOI: 10.19080/IJOPRS.2018.03.555611

Int J Pul & Res Sci

NMR Metabolomics to Explore Respiratory Disorders

P Iadarola[1]*, M Cagnone[2] and S Viglio[2]

[1]*Department of Biology and Biotechnologies "L. Spallanzani", University of Pavia, Italy*

[2]*Department of Molecular Medicine, Biochemistry Unit, University of Pavia, Italy*

Submission: April 20, 2018; **Published:** May 17, 2018

***Corresponding author:** P Iadarola, Department of Biology and Biotechnologies "L. Spallanzani", University of Pavia, Italy, Email: paolo.iadarola@unipv.it

Abbreviations: BALf: Bronchoalveolar Lavage Fluid; EBC: Exhaled Breath Condensate; ELF: Epithelial Lining Fluid; NMR: Nuclear Magnetic Resonance; MS: Mass Spectrometry; LC: Liquid Chromatography.

Introduction to Metabolomics

Metabolites are the end products of enzymatic activity inside the cells. Being in general characterized by molecular masses less than 1 kDa, they are represented by amino acids, carbohydrates, lipids, hormones, nucleotides and other small molecules. Due to the proximity of metabolites to a phenotype or disease, detecting and quantifying changes in the concentration of metabolites may reveal the range of biochemical effects induced by a disease condition or its therapeutic intervention. This is exactly the task of Metabolomics, the newest 'omics' science whose term was coined in analogy with those of the previously developed Genomics and Proteomics. Metabolomics is not only complementary to the other two approaches but, being able to provide information that allows a better understanding of cellular biology, it looks like the perfect tool suitable to integrate them. In fact, although genomics provides good fingerprints of hereditary information, it should be underlined that not all human diseases are associated with genetic defects. On the other hand, up- or down-regulation in protein(s) expression revealed by proteomics not necessarily correlates with a perturbation in their biological activity. Thus, given that the metabolome reflects changes that occur in the transcriptome, genome, or proteome, it can provide an instantaneous snapshot of cell physiology.

NMR Technology

Given the huge number, the chemical diversity and the dynamic range of metabolite concentration, analyzing their entire range would require the combination of different analytical methods. Nevertheless, very often a single technique is able to provide a good snapshot of the system under investigation. The most used methods applied are currently gas or liquid chromatography (GC or LC) in combination with mass spectrometry (MS) and nuclear magnetic resonance (NMR) spectroscopy. The peculiarities and advantages of NMR (it is rapid, quantitative, non-destructive and requires minimal sample pre-treatment) makes often this method more attractive than the others for providing a rapid and accurate metabolic picture of the sample. Briefly, the biological sample under investigation is placed in a strong magnetic field to align nuclei (e.g., 1H, 13C, 15N, 31P) contained in the analytes. The interaction of a high power short duration radio frequency pulse leads to the generation of small NMR signals which are translated into peaks that are displayed across a spectrum. In principle, by comparing the position of these signals with reference data present in the literature, NMR resonances of common metabolites can be identified. When dealing with overlapping of signals, the use of a more sophisticated procedure (two-dimensional NMR experiments) that improve resolution is required.

NMR applied to Pulmonary Disorders

The rapid expansion of NMR metabolomics in the field of lung disorders resulted in the publication of a wealth of articles focused on the identification of metabolites associated with different diseases including chronic obstructive pulmonary disease, asthma, cystic fibrosis, tuberculosis, sarcoidosis, invasive pulmonary aspergillosis, pulmonary arterial hypertension, pulmonary langerhans cell hystiocytosis, high altitude pulmonary edema, adult respiratory distress syndrome, bronchiolitis obliterans syndrome, pulmonary emphysema associated with α1-antitrypsin deficiency. In most cases the matrices investigated were those that much better than others reflect the local environment they came from, i.e. bronchoalveolar lavage fluid (BALf), induced sputum, exhaled breath condensate

(EBC), epithelial lining fluid (ELF). It was observed that profiles of patients with different pathological conditions shared largely the same panel of metabolites. However, while appearing similar, the patterns of peaks evidenced distinctive differences in terms of presence/absence of some specific metabolites and prompted investigators at focusing on their quantitative variations. In general, from among the numerous metabolites detected, those that allowed to discriminate patients from healthy controls were identified as Krebs cycle intermediates, mono- and disaccharides, nucleotides, phospholipid precursors, amino acids, alcohols, ketones, short-chain fatty acids. The fact that these molecules were "heterogeneous", other than being a source of confusion, was an incentive to the search of a rationale for reasoning on their potential role in the onset of the disorder. Although belonging to different chemical classes, these analytes contained a piece of information that was unequivocally useful to distinguish profiles of health from those of disease states. In most cases multivariate statistical analyses (i.e. principal component analysis and/or orthogonal partial least squares discriminant analysis) were carried out to confirm that data concerning discrimination between cohorts of subjects under investigation were statistically significant. Application of appropriate platforms to the lists of metabolites also allowed interpretation of acquired data and consequent generation of biochemical pathways aimed at defining their relationships. These studies allowed pointing out a good number of pathways that played a critical role in different lung disorders. These included cellular energy metabolism (alteration in β-oxidation of fatty acids, glycolysis, pentose phosphate pathway), the pyruvate and the taurine/hypotaurine pathways. The fact that a number of metabolites identified in these studies were common to a variety of pulmonary disorders could mean that they were not very specific to a given pathology. However, given the common clinical traits among several lung disorders, this finding was not surprising. Taken together, all NMR experimental data so far generated evidenced/confirmed that some relevant pathways shown to be involved in a lung disorder, most likely were deregulated also in other cognate pulmonary pathologies.

Conclusions

Although the application of NMR to metabolomic studies of respiratory disorders is still in its infancy, the data so far published represent a significant contribution to the identification of biomarkers which may aid in the diagnosis and/or treatment of lung diseases. Metabolome is characterized by a peculiar ability to change very quickly over time. Thus, succeeding in identifying molecules that nobody expected to be there (and the metabolic pathway they are involved in) would be an important contribution which may open the door to clinical studies.

DOI: 10.19080/IJOPRS.2018.03.555611

high-throughput

MDPI

Article

A Pilot Study to Investigate the Balance between Proteases and α1-Antitrypsin in Bronchoalveolar Lavage Fluid of Lung Transplant Recipients

Maddalena Cagnone [1,†], Davide Piloni [2,3,†], Ilaria Ferrarotti [2], Monica Di Venere [1], Simona Viglio [1], Sara Magni [3], Anna Bardoni [1], Roberta Salvini [1], Marco Fumagalli [4], Paolo Iadarola [4,*], Sabrina Martinello [2] and Federica Meloni [2,3]

1 Department of Molecular Medicine, Biochemistry Unit, University of Pavia, 27100 Pavia, Italy; maddalena.cagnone@gmail.com (M.C.); monica.divenere01@universitadipavia.it (M.D.V.); simona.viglio@unipv.it (S.V.); abardoni@unipv.it (A.B.); roberta.salvini@unipv.it (R.S.)
2 Department of Internal Medicine and Therapeutics, Section of Pneumology, University of Pavia, 27100 Pavia, Italy; davidepiloni@live.it (D.P.); I.Ferrarotti@smatteo.pv.it (I.F.); sabrinamartinello@hotmail.it (S.M.); f.meloni@smatteo.pv.it (F.M.)
3 IRCCS Foundation Policlinico San Matteo, Department of Medical Sciences and Infective Diseases, Unit of Respiratory Diseases, 27100 Pavia, Italy; sara.magni04@gmail.com
4 Department of Biology and Biotechnologies "L. Spallanzani", Biochemistry Unit, University of Pavia, 27100 Pavia, Italy; marco.fumagalli@unipv.it
* Correspondence: piadarol@unipv.it
† These authors contributed equally to this work.

Received: 11 December 2018; Accepted: 7 February 2019; Published: 13 February 2019

check Eoj updates

Abstract: The neutrophilic component in bronchiolitis obliterans syndrome (BOS, the main form of chronic lung rejection), plays a crucial role in the pathogenesis and maintenance of the disorder. Human Neutrophil Elastase (HNE), a serine protease responsible of elastin degradation whose action is counteracted by α1-antitrypsin (AAT), a serum inhibitor specific for this protease. This work aimed to investigate the relationship between HNE and AAT in bronchoalveolar lavage fluid (BALf) from stable lung transplant recipients and BOS patients to understand whether the imbalance between proteases and inhibitors is relevant to the development of BOS. To reach this goal a multidisciplinary procedure was applied which included: (i) the use of electrophoresis/western blotting coupled with liquid chromatography-mass spectrometric analysis; (ii) the functional evaluation of the residual antiprotease activity, and (iii) a neutrophil count. The results of these experiments demonstrated, for the first time, the presence of the complex between HNE and AAT in a number of BALf samples. The lack of this complex in a few specimens analyzed was investigated in relation to a patient's lung inflammation. The neutrophil count and the determination of HNE and AAT activities allowed us to speculate that the presence of the complex correlated with the level of lung inflammation.

Keywords: alpha 1-antitrypsin; bronchoalveolar lavage fluid; bronchiolitis obliterans syndrome; neutrophils; elastase; lung

1. Introduction

Much of the lung destruction in acute and chronic lung diseases is caused by the deleterious activities of multiple proteases, among which human neutrophil elastase (HNE) is the serine protease mostly responsible of elastin degradation [1,2]. HNE is a serine protease secreted by neutrophils and it was shown to orchestrate inflammation through the activation of cathepsin B and matrix metalloprotease 2 (MMP-2) whose upregulation contributes to pulmonary infection and tissue

destruction [3,4]. Given this role of HNE, it can be postulated that its neutralization with a specific anti-protease would automatically inhibit the upregulation of other proteases, thus lessening the overall protease burden. This could prevent/decrease lung destruction and contribute to the restoration of lung host defense [3]. The specific inhibitor of HNE is α1-antitrypsin (AAT), a 52 kDa glycoprotein mainly produced and secreted (70–80%) by hepatocytes. In small amounts, it is also synthesized by monocytes, macrophages, pulmonary alveolar cells and by intestinal and corneal epithelium [5–8]. AAT provides more than 90% of the anti-proteinase activity in human serum, the remaining 10% being provided by β-2 macroglobulin. Inherited α1-antitrypsin deficiency (AATD) is a clear example that the balance between proteases and antiproteases is one of the most important aspects of lung homeostasis. Being that the increased levels of HNE positively correlated with the severity of emphysema, a careful monitoring of the ratio between the amount of protease and its specific inhibitor is vital for these patients [9,10].

Despite the high specificity of AAT for HNE, additional skills which support the key role of this inhibitor in regulating inflammatory response have recently been evidenced. Numerous reports, in fact, have shown its ability to neutralize a broad range of other serine proteases and different classes of proteases, which include proteinase-3, myeloperoxidase, cathepsin G (Cat. G), metalloproteases and cysteine-aspartic proteases [11–17].

The role of the AAT/HNE balance in homeostasis of the lung was investigated by Pajdak et al. [14] by means of an immune-electrophoretic procedure. This approach allowed researchers to observe the presence of AAT-HNE complexes in bronchoalveolar lavage fluid (BALf) from patients with inflammatory lung disease, asthma and lung cancer.

More recently, both HNE activity and AAT concentration have been quantified by Hirsch et al. [16] in a cohort of lung transplant recipients by means of a titration assay and an enzyme-linked immunosorbent assay (ELISA). Their study was focused on the possible role of alterations in antiprotease defense and of oxidant activities for the pathogenesis of chronic rejection after lung transplantation, an increasingly widely applied therapy for end-stage lung diseases in the past two decades.

Long-term survival of a lung graft is hampered by the occurrence of chronic lung allograft dysfunction (CLAD) that occurs in nearly 50% of patients by the fifth post-transplant (Tx) year [17].

According to a recent classification, CLAD presents two major clinical phenotypes: the so-called obstructive form of bronchiolitis obliterans syndrome (BOS, nearly 70% of cases) [18], and the newly-described restrictive allograft syndrome (RAS) [19,20]. While being the most frequent one, the exact pathogenesis of BOS is still unknown, although the neutrophilic component seems to play a significant role in the maintenance of this condition. It has been speculated that BOS results from several noxious triggers which cause innate/adaptive immune reactions, leading to immune activation (mainly T helper 17, Th-17) responsible for inducing the neutrophilic inflammation characteristic of the disorder. Given the tissue-protective and anti-inflammatory properties of AAT, the interest in its influence in early and long-term complications post lung transplant has increased in recent years, also in light of the poor knowledge of complications which involve a high neutrophil recruitment, e.g., ischemia reperfusion injury and BOS [21–27]. In this context, BALf seems to meet the requirements for being an important tool for the study of changes in cell type and/or number and solutes that occur in the lower respiratory tract of lung transplant recipients. Identification in this fluid of potential biomarkers of BOS development/evolution would indeed offer a unique opportunity to actively intervene on the progression of the disease [28].

To obtain a global picture of the protease/antiprotease balance in the lungs of transplant recipients, BALf samples from these patients were investigated in this work. Data from electrophoretic and western blotting analysis were compared with those acquired from liquid chromatography–mass spectrometry (LC–MS). The neutrophil count, together with the determination of HNE and of Cat. G activities provided information on the functionality of AAT, its balance with HNE, and its correlation to the degree and type of inflammation of the deep graft tissue.

2. Materials and Methods

2.1. Reagents

Antibodies for detection of AAT and secondary anti-mouse antibodies were obtained from Abcam (Cambridge, UK). HNE, together with a bicinchoninic acid (BCA) protein assay kit were obtained from Thermo Scientific (Rockford, IL, USA). The standard *p*-nitroaniline (*p*-NA) and the peptide substrates used for the determination of human HNE and Cat. G activities (MeOSuc-Ala-Ala-Pro-Phe-NA and Suc-Ala-Ala-Pro-Phe-NA, respectively) were from Bachem (Bachem AG, Bubendorf, Switzerland). Unless otherwise stated, all other analytical grade reagents were purchased from Sigma-Aldrich (St. Louis, MO, USA). Double-distilled water used for the preparation of all buffers was prepared with a Millipore (Bedford, MA, USA) Milli-Q purification system.

2.2. Patients

The lung transplanted patients ($n = 13$) investigated in this study were enrolled at the Pneumology Unit of the IRCCS Policlinico San Matteo Foundation, Pavia, Italy. Based on their clinical features, they were classified as stable (S), potential BOS (BOS0p), BOSII (BOSII) and BOSIII (BOSIII) patients. Stable were individuals that, at >2 years post-transplantation, came up with still stable lung function, in the total absence of acute rejection or infection. Diagnosis of BOS and of its grades of severity were assessed according to published guidelines [29–31]. The current classification of BOS severity is based on changes in the forced expiratory volume in the first second (FEV1) and is indicated as BOS0p if FEV1 is 81–90% of the best FEV1 value obtained after transplantation; BOSI (patients not considered in this study) when FEV1 is 66–80% of the best value; BOSII when FEV1 is 51–65% of the best, and BOSIII if FEV1 is ≤50%. Individuals under investigation in this study were divided in two groups according to these characteristics. The first (Group1) contained seven subjects: six S and one BOS0p; the second (Group2) six subjects: four BOSII and two BOSIII. The immune suppression (IS) protocol applied to these patients was reported elsewhere [32]. All of them underwent surveillance and bronchoscopy at 1, 3, 6, 12, and 24 months plus on clinical need, which included the decline of lung function, and at diagnosis of chronic lung rejection. Biopsy-proven episodes of acute rejection (AR) [33] were treated with steroid boluses and, in case of AR recurrence or persistence, with a standard anti-thymoglobulin course and a modulation of the IS regimen. The surveillance protocol was reported elsewhere [34]. Patients diagnosed with BOS0p were prescribed a three-month course of chronic low-dose azithromycin. At the same time, patients underwent a gastro-esophageal reflux assessment and a maximization of anti-reflux medical treatment. In case of a further decline consistent with BOSI diagnosis, since 2003 patients have been referred to the Apheresis Unit for compassionate ECP (extracorporeal photopheresis) treatment [35]. Additionally, the cytomegalovirus surveillance protocol was detailed elsewhere [36]. Patients enrolled for this study were investigated for α1-antitripsin deficiency (AATD) at the time of listing for lung transplantation according to standard algorithm [37]. None of them resulted positive for intermediate or severe AATD. All transplanted patients were given a low-dose steroid treatment (0.05–0.1 mg/kg body weight of prednisone) as a part of the triple immunosuppressive regimen. Given that all patients were submitted to the same treatment, this was not expected to have any influence on the measurements performed on samples analyzed. All patients gave their informed consent to BALf collection.

The demographic and clinical features (including age, gender, CLAD occurrence and treatment strategies) of patients considered in this study are detailed in Table1.

Table 1. Demographic data of individuals considered in this study.

Sample #	Age	Sex	CLAD	Months from CLAD	Azithromycin	ECP	Immunosuppressive Therapy
1	65	M	Stable	n.d. *	No	No	CsA, AZA
2	51	M	Stable	n.d. *	No	No	TAC, MMF
3	64	M	Stable	n.d. *	No	No	TAC, MMF
4	56	M	Stable	n.d. *	No	No	CsA, AZA
5	34	M	Stable	n.d. *	No	No	CsA, AZA
6	57	M	Stable	n.d. *	No	No	CsA, AZA
7	42	M	BOS0p	13.57	Yes	No	TAC, MMF
8	62	M	BOS2	1.00	No	No	CsA
9	28	M	BOS2	2.57	Yes	No	TAC, MMF
10	62	M	BOS2	1.00	No	No	TAC, MMF
11	63	F	BOS2	1.00	Yes	No	TAC, AZA
12	26	M	BOS3	23.43	Yes	Yes	TAC
13	53	F	BOS3	38.87	No	Yes	CsA, RAD

* not determined. CsA: Cyclosporin A; TAC: Tacrolimus; RAD: Everolimus; MMF: Mycofenolate Mofetil; AZA: Azathioprine; CLAD: chronic lung allograft dysfunction. None of the samples were obtained during Azithromycin treatment.

2.3. BALf Collection and Processing

BALf collection was performed as previously described [28]. Briefly, the distal tip of the bronchoscope was wedged into the middle lobe or lingular bronchus and a total of 150 mL of warm sterile saline solution was instilled in five subsequent 30 mL aliquots which were sequentially retrieved by gentle aspiration. The first aliquot collected (20 mL) was used for a series of analyses which included microscopic and cultural examination of common bacteria and fungi and direct/cultural investigations for respiratory viruses. The returned fluid from the second to the fifth aliquots was pooled and further processed as BALf. Cells were recovered by centrifugation at 1500× *g* rpm for 10 min and supernatant divided in aliquots (30 mL each) which were stored at −80 °C immediately after processing, until use.

2.4. AAT Measurement

AAT was measured in BALf by a rate immune nephelometric method (Immage 800 Immunochemistry System, Beckman-Coulter, Brea, CA, USA).

2.5. BCA Protein Assay

The exact protein concentration in each sample was determined by applying the bicinchoninic acid (BCA) assay [38] using bovine serum albumin (BSA), in the range of concentration between 5 and 25 µg/mL, to produce the calibration curves.

2.6. 1D-PAGE

An aliquot of each sample (20 µg of protein) was submitted to protein precipitation with trichloroacetic acid (TCA), according to Yvon et al. [39]. After centrifugation, the pellet was reconstituted in 10 µL of 50 mM Tris–HCl pH 8.3 containing 5% 2-mercaptoethanol, 2% sodium dodecylsulphate (SDS), 0.1% bromophenol blue (BPB) and 10% glycerol. Samples were incubated at 90 °C for 10 min and then loaded on gel slabs. Electrophoresis was performed according to Laemmli [40] in 5% stacking gel and 12.5% running gel by applying a voltage of 150 V for 1 h. Gels were stained with colloidal Coomassie G-250, according to Candiano et al. [41]

2.7. Western Blotting

Ten micrograms of proteins were precipitated by addition of 1.22 M trichloroacetic acid (TCA) and the pellet recovered after centrifugation was submitted to sodium dodecyl sulphate - polyacrylamide gel electrophoresis (SDS-PAGE). Protein bands were transferred onto a Millipore polyvinyldivinyl fluoride (PVDF) membrane (Billerica, MA, USA) by using a trans blot turbo system (BioRad). After 1 h incubation in 5% milk diluted in phosphate buffer saline (PBS) and three washes with phosphate buffer saline containing 0.1% Tween 20 (PBST), the membrane was incubated overnight with AAT antibody (ab9400; Abcam, Cambridge, UK) at a 1:2500 dilution in 1% milk. The membrane was washed three times with PBST (10 mL), incubated with the secondary antibody, rabbit anti-mouse IgG H&L (HRP) (ab6728, Abcam), at a 1:2000 dilution in 1% milk in PBST, for 1 h at room temperature. The membrane was washed again (three times) with PBS and incubated in ECL Westar ηC Ultra (Cyanagen, Bologna, Italy) solution according to the provided protocol. The same procedure was applied for the identification of free and complexed HNE by using the anti HNE antibody (PA5-29659, Thermo Scientific) at a 1:1000 dilution.

All immunoblots were acquired with the ImageQuant LAS 4000 analyzer (GE Healthcare Chicago, IL, USA).

2.8. Enzymatic Assays

The determination of HNE and Cat. G activities was carried out by applying a previously described colorimetric assay [42–44]. The original sample solution was exchanged into the incubation buffer by withdrawing an aliquot of each sample (400 µL), which was lyophilized and the pellet taken up in 400 µL of 50 mM Tris HCl pH 7,8 containing 500 mM NaCl. The reaction was started by the addition of 5 µL of the appropriate substrate, i.e., MeOSuc-Ala-Ala-Pro-Phe-NA for HNE and Suc-Ala-Ala-Pro-Phe-NA for CatG. The final concentrations were 2 mM and 20 mM respectively. The mixture was incubated at 37 °C for 10 min and the reaction was stopped by addition of 40 µL of 0.27 M TCA. The values of absorbance at 410 nm provided the amount of *p*-nitroaniline (*p*-NA) released by peptide hydrolysis. The limit of detection (LOD) for *p*-NA was <1 µM. One unit of enzyme activity was defined as the amount of enzyme required for the release of 1 µmol/min of *p*-NA.

2.9. In-Situ Digestion

Enzymatic digestion of proteins was performed as previously described [45]. Briefly, the selected bands were carefully excised from the gel, placed into eppendorf tubes, broken into small pieces and washed with 100 mM ammonium bicarbonate (AmBic) buffer pH 7.8 containing 50% acetonitrile (ACN) until complete de-staining was achieved. The gel pieces were then dehydrated by adding 200 µL of ACN until they became opaque-white color. Acetonitrile was finally removed, gel pieces were dried under vacuum for 10 min and then rehydrated by adding 75 µL of 100 mM AmBic buffer pH 7.8, containing 20 ng/µL sequencing grade trypsin (Promega, Madison, WI, USA). The digestion was performed overnight upon incubation of the mixture at 37 °C and the resultant peptides were extracted from gel matrix by a three-step sequential treatment with 50 µL of 50% ACN, 5% trifluoroacetic acid (TFA) in water and finally with 100% ACN. Each extraction involved 10 min of stirring followed by centrifugation and removal of the supernatant. All supernatants were pooled, dried and stored at
−80 °C until mass spectrometric analysis. At the moment of use, the peptide mixture was solubilized in 0.1% formic acid (FA).

2.10. Liquid Chromatography Tandem Mass Spectrometry (LC–MS/MS)

Analyses were performed on a liquid chromatography-mass spectrometry system (Thermo Finnigan, San Jose, CA, USA) consisting of a thermostated column, a surveyor auto sampler controlled at 25 °C, a quaternary gradient surveyor MS pump equipped with a diode array (DA) detector, and a linear trap quadrupole (LTQ) mass spectrometer with electrospray ionization (ESI) ion

source controlled by Xcalibur software 1.4 (Thermo Fisher Scientific, Waltham, MA, USA). Analytes were separated by reverse-phase high performance liquid chromatography (RP-HPLC) on a Jupiter (Phenomenex, Torrance, CA, USA) C18 column (150 × 2 mm, 4 µM, 90 Å particle size) using a linear gradient (2–60% solvent B in 60 min) in which solvent A consisted of 0,1% aqueous FA and solvent B of ACN containing 0.1% FA. Flow rate was 0.2 mL/min. Mass spectra were generated in positive ion mode under constant instrumental conditions: source voltage 5.0 kV, capillary voltage 46 v, sheath gas flow 40 (arbitrary units), auxiliary gas flow 10 (arbitrary units), sweep gas flow 1 (arbitrary units), capillary temperature 200 °C, tube lens voltage −105 V. MS/MS spectra, obtained by collision-induced dissociation (CID) studies in the linear ion trap, were performed with an isolation width of 3 Th *m/z*, the activation amplitude was 35% of ejection RF amplitude that corresponds to 1.58 V. Data processing was performed using Peaks studio 4.5 software.

2.11. Workflow of the Procedure Followed in the Present Study

The workflow shown in Figure1summarizes the key steps of this study.

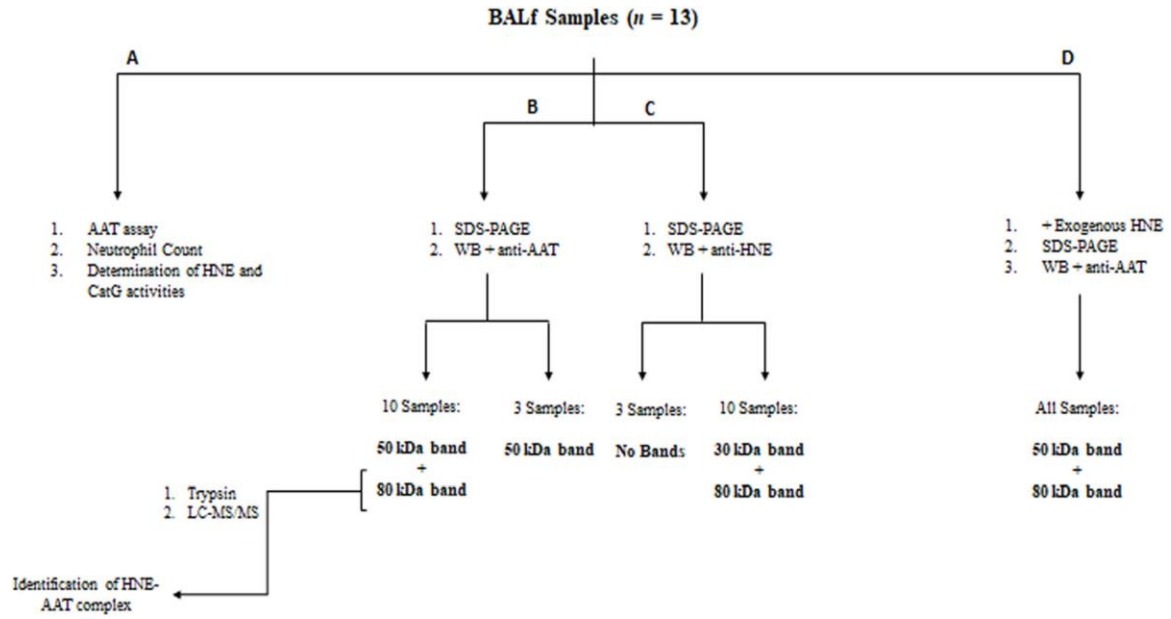

Figure 1. Workflow of the experimental procedure.

3. Results

3.1. Identification of the HNE-AAT Complex

The results of the electrophoretic runs performed on the BALf of all subjects investigated are shown in Figure2, panel A. Lanes 1 to 7 refer to the subjects grouped in Group 1 (Stable and BOS 0p) and 8 to 13 to those in Group 2 (BOSII and BOSIII). It can be observed that two bands, at approximately 80 and 55 kDa, exceed in abundance over others. Information on these two bands was obtained by blotting the gels on a PVDF membrane that was later incubated with an anti-AAT antibody. The results are shown in panel B of Figure2. Based on the presence/absence of the immune-reactive band at 80 kDa, individuals belonging to Group 1 could be divided in two sub-classes: those who did not exhibit this band (lanes 1 to 3) and those who showed it (lanes 4 to 7). Conversely, the image of the PVDF membrane obtained from patients belonging to Group 2 (lanes 8 to 13), mirrored that of the starting gel. The 80 kDa band was evident, although at different intensity, in all profiles, regardless of whether the BALf belonged to BOS II or BOS III patients. Based on the well-known molecular mass of AAT (Mr 52,0 kDa), the band at approximately 55 kDa was attributed to this protein. Likewise, on the basis of the sum of the theoretical molecular weights of AAT and HNE, the band at 80 kDa

was tentatively attributed to the complex between these two proteins. While experimental evidence was still lacking, the reactivity of the material under this band against the anti-AAT antibody was circumstantial evidence that it contained AAT.

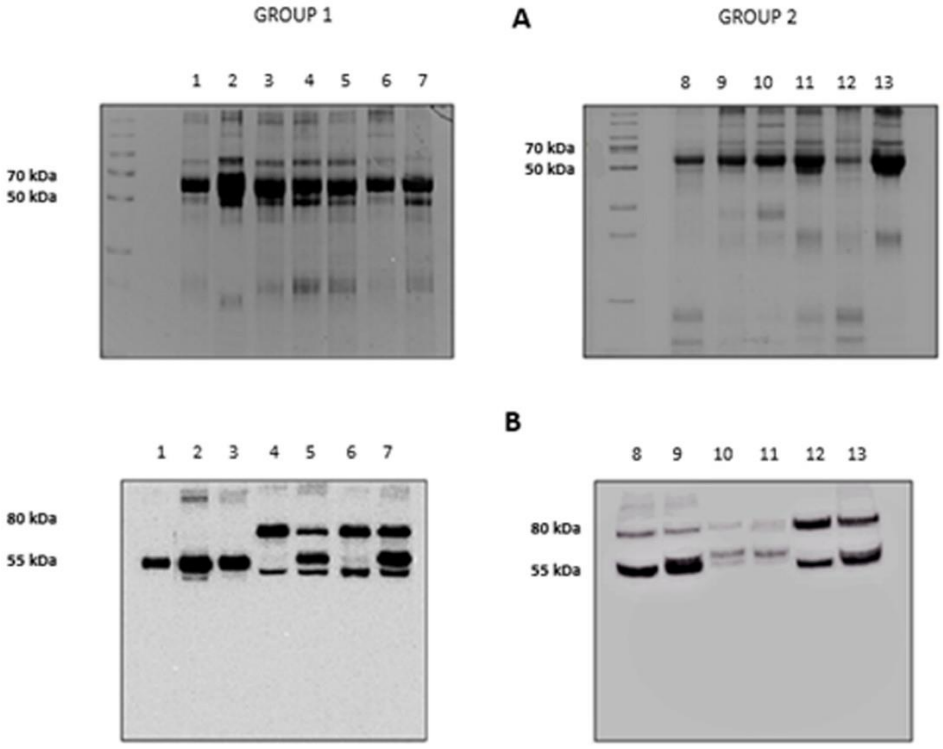

Figure 2. Panel A: 12.5% SDS-PAGE showing the protein profile of all the bronchoalveolar lavage fluid (BALf) samples considered. Group 1: lanes 1–7, Group 2: lanes 8–13. Panel B: Western blotting with anti-AAT antibody of the same samples as in panel A.

The presence of a band at approximately 80 kDa in SDS-PAGE had been previously observed in vitro also by other authors who speculated that it could correspond to the HNE-AAT complex [46,47]. To definitively prove the existence of this inhibitory complex in BALf samples that showed this band, it was carefully excised and the protein submitted to the procedure detailed in the experimental section. Peptides generated from tryptic digestion were separated by LC–MS/MS and fragmentation data searched against the Swiss-Prot database [48,49]. Data relative to the proteins present under the 80 kDa band (shown in Table2) allowed us to unambiguously identify both HNE and AAT. The same procedure was applied to the band at approximately 55 kDa to confirm that it contained AAT. The data of Table2show that this band contained AAT contaminated by proteins with similar molecular weight which co-migrated with the former due to the limits of resolution of 1D electrophoresis. Additional information concerning the primary sequence of all peptides identified for each protein analyzed is included in Table S1 of the Supplementary Information.

Table 2. Proteins identified by liquid chromatography–mass spectrometry (LC–MS/MS) under bands at 50 and 80 kDa.

Molecular Weight	Accession	Mass (kDa)	Score (%)	Coverage (%)	Description
80 kDa	sp|P01009|A1AT_HUMAN	46,737	67	9.33%	α1-antitrypsin OS = *Homo sapiens* GN = SERPINA1 PE = 1 SV = 3
	sp|P08246|ELNE_HUMAN	28,518	62	3.37%	Neutrophil elastase OS = *Homo sapiens* GN = ELANE PE = 1 SV = 1

Table 2. *Cont.*

Molecular Weight	Accession	Mass (kDa)	Score (%)	Coverage (%)	Description
55 kDa	sp|P02768|ALBU_HUMAN	69,367	98	11.82%	Serum albumin OS = *Homo sapiens* GN = ALB PE = 1 SV = 2
	sp|P01009|A1AT_HUMAN	46,737	85	6.70%	α1-antitrypsin OS = *Homo sapiens* GN = SERPINA1 PE = 1 SV = 3
	sp|P01859|IGHG2_HUMAN	35,901	60	4.29%	Ig γ-2 chain C region OS = *Homo sapiens* GN = IGHG2 PE = 1 SV = 2

3.2. Determination of AAT Amount and of Protease Activities

To answer the question of whether HNE had fully complexed AAT or was still partially present in BALf as a free, active enzyme, the activity of HNE was determined in all samples. The results summarized in Table3pointed out that significant levels of HNE activity were detectable only in BALf samples presenting the 80 kDa band. Conversely, the amount of AAT did not differ significantly among samples.

Table 3. Biochemical features of all samples analyzed.

Sample #	Clinical Classification of the Disorder	AAT Assay (mg/dL)	Neutrophil Count	Elastase Specific Activity (mU/mg)	Cathepsin G Specific Activity (mU/mg)	Presence of the 80 kDa Complex
1	Stable	0.57 *	1	n.d. **	n.d. **	NO
2	Stable	1.00	1	0.08	n.d.	NO
3	Stable	0.32	1	n.d.	n.d.	NO
4	Stable	0.79	34	0.725	n.d.	YES
5	Stable	0.37	30	1.06	0.14	YES
6	Stable	0.40	1	n.d.	n.d.	YES
7	BOS 0p	0.26	28	0.29	n.d.	YES
8	BOS II	2.50	94	4.44	0.57	YES
9	BOS II	0.56	56	2.16	0.254	YES
10	BOS II	0.12	40	2.98	n.d.	YES
11	BOS II	0.12	5	2.23	n.d.	YES
12	BOS III	0.13	10	n.d.	n.d.	YES
13	BOSIII	0.13	15	1.56	n.d.	YES

* Values reported are the mean of three independent determinations. Standard deviation was within 5%. ** n.d. = not detectable.

* Values reported are the mean of three independent determinations. Standard deviation was within 5%. ** n.d. = not detectable.

Being that the Cat. G activity levels are lower than the LOD of the procedure, they could be estimated only in two samples (samples 8 and 9).

As shown in Figure3, a reasonable correlation was observed between the specific activity of HNE and the number of neutrophils determined in all samples.

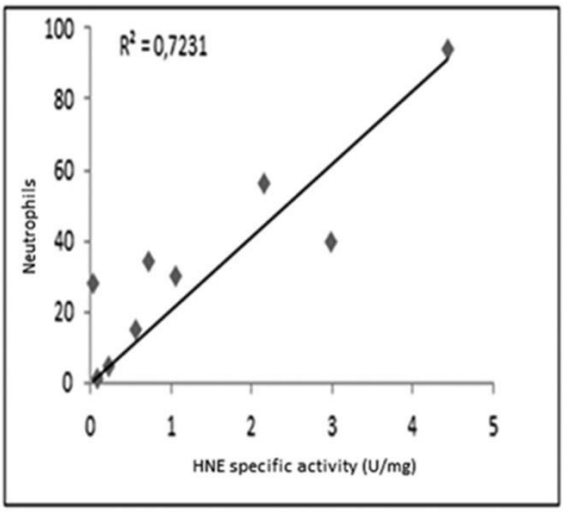

Figure 3. Correlation between the specific activity of HNE and the count of neutrophils in samples analyzed.

3.3. Use of Western Blotting for HNE Detection

The presence/absence of HNE in the BALfs of subjects investigated was checked by running the samples on SDS-PAGE and blotting the bands on a PVDF membrane that was incubated with anti-HNE antibody (Figure4). The absence of immune reactive bands in BALfs lacking the 80 kDa band (lanes 1 to 3) unambiguously demonstrates that these samples do not contain HNE. Conversely, the specimens that formed the complex showed the presence of two bands (lanes 4 to 13). Based on their migration on the gel, these bands were assigned to free and complexed HNE. Following the LC–MS procedure described above, HNE was identified in both bands (data not shown).

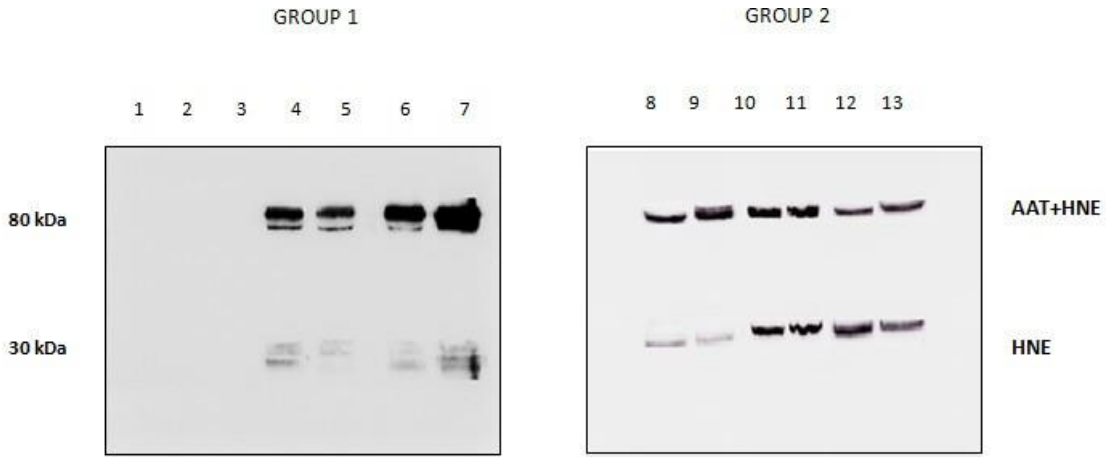

Figure 4. Western blotting profile obtained upon incubation of all BALfs with the anti-HNE antibody. Lanes 1–3: samples not showing the 80 kDa band when incubated with anti-AAT. Lanes 4–13: sample showing the 80 kDa band.

3.4. Inhibitory Capacity of AAT

The inflammation-mediated cell oxidative stress was previously observed to inactivate in vitro AAT through a sort of oxidative cascade [46,47]. This would prevent (partially or totally) its capacity to inhibit HNE. The efficiency of AAT towards HNE was checked in BALfs from subjects who did not show the HNE-AAT complex by adding exogenous HNE (2 µL; 0.2 mg/mL) to samples. After 15 min of incubation at 37 °C, an aliquot was submitted to SDS-PAGE and gels blotted on a PVDF membrane which was incubated with the anti-AAT antibody. Figure5, panel A, illustrates the results relative to these samples before (lanes 1; 2 and 3) and after incubation (lanes 1 *; 2 * and 3 *). The formation of

the 80 kDa band clearly indicated that the BALf sample was able to capture the “excess” of HNE thus suggesting that an amount of functional AAT was still present in these samples.

When the same amount of exogenous HNE was added to samples which presented the complex, the 80 kDa band was seen to increase considerably. Figure5, panel B, shows the results relative to a sample chosen at random among all available (sample #12). The results relative to other samples are shown in Figure S1 in the Supplementary Material. These data further support the hypothesis that AAT was functional in these samples.

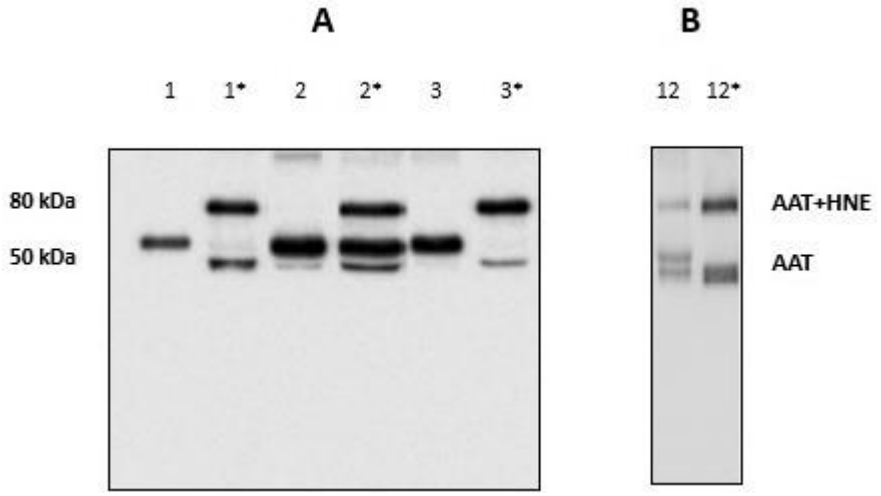

Figure 5. (**A**) Western blotting of BALfs from the three patients without the 80 kDa band, before (1; 2 and 3) and after incubation with exogenous HNE (1 *; 2 * and 3 *). (**B**) Western blotting of BALf from a patient with the 80 kDa band, before (12) and after incubation with exogenous HNE (12 *).

4. Discussion

Previous studies had already reported that BOS progression is associated with a protease/antiprotease imbalance [16]. To get insights into this mechanism of the control of inflammatory lung diseases, possible variations in the protease/antiprotease balance of BALf from two different cohorts were evaluated. Lung transplant recipients, both stable and developing BOS after lung transplantation, have been investigated. Since the mere assay of HNE and AAT involved in the process is not able to provide information on the level of activity of these proteins, we explored their capacity to interact. The existence of this complex in the BALf samples of cystic fibrosis patients had previously been demonstrated by a double-ligand ELISA [50]. The finding that a few samples of stable post-transplant subjects lacked this inhibitory complex was unexpected and opened the door to a series of questions. In fact, although the Western Blot analysis clearly indicated that all samples contained AAT, it did not provide information about the ability of this inhibitor to bind HNE in whole or in part. Thus, whether the lack of such complex in the BALf of the mentioned subjects should be ascribed to their pathological state, i.e., the low level of pulmonary inflammation, remained a speculation. In fact, while protease activity was undetectable in patients with a low level of lung inflammation, the formation of the complex could also have been prevented by possible inactivation processes at the expense of AAT occurring in the lungs of these individuals. This latter hypothesis was denied by the addition to the above samples of exogenous HNE, which lead to the formation of the complex. Instead, our findings supported the assumption that AAT was, at least in part, functional.

This result arouses a major question. On the assumption that any pathological condition leads to a number of pulmonary physiological changes, could this complex be considered a biomarker of lung status? It seems logical to argue that free HNE would be a marker of the degree of injury more relevant than the complex. In fact, if the rate of formation of AAT–HNE complexes is limited by the amount of

available AAT, then it would be easier to measure NE in excess in the lung. The fact that free elastase in inflamed tissues can only be detected if it is present in excess over AAT activity or if this anti-elastolytic function has been somehow modified, was previously observed by other authors [51,52]. This is not the case of the patients under investigation. In fact, given that both the initial lack of the complex and its formation by addition of exogenous HNE cannot reflect with certainty an excess of the protease, our results point to a different conclusion. The unifying view that apparently emerges from these data is that not necessarily all recipients classified as "stable" based on their clinical/functional status, display the same conditions at a molecular level. The neutrophil count and detection of active HNE in tissues and fluids recovered from inflammatory sites might represent a critical step in tissue pathogenesis. In fact, significantly lower neutrophil levels in BALf from healthy subjects compared to BOS patients and the tendency of both HNE activity and the concentration of HNE-AAT complex to increase in these latter, had been previously observed [16]. Neutrophils produce antioxidants and are indispensable in forming the first line of defense during infection. In addition to the well-known anti-protease traits, evidence has been increasing in the last years that AAT has tissue-protective, anti-inflammatory and immune-regulating properties that can affect most inflammatory cells [22]. As a consequence, the concern that AAT has a great influence in early and long-term outcomes post lung transplantation has gained much interest [53]. Despite this interest, knowledge about the complications of high neutrophil recruitment is still poor and bronchoscopy with bronchoalveolar lavage seems to be the best diagnostic approach to investigate the local alterations at bronchial and alveolar levels. As shown in Table3, while the number of neutrophils was very low in the BALf of the three stable individuals who did not present free elastase activity or complex formation, these numbers and the HNE activity were increasing along with the severity of the disease. In this context, it is no wonder that our attention has also been drawn to the investigation of AAT functionality. It has been recently reported that macrophages or neutrophils have the potential ability to alter its activity in a manner that would allow neutrophil elastase to accumulate [54]. However, while several studies have assumed that oxidation of AAT promotes detection of free HNE activity in vivo [46,47], very poor experimental evidence still supports this contention. The reason is that almost all studies of AAT function after its oxidation in vitro or in vivo have been limited to the determination of its ability to inhibit exogenous porcine pancreatic elastase [54]. Obviously, our data do not allow us to exclude the fact that the lack of formation of the complex in some of our BALf samples was due to AAT modifications that made it unable to completely inhibit neutrophil elastase activity. However, the addition of exogenous HNE to samples not showing the 80 kDa band and the consequent formation of this complex seemed to show the functionality of AAT present in these samples. The great increase observed in the 80 kDa band by addition of exogenous HNE was a further evidence that this hypothesis was most likely correct.

5. Limitations of the Study

The sample size of individuals investigated represents a limitation of the present study. We would like to note that this research was conceived as a feasibility study whose aim was of acquiring a global vision of the protease/antiprotease balance in patients affected by BOS at different levels of severity. In an effort to work with well-characterized cohorts, great attention was paid to excluding sources of excessive variability and this choice necessarily lessened the sample size. Thus, the distribution of single versus double lung transplant procedures was similar, recipients affected by AATD were excluded, as were similar types of transplant indications, analogous IS regimen, NO azithromycin treatment at time of sampling, and appreciable length of post-transplant FU for enrolled stable recipients. The observed variability in sampling time is related to the evolution of BOS, whose grading reflects disease severity. While in some cases the evolution towards more severe disease is fast, in other cases patients evolve to BOSIII grade more slowly. Patients numbers 12 and 13 had been sampled after several months of disease course. The severity of disease however was not necessarily associated with a higher degree of inflammation.

That the investigation was limited to subjects with stable pulmonary function and patients affected by BOS II and BOS III can be considered another limitation of this work. However, the decision of not considering the BOSI patients at this stage of the work reflects the abovementioned need to avoid potential sources of variability. In fact, the possible reversibility of pulmonary alterations, common to this stage of BOS, could represent a confounding factor that may have affected the results. Finally, the demographic data shown in Table1might highlight the heterogeneity of the lung transplant recipients considered in this study. We consider this hypothetical heterogeneity not relevant for the purposes of our work. In fact, we focused our investigation only on the assessment of the AAT/HNE balance at graft level in patients submitted to double lung transplantation that were influenced only by graft acceptance/rejection status.

Of course, we are aware that a high-quality set of samples does not necessarily eliminate the risk of relying on poor evidence of data and that, to obtain more concrete answers about a condition that is largely still shrouded in mystery, larger-scale studies will be essential.

These results are preliminary and must, obviously, be validated on a larger cohort of patients that should involve individuals with different levels of BOS severity and co-morbidities associated with the presence of chronic rejection that could affect the protease/antiprotease balance.

6. Conclusions

This pilot work aimed to obtain a global picture of the protease/antiprotease balance in the BALf of two different cohorts of lung transplant recipients. The results of our study allowed us to demonstrate, for the first time, that not all BALf samples contain the complex between HNE and its specific inhibitor AAT. The lack of this complex in some subjects seems to be correlated with the low level of pulmonary inflammation, as suggested by the count of neutrophils and the determination of HNE/AAT activities in these subjects. The confirmation of these data on a larger cohort of individuals would allow us to consider the AAT-HNE complex a marker of pulmonary inflammation. This could indeed represent a new frontier in the field of biomarker discovery of lung inflammation in subjects with HNE/AAT unbalance. The identification of markers that could predict the development and progression of BOS is crucial for preventing the irreversible phase of the disorder with the final goal of improving the survival of lung transplant recipients.

Supplementary Materials: The following are available online athttp://www.mdpi.com/2571-5135/8/1/5/s1, Table S1. Primary sequence of all peptides identified for each protein analyzed. Figure S1- Western blotting of BALf from patients with the 80 kDa band before and after incubation with exogenous HNE * (left to right in both panels).

Author Contributions: Conceptualization, F.M., A.B., R.S.; methodology, M.C., M.D.V., I.F.; software, M.F., S.M. (Sara Magni); validation, M.C.; formal analysis, S.V., D.P.; investigation, M.C., D.P., I.F.; resources, F.M., P.I., A.B.; data curation, F.M., S.M. (Sara Magni), S.M. (Sabrina Martinello); writing—original draft preparation, P.I., M.C.; writing—review and editing, P.I., F.M.; supervision, S.V., A.B., R.S.; project administration, F.M.

Funding: This research received no external funding.

Conflicts of Interest: The authors declare no conflicts of interest.

References

1. Janciauskiene, S.M.; Bals, R.; Koczulla, R.; Vogelmeier, C.; Köhnlein, T.; Welte, T. The discovery of α1-antitrypsin and its role in health and disease. *Respir. Med.* **2011**, *105*, 1129–1139. [CrossRef] [PubMed]
2. De Serres, F.; Blanco, I. Role of alpha-1 antitrypsin in human health and disease. *J. Intern. Med.* **2014**, *276*, 311–335. [CrossRef] [PubMed]
3. Geraghty, P.; Rogan, M.P.; Greene, C.M.; Brantly, M.L.; O'Neill, S.J.; Taggart, C.C.; McElvane, N.G. Alpha-1-antitrypsin aerosolized augmentation abrogates neutrophil elastase-induced expression of cathepsin B and matrix metalloprotease 2 in vivo and in vitro. *Thorax***2008**, *63*, 621–626. [CrossRef] [PubMed]

4. Gaggar, A.; Li, Y.; Weathington, N.; Winkler, M.; Kong, M.; Jackson, P.; Blalock, J.E.; Clancy, J.P. Matrix metalloprotease-9 dysregulation in lower airway secretions of cystic fibrosis patients. *Am. J. Physiol. Lung Cell. Mol. Physiol.* **2007**, *293*, L96–L104. [CrossRef] [PubMed]
5. Perlmutter, D.H.; Kay, R.M.; Cole, F.S.; Rossing, T.H.; Van Thiel, D.; Colten, H.R. The cellular defect in alpha 1-proteinase inhibitor (alpha 1-PI) deficiency is expressed in human monocytes and in xenopus oocytes injected with human liver mRNA. *Proc. Natl. Acad. Sci. USA* **1985**, *82*, 6918–6921. [CrossRef] [PubMed]
6. Ray, M.B.; Geboes, K.; Callea, F.; Desmet, V.J. Alpha-1-antitrypsin immunoreactivity in gastric carcinoid. *Histopathology* **1982**, *6*, 289–297. [CrossRef] [PubMed]
7. Geboes, K.; Ray, M.B.; Rutgeerts, P.; Callea, F.; Desmet, V.J.; Vantrappen, G. Morphological identification of alpha-I-antitrypsin in the human small intestine. *Histopathology* **1982**, *6*, 55–60. [CrossRef] [PubMed]
8. Boskovic, G.; Twining, S.S. Local control of alpha1-proteinase inhibitor levels: Regulation of alpha1-proteinase inhibitor in the human cornea by growth factors and cytokines. *Biochim. Biophys. Acta* **1998**, *27*, 37–46. [CrossRef]
9. Gadek, J.E.; Fells, G.A.; Zimmerman, R.I.; Rennard, S.I.; Crystal, R.G. Antielastases of the human alveolar structures. Implications for the protease-antiprotease theory of emphysema. *J. Clin. Investig.* **1981**, *68*, 889–898. [CrossRef] [PubMed]
10. Greene, C.M.; Marciniak, S.J.; Teckman, J.; Ferrarotti, I.; Brantly, M.L.; Lomas, D.A.; Stoller, J.K.; McElvaney, N.G. α1-Antitrypsin deficiency. *Nat. Rev. Dis. Primers* **2016**, *2*, 16051. [CrossRef] [PubMed]
11. Brantly, M. Alpha-1 antitrypsin: Not just an antiprotease. Extending the half-life of a natural anti-inflammatory molecule by conjugation with polyethylene glycol. *Am. J. Respir. Cell Mol. Biol.* **2002**, *27*, 652–654. [CrossRef] [PubMed]
12. Janciauskiene, S.; Nita, I.; Subramaniyam, D.; Li, Q.; Lancaster, J.R., Jr.; Matalon, S. Alpha1-antitrypsin inhibits the activity of the matriptase catalytic domain in vitro. *Am. J. Respir. Cell Mol. Biol.* **2008**, *39*, 631–637. [CrossRef] [PubMed]
13. Bergin, D.A.; Reeves, E.P.; Meleady, P.; Henry, M.; McElvaney, O.J.; Carroll, T.P.; Condron, C.; Chotirmall, S.H.; Clynes, M.; O'Neill, S.J.; et al. α-1 Antitrypsin regulates human neutrophil chemotaxis induced by soluble immune complexes and IL-8. *J. Clin. Investig.* **2010**, *120*, 4236–4250. [CrossRef] [PubMed]
14. Pajdak, W.; Sieradzak-Fleituch, M.; Dubin, A.; Owsiński, J. Alpha-1-antitrypsin and alpha-1-antitrypsin-neutrophil elastase complex in bronchoalveolar lavage fluid of patients with pulmonary diseases (pilot study). *Acta Med. Hung.* **1991**, *48*, 103–109. [PubMed]
15. Fujita, J.; Bungo, M.; Hata, Y.; Nakamura, H.; Shiotani, T.; Irino, S. Evaluation of the elastase: Alpha 1-antitrypsin balance in patients with bacterial pneumonia using bronchoalveolar lavage. *Nihon Kyobu Shikkan Gakkai Zasshi* **1989**, *27*, 712–717. [PubMed]
16. Hirsch, J.; Elssner, A.; Mazur, G.; Maier, K.L.; Bittmann, I.; Behr, J.; Schwaiblmair, M.; Reichenspurner, H.; Fürst, H.; Briegel, J.; et al. Bronchiolitis obliterans syndrome after (heart-)lung transplantation. Impaired antiprotease defense and increased oxidant activity. *Am. J. Respir. Crit. Care Med.* **1999**, *160*, 1640–1646. [CrossRef] [PubMed]
17. Yusen, R.D.; Edwards, L.B.; Kucheryavaya, A.Y.; Benden, C.; Dipchand, A.I.; Dobbels, F. The registry of the International Society for Heart and Lung Transplantation: Thirty-first adult lung and heart-lung transplant report–2014; focus theme: Retransplantation. *J. Heart Lung Transplant.* **2014**, *33*, 1009–1024. [CrossRef] [PubMed]
18. Sato, M.; Ohmori-Matsuda, K.; Saito, T.; Matsuda, Y.; Hwang, D.M.; Waddell, T.K. Time-dependent changes in the risk of death in pure bronchiolitis obliterans syndrome (BOS). *J. Heart Lung Transplant.* **2013**, *32*, 484–491. [CrossRef] [PubMed]
19. Sato, M.; Hwang, D.M.; Waddell, T.K.; Singer, L.G.; Keshavjee, S. Progression pattern of restrictive allograft syndrome after lung transplantation. *J. Heart Lung Transplant.* **2013**, *32*, 23–30. [CrossRef][PubMed]
20. Ofek, E.; Sato, M.; Saito, T.; Wagnetz, U.; Roberts, H.C.; Chaparro, C.; Waddell, T.K.; Singer, L.G.; Hutcheon, M.A.; Keshavjee, S.; et al. Restrictive allograft syndrome post lung transplantation is characterized by pleuroparenchymal fibroelastosis. *Mod. Pathol.* **2013**, *26*, 350–356. [CrossRef] [PubMed]
21. Iskender, I.; Sakamoto, J.; Nakajima, D.; Lin, H.; Chen, M.; Kim, H.; Guan, Z.; Del Sorbo, L.; Hwang, D.; Waddell, T.K.; et al. Human α1-antitrypsin improves early post-transplant lung function: Pre-clinical studies in a pig lung transplant model. *J. Heart Lung Transplant.* **2016**, *35*, 913–921. [CrossRef] [PubMed]

22. Fisichella, P.M.; Davis, C.S.; Lowery, E.; Ramirez, L.; Gamelli, R.L.; Kovacs, E.J. Aspiration, localized pulmonary inflammation, and predictors of early-onset bronchiolitis obliterans syndrome after lung transplantation. *J. Am. Coll. Surg.* **2013**, *217*, 90–100. [CrossRef] [PubMed]
23. Gao, W.; Zhao, J.; Kim, H.; Xu, S.; Chen, M.; Bai, X.; Toba, H.; Cho, H.R.; Zhang, H.; Keshavjeel, S.; et al. α1-Antitrypsin inhibits ischemia reperfusion-induced lung injury by reducing inflammatory response and cell death. *J. Heart Lung Transplant.* **2014**, *33*, 309–315. [CrossRef] [PubMed]
24. Sundaresan, S.; Mohanakumar, T.; Smith, M.A.; Trulock, E.P.; Lynch, J.; Phelan, D.; Cooper, J.D.; Patterson, G.A. HLA-A locus mismatches and development of antibodies to HLA after lung transplantation correlate with the development of bronchiolitis obliterans syndrome. *Transplantation* **1998**, *65*, 648–653. [CrossRef] [PubMed]
25. Gerna, G.; Lilleri, D.; Furione, M.; Castiglioni, B.; Meloni, F.; Rampino, T.; Agozzino, M.; Arbustini, E. Human cytomegalovirus end-organ disease is associated with high or low systemic viral load in preemptively treated solid-organ transplant recipients. *New Microbiol.* **2012**, *35*, 279–287. [PubMed]
26. Kotsimbos, T.C.; Snell, G.I.; Levvey, B.; Spelman, D.W.; Fuller, A.J.; Wesselingh, S.L.; Williams, T.J.; Ostergaard, L. *Chlamydia pneumoniae* serology in donors and recipients and the risk of bronchiolitis obliterans syndrome after lung transplantation. *Transplantation* **2005**, *79*, 269–275. [CrossRef] [PubMed]
27. Daud, S.A.; Yusen, R.D.; Meyers, B.F.; Chakinala, M.M.; Walter, M.J.; Aloush, A.A.; Patterson, G.A.; Trulock, E.P.; Hachem, R.R. Impact of immediate primary lung allograft dysfunction on bronchiolitis obliterans syndrome. *Am. J. Respir. Crit. Care Med.* **2007**, *175*, 507–513. [CrossRef] [PubMed]
28. Ciaramelli, C.; Fumagalli, M.; Viglio, S.; Bardoni, A.M.; Piloni, D.; Meloni, F.; Iadarola, P.; Airoldi, C. ^{1}H NMR To Evaluate the Metabolome of Bronchoalveolar Lavage Fluid (BALf) in Bronchiolitis Obliterans Syndrome (BOS): Toward the Development of a New Approach for Biomarker Identification. *J. Proteome Res.* **2017**, *16*, 1669–1682. [CrossRef] [PubMed]
29. Piloni, D.; Morosini, M.; Magni, S.; Balderacchi, A.; Scudeller, L.; Cova, E.; Oggionni, T.; Stella, G.; Tinelli, C.; Antonacci, F.; et al. Analysis of long term CD4+CD25highCD127- T-reg cells kinetics in peripheral blood of lung transplant recipients. *BMC Pulm. Med.* **2017**, *17*, 102. [CrossRef] [PubMed]
30. Stewart, S.; Fishbein, M.C.; Snell, G.I.; Berry, G.J.; Boehler, A.; Burke, M.M.; Glanville, A.; Gould, F.K.; Magro, C.; Marboe, C.C.; et al. Revision of the 1996 working formulation for the standardization of nomenclature in the diagnosis of lung rejection. *J. Heart Lung Transplant.* **2007**, *26*, 1229–1242. [CrossRef] [PubMed]
31. Meloni, F.; Solari, N.; Miserere, S.; Morosini, M.; Cascina, A.; Klersy, C.; Arbustini, E.; Pellegrini, C.; Viganò, M.; Fietta, A.M. Chemokine redundancy in BOS pathogenesis. A possible role also for the CC chemokines: MIP3-beta, MIP3-alpha, MDC and their specific receptors. *Transpl. Immunol.* **2008**, *18*, 275–280. [CrossRef] [PubMed]
32. Estenne, M.; Hertz, M.I. Bronchiolitis obliterans after human lung transplantation. *Am. J. Respir. Crit. Care Med.* **2002**, *166*, 440–444. [CrossRef] [PubMed]
33. Sato, M.; Waddell, T.K.; Wagnetz, U.; Roberts, H.C.; Hwang, D.M.; Haroon, A.; Wagnetz, D.; Chaparro, C.; Singer, L.G.; Hutcheon, M.A.; et al. Restrictive allograft syndrome (RAS): A novel form of chronic lung allograft dysfunction. *J. Heart Lung Transplant.* **2011**, *30*, 735–742. [CrossRef] [PubMed]
34. Verleden, G.M.; Vos, R.; Vanaudenaerde, B.; Dupont, L.; Yserbyt, J.; Van Raemdonck, D.; Verleden, S. Current views on chronic rejection after lung transplantation. *Transpl. Int.* **2015**, *28*, 1131–1139. [CrossRef] [PubMed]
35. Del Fante, C.; Scudeller, L.; Oggionni, T.; Viarengo, G.; Cemmi, F.; Morosini, M.; Cascina, A.; Meloni, F.; Perotti, C. Long-Term Off-Line Extracorporeal Photochemotherapy in Patients with Chronic Lung Allograft Rejection Not Responsive to Conventional Treatment: A 10-Year Single-Centre Analysis. *Respiration* **2015**, *90*, 118–128. [CrossRef] [PubMed]
36. Lilleri, D.; Gerna, G.; Bruno, F.; Draghi, P.; Gabanti, E.; Fornara, C.; Meloni, F. Systemic and local human cytomegalovirus-specific T-cell response in lung transplant recipients. *New Microbiol.* **2013**, *36*, 267–277. [PubMed]
37. Ferrarotti, I.; Gorrini, M.; Scabini, R.; Ottaviani, S.; Mazzola, P.; Campo, I.; Zorzetto, M.; Luisetti, M. Secondary outputs of alpha1-antitrypsin deficiency targeted detection programme. *Respir. Med.* **2008**, *102*, 354–358. [CrossRef] [PubMed]

38. Smith, P.K.; Krohn, R.I.; Hermanson, G.T.; Mallia, A.K.; Gartner, F.H.; Provenzano, M.D.; Fujimoto, E.K.; Goeke, N.M.; Olson, B.J.; Klenk, D.C. Measurement of protein using bicinchoninic acid. *Anal. Biochem.* **1985**, *150*, 76–85. [CrossRef]
39. Yvon, M.; Chabanet, C.; Pélissier, J.P. Solubility of peptides in trichloroacetic acid (TCA) solutions. Hypothesis on the precipitation mechanism. *Int. J. Pept. Protein Res.* **1989**, *34*, 166–176. [CrossRef] [PubMed]
40. Laemmli, U.K. Cleavage of structural proteins during the assembly of the head of bacteriophage T4. *Nature* **1970**, *227*, 680–685. [CrossRef] [PubMed]
41. Candiano, G.; Bruschi, M.; Musante, L.; Santucci, L.; Ghiggeri, G.M.; Carnemolla, B. Blue silver: A very sensitive colloidal coomassie G-250 staining for proteome analysis. *Electrophoresis* **2004**, *25*, 1327–1333. [CrossRef] [PubMed]
42. Pollack, R.M.; Dumsha, T.C. On the use of p-nitroanilides as substrates for proteolytic enzymes. *FEBS Lett.* **1974**, *38*, 292–294. [CrossRef]
43. Viglio, S.; Zanaboni, G.; Luisetti, M.; Cetta, G.; Guglielminetti, M.; Iadarola, P. Micellar electrokinetic chromatography: A convenient alternative to colorimetric and high performance liquid chromatographic detection to monitor protease activity. *Electrophoresis* **1998**, *19*, 2083–2089. [CrossRef] [PubMed]
44. Iadarola, P.; Lungarella, G.; Martorana, P.A.; Viglio, S.; Guglielminetti, M.; Korzus, E.; Gorrini, M.; Cavarra, E.; Rossi, A.; Travis, J.; et al. Lung injury and degradation of extracellular matrix components by *Aspergillus fumigatus* serine proteinase. *Exp. Lung Res.* **1998**, *24*, 233–251. [CrossRef] [PubMed]
45. Di Venere, M.; Fumagalli, M.; Cafiso, A.; De Marco, L.; Epis, S.; Plantard, O.; Bardoni, A.; Salvini, R.; Viglio, S.; Bazzocchi, C.; et al. Ixodes ricinus and Its Endosymbiont Midichloria mitochondrii: A Comparative Proteomic Analysis of Salivary Glands and Ovaries. *PLoS ONE* **2015**, *10*, e0138842. [CrossRef] [PubMed]
46. Subramaniyam, D.; Virtala, R.; Pawłowski, K.; Clausen, I.G.; Warkentin, S.; Stevens, T.; Janciauskiene, S. TNF-α-induced self-expression in human lung endothelial cells is inhibited by native and oxidized α1-antitrypsin. *Int. J. Biochem. Cell Biol.* **2008**, *40*, 258–271. [CrossRef] [PubMed]
47. Montecucco, F.; Bertolotto, M.; Ottonello, L.; Pende, A.; Dapino, P.; Quercioli, A.; Mach, F.; Dallegri, F. Chlorhexidine prevents hypochlorous acid-induced inactivation of α1-antitrypsin. *Clin. Exp. Pharmacol. Physiol.* **2009**, *36*, e72–e77. [CrossRef] [PubMed]
48. Giuliano, S.; Agresta, A.M.; De Palma, A.; Viglio, S.; Mauri, P.; Fumagalli, M.; Iadarola, P.; Montalbetti, L.; Salvini, R.; Bardoni, A. Proteomic analysis of lymphoblastoid cells from Nasu-Hakola patients: A step forward in our understanding of this neurodegenerative disorder. *PLoS ONE* **2014**, *9*, e110073. [CrossRef] [PubMed]
49. Fietta, A.M.; Bardoni, A.M.; Salvini, R.; Passadore, I.; Morosini, M.; Cavagna, L.; Codullo, V.; Pozzi, E.; Meloni, F.; Montecucco, C. Analysis of bronchoalveolar lavage fluid proteome from systemic sclerosis patients with or without functional, clinical and radiological signs of lung fibrosis. *Arthritis Res. Ther.* **2006**, *8*, R160. [CrossRef] [PubMed]
50. Meyer, K.C.; Lewandoski, J.R.; Zimmerman, J.J.; Nunley, D.; Calhoun, W.J.; Dopico, G.A. Human neutrophil elastase and elastase/alpha 1-antiprotease complex in cystic fibrosis. Comparison with interstitial lung disease and evaluation of the effect of intravenously administered antibiotic therapy. *Am Rev. Respir. Dis.* **1991**, *144*, 580–585. [CrossRef] [PubMed]
51. Magi, B.; Bini, L.; Perari, M.G.; Fossi, A.; Sanchez, J.C.; Hochstrasser, D.; Paesano, S.; Raggiaschi, R.; Santucci, A.; Pallini, V.; et al. Bronchoalveolar lavage fluid protein composition in patients with sarcoidosis and idiopathic pulmonary fibrosis: A two-dimensional electrophoretic study. *Electrophoresis* **2002**, *23*, 3434–3444. [CrossRef]
52. Heutinck, K.M.; Ten Berge, I.J.; Hack, C.E.; Hamann, J.; Rowshani, A.T. Serine proteases of the human immune system in health and disease. *Mol. Immunol.* **2010**, *47*, 1943–1955. [CrossRef] [PubMed]
53. Bergin, D.A.; Hurley, K.; McElvaney, N.G.; Reeves, E.P. Alpha-1 antitrypsin: A potent anti-inflammatory and potential novel therapeutic agent. *Arch. Immunol. Ther. Exp. (Warsz.)* **2012**, *60*, 81–97. [CrossRef] [PubMed]
54. Ossanna, P.J.; Test, S.T.; Matheson, N.R.; Regiani, S.; Weiss, S.J. Oxidative regulation of neutrophil elastase-alpha-1-proteinase inhibitor interactions. *J. Clin. Investig.* **1986**, *77*, 1939–1951. [CrossRef] [PubMed]